Addis Ababa University

Addis Ababa Institute of Technology (AAiT)

School of Graduate Studies

Modelling and Dynamic Analysis of Bus Body Built in Ethiopia

by

Besufekad Getachew

Thesis submitted to the Addis Ababa Institute of Technology

in partial fulfilment of the requirements for the degree of

Master of Science

in

Mechanical Engineering

(Mechanical Design Stream)

Dr.-Ing. Leul Fesseha (Advisor)

February 2012

Addis Ababa, Ethiopia

Addis Ababa Institute of Technology (AAiT)

School of Graduate Studies

Modelling and Dynamic Analysis of Bus Body Built in Ethiopia

Submitted by:

Besufekad Getachew	_____	_____
Student	Signature	Date

Approved by:

1. Dr. Daniel Tilahun	_____	_____
Chairman, Dep.'s Graduate Committee	Signature	Date
2. Dr.-Ing. Leul Fesseha	_____	_____
Thesis Advisor	Signature	Date
3. Dr.-Ing. Zewdu Abdi	_____	_____
Internal Examiner	Signature	Date
4. Dr.-Ing. Tamirat Tesfaye	_____	_____
External Examiner	Signature	Date

Dedication

To my beloved family, for their immeasurable support, encouragement, and patience.

Acknowledgement

First of all, I would like to thank God for the endless blessings and gifts.

I would like to thank Dr.-Ing. Leul Fesseha for his scientific and technical guidance and support throughout this research, without his continuous corrections and constructive comments this project wouldn't have been successful.

I am grateful to all staff of Ultimate Motor P.L.C. Specially, I want to express my sincere appreciation and gratitude to Mr. Melkau Yirga for his valuable advice and for always having time for discussions.

I would also like to thank my father *Getachew*, my mother *Meaza*, my sisters *Tingirt* and *Melat*, and my brother *Dawit* for their love, understanding, support and encouragement.

Last but certainly not least, I would like to thank all of my friends for their encouragement, and support with different materials and ideas.

Abstract

Bus is a popular and common means of transport in Ethiopia. The structural strength and speed is a fundamental concern. Unnecessary weight of the bus structure leads to reduction of speed, high fuel consumption and reducing the overall performance of bus.

The primary objective of this research is to improve the bus structure weight. The improvement is carried out by analysing the structure for two main loading cases, bending load and torsional stiffness. This study examines the stresses and deformation responses of a typical bus structure during application of the load in service. A bus structure was modelled using computer aided design (CAD) CATIA V5R16 software and exported to finite element analysis ANSYS 12 software and simulated by applying boundary conditions. The structure weight improvement of the bus is made by reducing the size and thickness of metal used in the structure. In this analysis a new model of the bus was made and analysed. Two loading cases were incorporated in the analysis. Bending load case was used to simulate the bus travelling on smooth road and twisting moment is used to simulate a bus travelling on a bumpy road. This re-modelled bus is again simulated by finite element analysis software and found to be structurally safe. The simulation of the re-modelled bus was conducted using the same inputs used in the original model simulation. The remodelled result shows that the stress and displacement results are safe.

A simply supported overhanging beam model was made to validate the results obtained from finite element analysis simulation. Finally, cost analysis is carried out to compare the original structure cost with the improved. It is found that by reducing the size of the members used in the bus structure the cost is reduced. The cost reduced in the considered company reaches 520, 938.00 Birr annually.

Table of Contents

Chapter One 1

Introduction 1

1.1. Background 1

1.2. Motivation 2

1.3. Problem statement 2

1.4. Objective of the Study 2

1.5. Scope of the project 3

Chapter Two 4

Literature Survey 4

2.1. Introduction 4

2.2. Literature Review 4

Chapter Three 8

Research Methodology 8

3.1. Introduction 8

3.2. Methodology of the research 8

3.3. The steps of the analysis 9

3.4. Finite Element Analysis 10

3.5. Vibration of Beams 10

3.6. Modal Analysis 12

3.6.1. Analysis of free vibration 13

Chapter Four 16

Modelling and Finite Element Analysis 16

4.1. Introduction 16

4.2. Bus specification 16

4.3. Modelling of bus structure 17

4.4. Finite element modelling of the bus structure 18

4.5. Consideration of welding effect in finite element modelling of the structure 19

4.6. Finite element meshing of the bus 20

4.7. Inputs for Finite Element Analysis 22

4.8. Boundary conditions used in the analysis 24

4.9. Results and discussion of static structure analysis 25

4.9.1. Bending load case 26
4.9.2. Torsional Moment case 34
4.10. Vibration analysis of original structure 46
4.11. Improvement process 54
4.11.1. Changing the size of RHS 55
4.12. Improved structure analysis 56
4.12.1. Finite element mesh of the improved model 56
4.12.2. Boundary conditions of the improved structure analysis 56
4.12.3. Bending loading case 57
4.12.4. Torsional moment case 64
4.12.5. Vibration analysis of the improved structure 74
4.13. Comparison between original and improved structure 78
4.14. Verification of the method used 79
4.14.1. Bending Moment 79
4.14.2. Deflection of the beam 83
4.14.3. Verification of manual analysis of the beam with ANSYS 12 Workbench 85
Chapter Five 87
Cost Analysis 87
Chapter Six 91
Conclusions and Recommendations 91
6.1. Conclusions 91
6.2. Limitations of the study 91
6.3. Recommendation for Future Study 92
References 93
Bibliography 95

Table of Figures

Figure 3.1 Analysis flow diagrams 9
Figure 4.1 RHS profiles employed (dimensions in mm) 17
Figure 4.2 CAD model of bus structure 18
Figure 4.3 Imported model of bus to ANSYS 12 window 19
Figure 4.4 Tetrahedron element 20
Figure 4.5 a) Tetrahedron element cross section construction b) SOLID186 Structural solid geometry (Tetrahedral Element) 21
Figure 4.6 Finite element model mesh of the bus 22
Figure 4.7 Bus structure load applied 23
Figure 4.8 Boundary condition during torsional moment case 25
Figure 4.9 Equivalent stresses (Von miss stress) of original structure in bending load case ..27
Figure 4.10 Normal stresses of original structure in bending load case 29
Figure 4.11 Total displacements of original structure in bending load case 31
Figure 4.12 Vertical displacements (Z-Axis) of original structure in bending load case 33
Figure 4.13. Boundary condition during torsional moment case 1 34
Figure 4.14 Total displacement of original structure in twisting moment case 36
Figure 4.15 Directional displacements (z-direction) of original structure in twisting moment case 37
Figure 4.16 Von-Miss Stress of original structure in torsional moment case 39
Figure 4.17 Normal Stress (y-direction) of original structure in torsional moment case 40
Figure 4.18 Shear stress of original structure in torsional moment case 1 41
Figure 4.19 Boundary condition during torsional moment case 2 41
Figure 4.20 Total displacement of the original structure during torsional moment case 2 42
Figure 4.21 Equivalent stress of the original structure during torsional moment case 2 44
Figure 4.22 Shear stress of the original structure during torsional moment case 2 45
Figure 4.23 MATLAB plot of PSD of Road Roughness 47
Figure 4.24 Displacement PSD of Class H road for 20 km/hr and 70 km/hr 48
Figure 4.25 Deformation of bus for mode 1 and mode 2 of original structure 49
Figure 4.26 Displacement of bus for mode 4 and mode 3 of original structure 50
Figure 4.27 Equivalent Stress Values for modes 1, 2, 3, and 4 51
Figure 4.28 PSD responses of selected nodes due to road roughness of original structure 53
Figure 4.29 Passenger door side structure showing members which use same RHS 54

Figure 4.30 Driver side door structure showing members which use same RHS.....55
Figure 4.31 Finite element mesh of the improved bus structure.....56
Figure 4.32 Von-Miss stress of improved structure in bending load case.....58
Figure 4.33 Normal stresses (y-direction) of improved structure in bending load case.....60
Figure 4.34 Directional displacements (z-direction) of improved structure in bending load case.....62
Figure 4.35 Total displacement of improved structure in bending load case.....63
Figure 4.36 Equivalent stress of improved structure in torsional load case 1.....65
Figure 4.37 Normal Stress (vertical-direction) of improved structure in torsional load case 1 67
Figure 4.38 Shear stress of the improved structure for torsional moment case 1.....68
Figure 4.39 Directional displacements (vertical direction) of improved structure in torsional load case 1.....69
Figure 4.40 Total Displacement of improved structure in torsional load case 1.....70
Figure 4.41 Equivalent stress in the improved structure for torsion moment case 2.....71
Figure 4.42 Shear stress of the improved structure for torsion moment of case 2.....72
Figure 4.43 Total displacement of the improved structure for torsion moment case 2.....73
Figure 4.44 Displacement of improved bus structure for mode 1and mode 2.....74
Figure 4.45 Displacement of improved bus structure for mode 3and mode 4.....75
Figure 4.46 Equivalent stress values for the improved structure.....75
Figure 4.47 PSD responses of selected nodes due to road roughness of original structure.....77
Figure 4.48 Loads applied on the beam.....79
Figure 4.49 Cross section of the beam used in the verification.....79
Figure 4.50 Reaction forces of the beam.....80
Figure 4.51 Cross section of beam for shear stress.....81
Figure 4.52 Shear force diagram.....82
Figure 4.53 Section X-X of Beam.....83
Figure 4.54 Deflection curve of the beam plotted in Microsoft Excel.....84
Figure 4.55 Finite element mesh of the beam.....85
Figure 4.56 Minimum bending stress.....85
Figure 4.57 Maximum bending stress.....86
Figure 4.58 Deformation of the beam.....86

List of Tables

Table 4.1 Bus specification 16

Table 4.2 Material property of RHS used 17

Table 4.3 Overall dimension of bus model 18

Table 4.4 Loads applied on the structure 23

Table 4.5 Stress and displacements values in bending load case of original structure 26

Table 4.6 Stress and displacement Values of original structure in twisting moment Case 35

Table 4.7 Frequency value at each mode shape of original structure 49

Table 4.8 Values of stress and displacement for the improved bus 57

Table 4.9 Stress and displacement values in torsional loading case 64

Table 4.10 Mode shape and frequencies of improved structure 74

Table 4.11 Comparison between original and improved structure during bending load case . 78

Table 4.12 Comparison between original and improved structure during torsion load case ... 78

Table 4.13 Deformation values of the beam calculated analytically 84

Table 4.14 Sizes of RHS used in the bus Structure 87

Table 4.15 Total length of RHS 70X50X3mm used in passenger door side structure 88

Table 4.16 Total length of RHS 50X30X3mm used in passenger door side structure 88

Table 4.17 Total length of RHS 70X50X3mm used in Driver door side structure 89

Table 4.18 Total length of RHS 50X30X3mm used in passenger door side structure 89

Table 4.19 Prices of RHS 90

Table 4.20 Length of RHS and cost saved 90

Chapter One

Introduction

1.1. Background

Transportation industry plays a major role in the economy of modern industrialized and developing countries. The major means of transport include automobile, buses, trains, ship aeroplanes, etc. In our country, buses are major means of transport used both for short and long distances and as a result warranted its local fabrication. Consequently, many companies have grown dramatically, from small repair shops to their present day level. To date, the fabrication of these vehicles has been done without the necessary analysis that ensures their reliability on safety and performance. Therefore, considering their growing trend of demand and use, it is essential to give due attention to the fabrication design of these vehicles, to make sure of their road worthiness, safety and overall performance.

A bus body (compartment) structure is fabricated from welded beams of rectangular cross section which makes up the four sides of and covered by sheet metal. The main components of the bus structure parts include right side, left side, front side, rear side, roof and floor. The body structure, which is the main part of the body, should support the engine, seats, luggage, fuel tank and passengers. Besides these, the structure is subjected to dynamic and impact loads which could be detrimental to the strength and rigidity of the overall structure. To make the bus structure strong enough, the local bus builders use large amount of steel. Simple modification of structural parts is limited by the body strength, stiffness and crashworthiness. The production process is not supported by modern design principles. As a result, during the operation phase, these buses are not as such efficient because of the large amount of self weight of the buses. In order to make improvement on the design of the structure, it is basic to analyze the structure for stresses and deformations to find parts which are subjected to maximum and minimum stresses and deformations. This indirectly tells whether parts are highly loaded or not. Therefore, understanding of this lays the foundation for improvement of the bus in weight.

1.2. Motivation

The increasing demand for public transportation forces responsible governments to find a solution. To meet the need and simultaneously save foreign currency, local fabrications has been strongly supported. As a result, there are large numbers of bus body builders in Ethiopia, mainly located in Addis Ababa. All, build the bus body on imported regular trucks, mostly ISUZU's, IVECO's and DEWOO's and mainly based on vehicle body repair experience. Most, do not have any designs and worse, none have any design analysis which ought to be a requirement for the certification for these vehicles. The operation of these vehicles in service though alleviates the transportation need, causes unnecessary accidents with loss of life and property damage. Further, use of large number of components with the false assumption "any strong structure is good" which adds up unnecessary weight to the body and impact the overall efficiency.

The motivation of this research is to propose a design modification to find improved structure of a locally built bus. By analysing the strength behaviour of the bus structure, improvement on the bus structure is made.

1.3. Problem statement

The modeling and investigation (both static and the dynamic), of the structure of buses on the road today will indicate the shortcomings of the current designs. This shortcomings include over weight of structure, which leads to high fuel consumption. An improved bus body structure based on finite element analysis will be proposed to alleviate these shortcomings. The result of the analysis and the implementation of the design will contribute to the improvement of the locally built buses.

1.4. Objective of the Study

The primary objective of this research is to make weight improvement on the currently produced bus body structure in Ethiopia. This is done by investigating the current bus structure manufactured in Ethiopia and come up with improved design to alleviate the shortcomings. The structure is to be lighter in weight and as a result efficient in fuel saving.

Analysis of structural strength and stiffness will be carried out, and the comparison of the original and improved structures in terms of strength and rigidity shall be made.

The major objective of the dynamic analysis processes shall be simulation of the bus while traveling with *20 km/hr* and *70 km/hr* on ISO standard low quality road and finding responses of the original and improved structure (i.e. stresses and displacements) at selected nodes of the bus structure. Meanwhile, the determination of the natural frequency and mode shape of bus structure will be made.

1.5. Scope of the project

The scope of this project includes the following analysis,

1) Modeling of the bus body using CATIA V5R16 software;
2) Structural integrity (strength and stiffness) analysis will be carried out to observe the structure strength (stress and deformation) using finite element analysis software.
3) Dynamic analysis of the model using the proper finite element analysis and simulation software to investigate the performance of the model; and
4) Re-modelling of the original structure with newly replaced members of the structure
5) Structural integrity (Strength and stiffness) analysis will be carried out for the new structure to observe the structure strength (stress and deformation) using finite element analysis software
6) Dynamic analysis of the model using the proper finite element analysis and simulation software to investigate the performance of the model
7) Cost Analysis will be carried out
8) To recommend the possible and relevant improvements in the design of bus frame

Chapter Two

Literature Survey

2.1. Introduction

The design of vehicle body has evolved from a simple, all steel structure that meets the basic requirement of strength and functionality, to the current day complex and efficient structure. Lightweight composite materials, such as glass-fiber reinforced polymers, have been used to replace traditional steel and aluminium components. This is because composites offer significant opportunities for enhancement of product performance in terms of strength, stiffness and energy absorption, combined with weight reduction and space saving. Today, design procedures of vehicles body that ensures reliability and road worthiness is well established. However, as a result of advancements in the areas of material, production methods, computational & design tools, optimization technique, etc., further improvement on vehicle structural design is still an active topic of research.

A wealth of analytical and experimental investigations addressing the issue and methodology of structural optimization to reduce the overall weight of vehicle body, maintaining the integrity and performance, now exists [1, 3, 6]. The optimization of the structural design, is pursued by either employing new materials [1, 15] or optimizing the structure using the traditional material steel [9].

2.2. Literature Review

Boada et al. (2007) presented a genetic-algorithm based optimization of a bus structure as a design methodology. The structure of the bus has been optimized by using genetic algorithms. The optimized bus is then checked for stress distribution and stiffness calculations by means of a developed finite element model of the bus structure. By applying this method, an optimized structure in weight and torsional stiffness has been achieved.

Lan et al. (2004) investigated medium-sized bus- body structure. In this investigation, they used computer-aided design (CAD) package for modelling and the analysis was made using finite element (FE) solver, ANSYS.

Sensitivity analyses were carried out on body structural parameters with the objective of minimizing body weight while maintaining the required performance. Based on the sensitivity analyses, it was found the upper cross-beam of the chassis frame, the vertical middle posts, the bridging bars of the chassis frame and the lower cross-beam of the chassis frame are more sensitive to rigidity/weight and frequency/weight. The body weight is reduced by 5.7 %. The results of the analysis were verified by experimental test.

Zhang Xingwang and Tao Zhen (2009) studied Shape Optimization of Bus Body Structure based on stiffness sensitivity analysis. Optimization of the design of structure and dimension of the body parts was made. The stiffness sensitivity of the whole auto body structure parts were analysed for torsion and bending loads and proved to be more reasonable, numerically. They achieved to reduce the mass of original body structure by 8.9 kg which is 2.95 % of the total weight.

Butdee and Vignat (2008) implemented the Theory of Inventive Problem Solving (TRIZ) method and claims to achieve a light bus body structure, design. Light weight bus body design is supported by TRIZ. The designed bus model is transferred to CAD and transfer data to CAE using finite element analysis. Then the weight reduction of bus is made. Re-analysis of this structure is made with same finite element method as done for the original structure. The comparison of mass before and after improvement was claimed to have reduced the weight by 0.93%.

Manokruang and Butdee (2009) presented the 2nd approach of light weight design. Used expert system, to eliminate less priority parts and reduced the overall vehicle weight by 4.62% while maintaining the stress level below the allowable.

Martin Hornung and Michael Hajj (2009) presented the use of structural adhesive and structural foam as a way of reducing vehicle weight. They showed that engineering plastics in combination with structural foam are good alternatives to replace steel reinforcements. Components made of steel have been replaced by three parts with structural foam on nylon

carriers, one steel part was upgraded in quality, and another steel part was significantly downgraded in quality. By these means, a weight saving of 12.5 kg/car was achieved.

Cho-Chung Liang and Giang-Nam Le (2009) used successive response surface method (SRSM) for optimal analysis of bus superstructure strength. Optimisation was performed by SRSM and finite element was solved by LS-DYNA. Vehicle weight at existing level was maintained while improving the crashworthiness. The result obtained shows that the deformation of the bus frame was reduced by 49.2% for lower and 39.4% for upper side frames.

A new approach for optimum design of the bus window pillar member was investigated by Kim et al. (2000). Stress distribution and fatigue strength were estimated through finite element analysis and experiment. To verify the results, stress analyses on the spot welding points, which were fatigue crack initiation points, were performed.

A new concept is introduced to optimise the computational costs and the reliability of the analysis of bus frame dynamics by Balazs Gombor (2005). A relatively simple finite element model was used and modal parameters (modal, damping, and mass) belonging only to the most significant modes were extracted. The reliability and applicability of the results gained from this method were verified by the stress measurements made on 412 low floor bus type of IKARUSBUS Inc.

Theodosiou, G. Georgiou and S. Natsiavas (2008) investigated the periodic steady state response of a large scale city bus model with nonlinear characteristics. They used a method to reduce the degree of freedom (DOF) to reduce the computational difficulty. Finite element model of the whole bus body including the accessories (Engine, AC, fuel tanks) were made. They considered non-linear spring and damper of the supports. The employed method was validated by presenting numerical results obtained under periodic road excitation.

A fundamental theoretical study is performed for the computation of the fatigue damage of the main structures of a road vehicle running on a randomly profiled road by Gobbi and Mastinu (1998). They considered a simple quarter car vehicle model. The expected fatigue damage was analysed according to Miner’s rule and Rain-Flow counting employing Rychlik

method. The research showed vehicle parameters (namely masses, dampings, and stiffnesses) have an influence on fatigue damage.

Structural reliability analysis of bus body in consideration to the correlation of working conditions was done by Zhang et al. (2009). They used structural reliability analysis for optimal design of bus structure. The results showed that in the two typical load cases (Bending and Torsion), the cross-area of beam element has a significant influence on the bus body structure reliability and a less influential effect has been found on the thickness of skin.

Ahmed et al. (1997) investigated the ride comfort of city bus body mounted on lorry chassis. In their work, experimental investigations were made on the actual bus and analytical investigations were carried out on half vehicle model. Focus was made to evaluate and improve the ride performance parameters. Results obtained showed that this bus has very poor ride performance when compared to buses which were manufactured on a bus chassis.

Sidhu et al. (2003) made a study on shape optimization of vehicle for improved safety and reliability. HEEDS (Hierarchical Evolutionary Engineering Design System) software package was used as optimization technique. Using ABAQUS and HEEDS optimization environment, this process has been applied to several automotive lower compartment rail designs. Results showed that significant gains in performance along with up to 20% reductions in mass were achieved.

Chapter Three

Research Methodology

3.1. Introduction

This research focuses on the improvement of bus body structure built in Ethiopia. For the purpose of the data collection, Ultimate Motor Bus Body Builder is selected. This company is selected based on its large market coverage both for private and governmental companies. Currently, Ministry of Education is the number one client. The factory uses RHS 70X50X3 mm, RHS 50X30X3 mm and RHS40X40X2.5 mm to build the bus structure. Using the data found from the company the modeling is made.

The research focuses on weight improvement of bus body structure produced in the above stated company. It includes strength analysis, stiffness analysis, dynamic analysis and simulation of bus frame. Strength and stiffness analysis is concerned with stress and deformation analysis of bus frame using ANSYS 12 workbench finite element analysis. Dynamic analysis incorporates natural frequencies and mode shapes of bus frame and acceleration responses at selected nodes of the structure while the bus is travelling on standard road.

The research commences by modeling the bus structure with the data gained from the bus manufacturer. This model is then analyzed for strength property i.e. stress and deformations. Then re-modeling of the bus is made with newly replaced RHS. This model is again analyzed for stress and deformations. Besides, dynamic analysis is made in order to find PSD of acceleration response, when the bus is excited by the road. Finally, the two results are compared.

3.2. Methodology of the research

1) **Data collection**: measuring of the real bus body structure components.
2) **CAD modeling of the structure**: this is made by using the data recorded from the bus body builder.
    - CATIA V5R16 software is used to build the computer model.

3) **Finite element (FE) analysis:** analyzing of structure for the required results using ANSYS Workbench software.

   i.e. Stress, displacement, mode shapes, PSD of acceleration

4) **Re-modeling of the structure:** using new size of components
5) **Finite element (FE) analysis of the re-modeled structure:** analyzing of structure for the required results using ANSYS software.

   i.e. Stress, displacement, mode shapes, PSD of acceleration

6) **Comparison of the original and improved structure**
   - In terms of Stress, displacement and weight of the original and improved structure

3.3. The steps of the analysis

The flow diagram shown below describes the method followed in the overall analysis and improvement of the bus structure weight on the base of bending load and torsional stiffness. The re-modelling is made till the stress result is reasonably below the allowable stress for both loading cases.

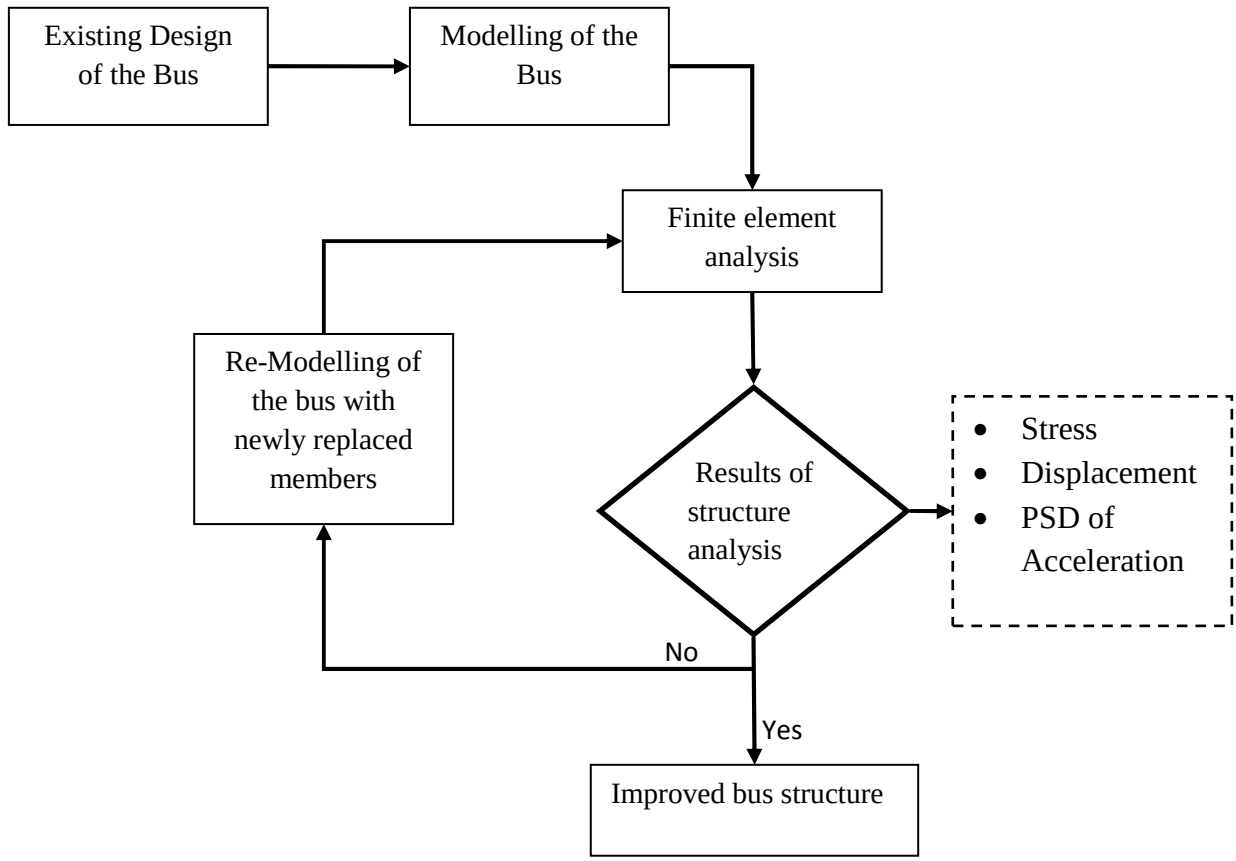

Figure 3.1 Analysis flow diagrams

3.4. Finite Element Analysis

The finite element method (FEM) is a numerical method seeking an approximated solution of the distribution of field variables in the problem domain that is difficult to obtain analytically. It is done by dividing the problem domain into several elements. Known physical laws are then applied to each small element, each of which usually has a very simple geometry. A continuous function of an unknown field variable is approximated using piecewise linear functions in each sub-domain, called an element formed by nodes. The unknowns are then the discrete values of the field variable at the nodes.

Next, proper principles are followed to establish equations for the elements, after which the elements are 'tied' to one another. This process leads to a set of linear algebraic simultaneous equations for the entire system that can be solved easily to yield the required field variable. Traditionally, structures have been analyzed either as continuous or as discretized ('lumped') systems.

Some structures, such as uniform beams, can still usefully be treated as continuous systems, but most are now regarded as discrete multi-DOF systems. The finite element method, in fact, can be said to combine both approaches: it is continuous within the elements, but discrete at the global coordinate level.

The general procedure of FEM for structure analysis is

- Divide structure in to pieces (elements with nodes)
- Describe the behavior of the physical quantities on each element
- Assemble the elements at the nodes to form an approximate system of equation for the whole structure
- Solve the system of equations involving unknown quantities at the nodes (e.g. displacements)
- Calculate the desired quantities (e.g. deformation and stresses) at selected elements

3.5. Vibration of Beams

It is still useful to be able to calculate the natural frequencies and vibration modes of uniform beams, plates, cables, membranes, etc. These are sometimes used in structures, and they are also useful as test cases for unfamiliar programs, since the exact analytic answers are known.

As an example, the bending modes of a uniform beam are now derived. From simple beam theory, for static loading, the following well-known relationships apply:

$$EI\frac{d^2y}{dx^2} = M(x) \quad 3.1$$

$$EI\frac{d^3y}{dx^3} = S(x) \quad 3.2$$

$$EI\frac{d^4y}{dx^4} = W(x) \quad 3.3$$

Where *E* is the Young's modulus, *I* is the second moment of area about bending axis, *y* is the displacement normal to the beam centerline at distance *x* along the beam, *M(x)* is the bending moment at *x*, *S(x)* is the shear at *x*, and *W(x)* is the load per unit length at *x*.

If there is no applied force or damping, the load distribution *W(x)* will be the inertia loading due to the mass of the beam:

$$W(x) = -\mu\frac{\partial^2y}{\partial t^2} \quad 3.4$$

Where μ is the mass of the beam per unit length, constant in this case, and *y* is now a function of time, *t*, as well as of *x*. The negative sign in Eq. 3.4 is due to D'Alembert's principle.

$$EI\frac{d^4y}{dx^4} = -\mu\frac{\partial^2y}{\partial t^2} \quad 3.5$$

Due to the assumption that there is no applied force, or damping, only simple harmonic motion is possible, i.e.,

$$y = \bar{y}sin\omega t \quad 3.6$$

$$\frac{\partial^2y}{\partial t^2} = -\omega^2\bar{y}sin\omega t \quad 3.7$$

Where $\bar{y}$ is a mode shape factor which is a function of *x*. The maximum loading corresponds to $sin\omega t = 1$, so for this condition, $\frac{\partial^2y}{\partial t^2} = -\omega^2\bar{y}$. Substituting this into Eq. 3.7 gives:

$$\frac{d^4y}{dx^4} = \frac{\mu\omega^2}{EI}\bar{y} = \beta^4\bar{y} \quad 3.8$$

Where $\beta^2 = \frac{\omega}{\sqrt{EI/\mu}}$

The general solution for the above equation becomes

$$\bar{y} = Asin\beta x + Bcos\beta x + Csinh\beta x + Dcosh\beta x \quad 3.9$$

The constants A, B, C and D depend upon the boundary conditions, i.e. whether an end is fixed, pinned (simply supported), and free.

3.6. Modal Analysis

A modal analysis determines the vibration characteristics (natural frequencies and mode shapes) of a structure or a machine component. It can also serve as a starting point for another, more detailed, dynamic analysis, such as random vibration, transient dynamic analysis, a harmonic response analysis, or a spectrum analysis. The natural frequencies and mode shapes are important parameters in the design of a structure for dynamic loading conditions. In addition, a modal analysis can be done on a prestressed structure, such as a spinning turbine blade.

The intention of computer simulation is to predict the behaviour of a component or vehicle under given loading conditions, before manufacture of a prototype. Finite element analysis (FEA) has been an integral part of the design and development process for commercial vehicles for many years. FEA is applied to ensure that all parts, linkages and systems, which make up a vehicle, are strong enough to withstand the loads placed on them in service. Beyond this analysis, however, as described previously, the dynamic behaviour of vehicles in service has been the result of testing, development and judgment, based on the experience of the design team. This is where the use of multi-body simulation (MBS) software can give real benefits. Whereas finite-element analysis looks at the stresses and deflections of parts, to ensure that they are strong enough for their intended uses, MBS software packages look at the dynamic behaviour and interaction of mechanisms and systems, under loads and conditions that replicate real life.
Computer simulation, if applied properly, brings many benefits to the analysis of static and dynamic systems. It opens up opportunities to analyse behaviour previously too complex to interpret, it can reduce the time required to investigate systems and it reduces some of the safety risks associated with prototype testing. All these factors contribute to reducing the cost of analysis, improving confidence in a design and achieving a higher added value to the analysis service and the products produced.

The tool, known as *modal analysis,* has its basis in the fact that every mechanical structure exhibits natural modes of vibration (dynamic response) and these modes can be readily computed given the elastic and inertia characteristics of the structure.

3.6.1. Analysis of free vibration

An independent multi-degree of freedom (MDOF) system can be considered with N degrees of freedom. The governing equation of motion of the system can be expressed in matrix form as,

$$\boldsymbol{KD} + \boldsymbol{M\ddot{D}} = \boldsymbol{F} \qquad 3.10$$

Where **K** and **M** are the globe stiffness and mass matrix, **D** is a vector of all the displacements at all the nodes in the entire problem domain, and **F** is a vector of all the equivalent nodal force vectors.

For a structural system with a total DOF of N, the stiffness matrix **K** and mass matrix **M** in Eq. 3.10 have a dimension of N ×N. By solving the equation we can obtain the displacement field, and the stress and strain. The question now is how to solve this equation, as N is usually very large for practical engineering structures. One way to solve this equation is using the so-called direct integration method. An alternative way of solving Eq. 3.10 is using the so-called modal analysis technique (or mode superposition technique). In this technique, we first have to solve the homogenous equation of Eq. 3.10.

The homogeneous equation is when we consider the case of **F** = 0, therefore it is also called *free vibration* analysis, as the system is free of external forces. For a solid or structure that undergoes a free vibration, the discretized system equation Eq. 3.10 becomes

$$\boldsymbol{KD} + \boldsymbol{M\ddot{D}} = 0 \qquad 3.11$$

The solution for the free vibration problem can be assumed as

$$\boldsymbol{D} = \varphi \exp(i\omega t) \qquad 3.12$$

Where $\boldsymbol{\varphi}$ is the amplitude of the nodal displacement, ω is the frequency of the free vibration, and *t* is the time. By substituting Eq. 3.12 into Eq. 3.11, we obtain

$$[\boldsymbol{K} - \omega^2 \boldsymbol{M}]\varphi = 0 \qquad 3.13(a)$$

Or

$$[\boldsymbol{K} - \lambda \boldsymbol{M}]\varphi = 0 \qquad 3.13(b)$$

Where

$$\lambda = \omega^2$$

Equation Eq. 3.13(a) and Eq. 3.13(b) are called the eigenvalue equation.

To have a non-zero solution for φ, the determinate of the matrix must vanish:

$$\det[\boldsymbol{K} - \lambda \boldsymbol{M}] = |\boldsymbol{K} - \lambda \boldsymbol{M}| = 0 \qquad 3.14$$

The expansion of the above equation will lead to a polynomial of λ of order N. This polynomial equation will have N roots, λ_1, *and* $\lambda_2 \ldots \lambda_N$, called *eigenvalues*, which relate to the *natural frequency* of the system by Eq. 3.13(a).

The natural frequency is a very important characteristic of the structure carrying dynamic loads. It has been found that if a structure is excited by a load with a frequency of one of the structure's natural frequencies, the structure can undergo extremely violent vibration, which often leads to catastrophic failure of the structural system. Such a phenomenon is called resonance. Therefore, an eigenvalue analysis has to be performed in designing a structural system that is to be subjected to dynamic loadings.

By substituting an eigenvalue λ_i back into the eigenvalue equation, Eq. 3.13(b), we have

$$[\boldsymbol{K} - \lambda_i \boldsymbol{M}]\varphi = 0 \qquad 3.15$$

This is a set of algebraic equations. Solving the Eq. 3.15 for φ, a vector denoted by φ_i can then be obtained. This vector corresponding to the ith eigenvalues λ_i is called the ith *eigenvector* that satisfies the following equation:

$$[\boldsymbol{K} - \lambda_i \boldsymbol{M}]\varphi_i = 0 \qquad 3.16$$

An eigenvector φ_i corresponds to a *vibration mode* that gives the shape of the vibrating structure of the ith mode. Therefore, analysis of the eigenvalues equation also gives very important information on possible vibration modes experienced by the structure when it undergoes a free vibration and can also be used to determine the steady state response modal analysis. Vibration modes of a structure are therefore another important characteristic of the structure.

Mathematically, the eigenvectors can be used to construct the displacement fields. Using a few of the lowest modes, one can obtain very accurate results for many engineering

problems. Modal analysis techniques have been developed to take advantage of these properties of natural modes.

In Eq. 3.13(b), since the mass matrix **M** is symmetric positive definite and the stiffness matrix **K** is symmetric and either positive or positive semi-definite, the eigenvalues are all real and either positive or zero. It is possible that some of the eigenvalues may coincide.

Chapter Four

Modelling and Finite Element Analysis

4.1. Introduction

Computer aided design and analysis has great significance to study vehicles structure property and improve the vehicle structure. The vehicle structure strength and dynamic property can easily be found using this tool. Simulation is useful to study and examine the behaviour of a body under different operating scenarios without the need of physical test of the actual. Further, simulation results can be used to demonstrate and communicate the reliability of the vehicle to the authority approving the certification. This procedure will have an advantage both to the manufacturers to have confidence on what they do (provided they fabricate the body as per the design) and the country at large that benefits from reliable locally built vehicles.

4.2. Bus specification

The following table shows bus specification used in the analysis. The factory uses DAEWOO trucks to build the bus.

Table 4.1 Bus specification

Overall Dimension	Width = 2.5 m Length = 11.5 m Height = 2.8 m
Capacity	61 Passengers
Wheel Drive	4X2
Wheel Base	6.1 m
Maximum Speed	100 km/hr
Fuel Tanker Capacity	250 L
Engine type	Diesel, Inline 6 cylinder
Maximum Torque	90 kg.m / 1200 rpm
Maximum Horse Power	240 Hp / 2300 rpm

4.3. Modelling of bus structure

The modeling of the bus structure is made with data collected from Ultimate Motors bus body builder. Before measuring of the structure, drawing of the bus structure is made. This helps for easy placement of the measured length on the corresponding members on the drawing. During the data collection of the structure, all members of the structure are measured with length measuring tape. The modelling of the bus structure is made with CATIA V5R16 software. The bus structure is made with steel beams of rectangular hollow section (RHS), with different size. The sizes of RHS used are RHS 70X50X3 mm, 50X30X3 mm and 40X40X2.5mm. This bus has a capacity of 61 passengers.

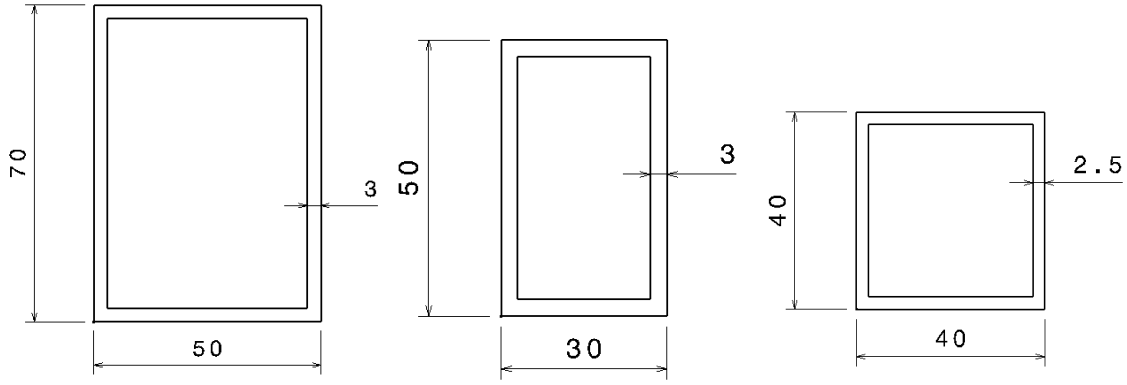

Figure 4.1 RHS profiles employed (dimensions in mm)

RHS (Rectangular Hollow Section) steel is used to build the bus structure. The steel used in this analysis is DIN standard of St 37.2 with material property given in table 4.2.

Table 4.2 Material property of RHS used

Material Property	Structural steel
Tensile yield strength	230 MPa
Compressive yield strength	230 MPa
Tensile ultimate strength	440 MPa
Density	7850 kg/m^3
Young's modulus	200 GPa
Elongation	26%

Table 4.3 Overall dimension of bus model

Length of model	11.5m
Width of model	2.5m
Height of model	2.8m

Before going to the finite element analysis, the modeling of the bus structure should be made. The figure given below shows the model of the bus made in CATIA V5R16 window. The structure parts are made with the real profiles and dimension used in the factory.

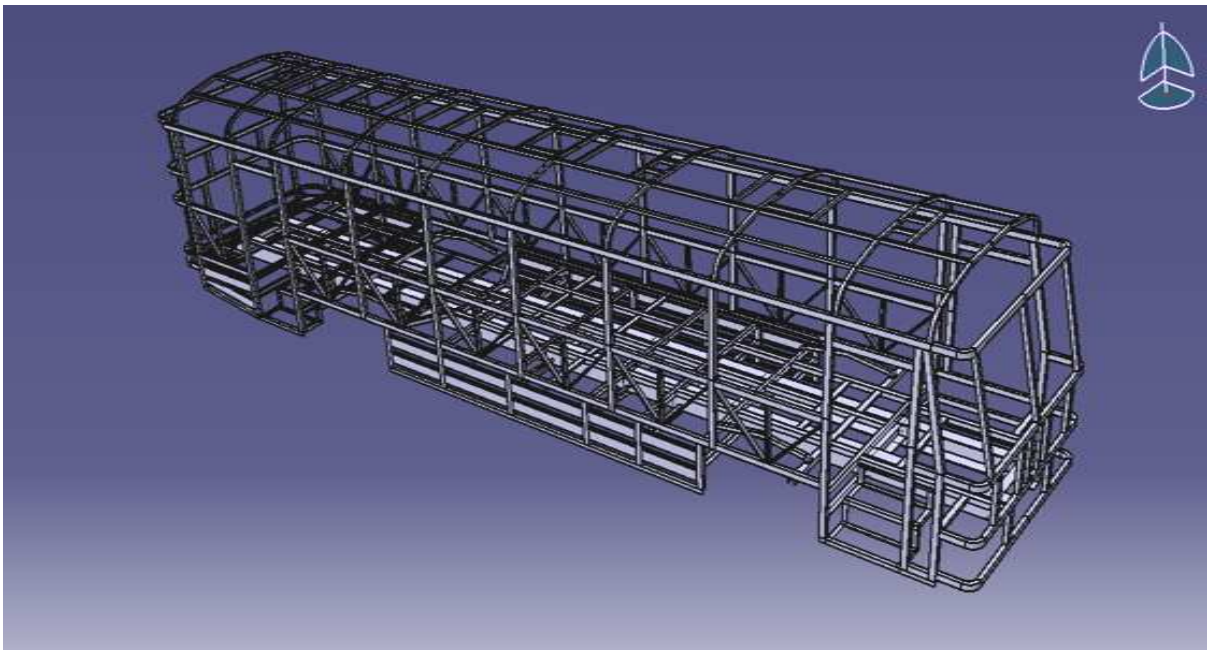

Figure 4.2 CAD model of bus structure

4.4. Finite element modelling of the bus structure

Finite element modelling is made with ANSYS 12 Workbench. The structure model made by CATIA V5R16 software is imported to ANSYS 12 workbench. In order to import the CATIA made model to ANSYS 12 window, both softwares run at the same time. The model in CATIA is opened. Then with the import option found in ANSYS workbench, the modelling is imported. Figure 4.2 shows the model of the bus structure in ANSYS workbench window.

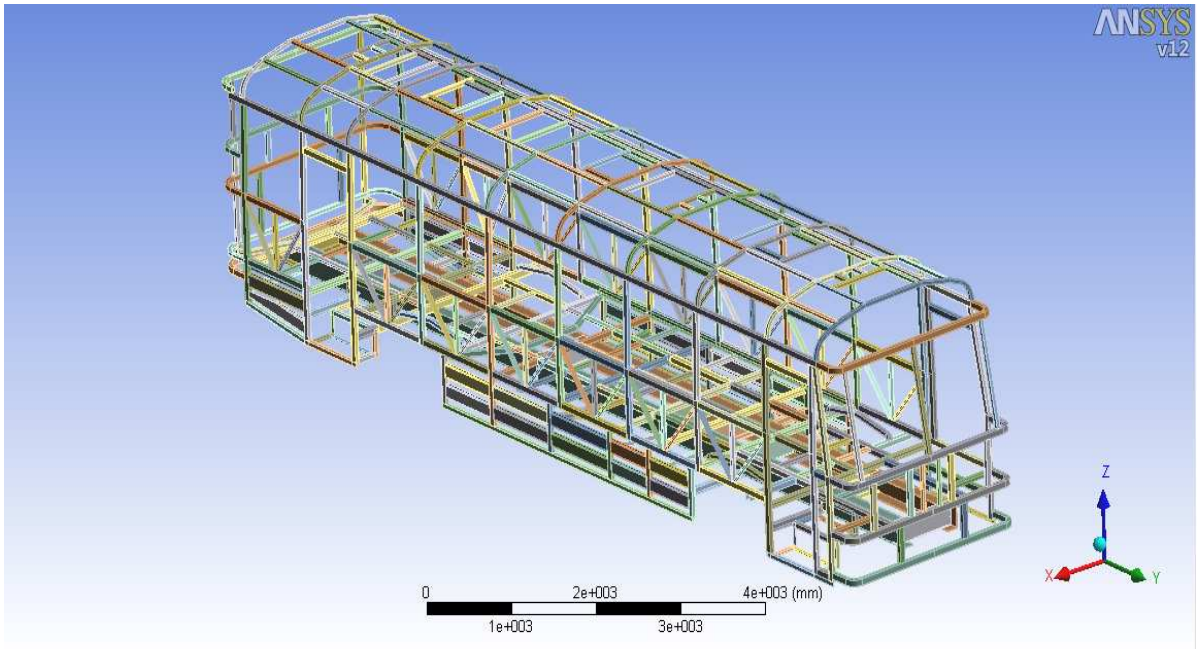

Figure 4.3 Imported model of bus to ANSYS 12 window

The imported model to ANSYS window has different colour from the CAD model because the ANSYS window recognizes each assembled part and assigns its own colour to individual parts of the structure.

4.5. Consideration of welding effect in finite element modelling of the structure

The model constitutes assemblies of individual members to form the whole structure. When the model is imported in to ANSYS 12 workbench, the ANSYS 12 workbench automatically recognizes the members in contact. The contact surfaces in reality are the places where welds are found. But to in incorporate the weld effects in to the analysis, we need to use ANSYS 12 workbench weld representative element. Therefore, in ANSYS 12 workbench, there are two ways of considering welded assemblies. The first one is contact element where it is used when we have a solid model. The other one called spot-weld connection is used when we have model of surface bodies assembled together [18]. The model in this analysis is a solid model. Therefore, contact element of type CONTA 174 is used.

The assumption in ANSYS 12 workbench is that contact elements transfer structural loads and structural effects between solid body parts. Therefore they are used for stress, displacement, frequency, strain, and solutions.

4.6. Finite element meshing of the bus

Finite element meshing is made with ANSYS 12 workbench. Meshing is an integral part of the computer-aided engineering (CAE) simulation process. The mesh influences the accuracy, convergence and speed of the solution. Furthermore, the time it takes to create a mesh model is often a significant portion of the time it takes to get results from a CAE solution.

Tetrahedral mesh elements are used in meshing of the bus structure. In ANSYS 12 Workbench, Tetra mesh method provides:

- Support for 3D inflation
- Built-in growth and smoothness control. The mesher will try to create a smooth size variation based on the specified growth factor.

A tetrahedron element is 3-D solid element which has 4 triangle faces and 6 triangle cross-sections. For this case, SOLID 186 elements are used to mesh the bus body structure.

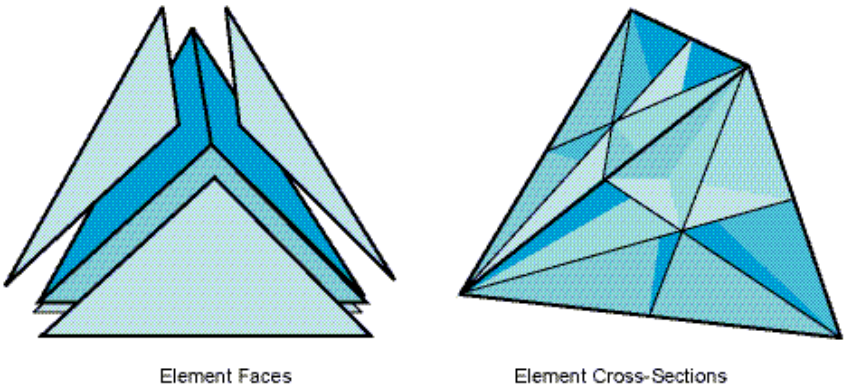

Figure 4.4 Tetrahedron element

As shown below, each tetrahedron cross-section is constructed by passing a plane through one of the edges and the closest point on the straight line containing the opposite edge. (Midside nodes, if any, are ignored.)

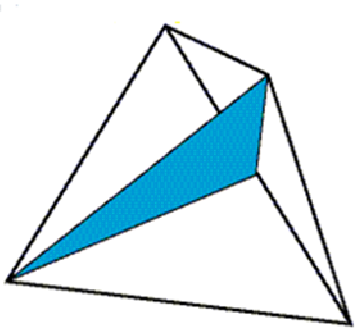

a

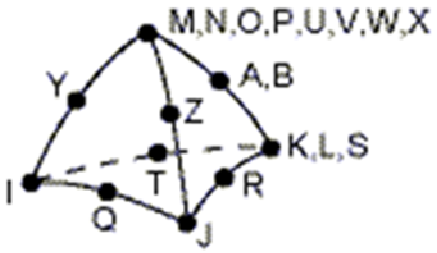

b

Figure 4.5 a) Tetrahedron element cross section construction b) SOLID186 Structural solid geometry (Tetrahedral Element)

The CAD model is an assembly of *370* individual parts and shown in figure 4.6. The finite element model consists of *207,046* nodes and *36,071* elements.

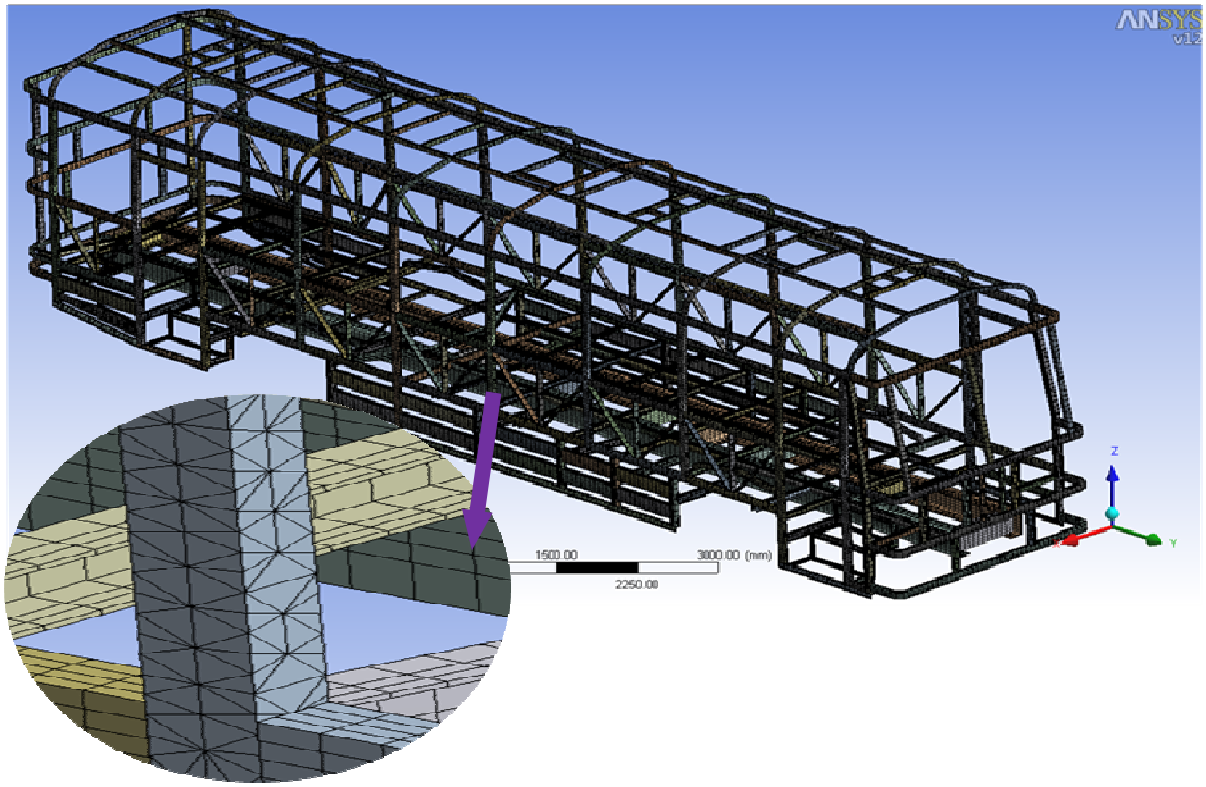

Figure 4.6 Finite element model mesh of the bus

4.7. Inputs for Finite Element Analysis

The inputs for the finite element analysis are all the loads carried by the bus. This loads carried by the bus during operation are self weight of bus, passenger weight, luggage, engine weight, fuel weight and extra tyre weight. There are different loading cases that act on the bus structure. But the two main loading cases are bending load due to the weight and torsional stiffness due to the relative vertical movement of the wheels. When analysing the total weight (self weight of bus, passenger weight, luggage, engine weight, fuel weight), the displacement in vertical direction at the nodes of the wheels is constrained. Therefore, weight of bus is the reaction force.

As shown in figure 4.7, all the loads considered are applied on the structure. The dark black arrows indicate the places of the four nodes where the wheel of the bus structure is mounted. The applied loads are indicated by red colour. The loads on the bed of structure are lumped and placed on the respective nodes. The luggage weight carried on the bus structure is distributed on the roof section.

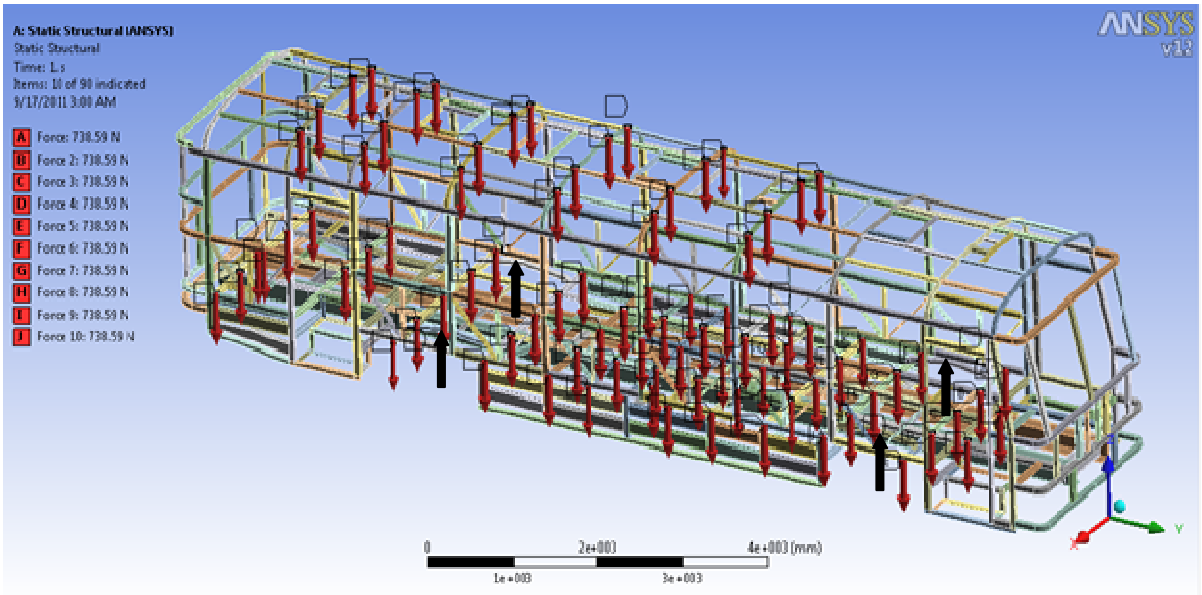

Figure 4.7 Bus structure load applied

When analysing the torsional stiffness, the rear wheels and front left wheel displacement in vertical direction is zero. But the front right wheel displacement is given a value of 100mm used to act twisting moment on the structure.

Loads applied to find the torsional stiffness are passenger weight, weight of individual seat, weight of engine, self weight of the structure, weight of luggage and fuel tank.

Self weight of the bus taken from the result of the reaction force calculated from the static analysis of the structure to be 2999.29 kg.

Table 4.4 Loads applied on the structure

No.	Component	Amount in number	Average Individual mass (kg)	Total mass (kg)	Total weight (N)
1	Passenger	61	65	3,965	38,896.65
2	Seat	61	10.29	627.69	6,157.64
3	Luggage on Roof	-	1200	1200	11,772
4	Luggage on rear and side compartment	-	200	200	1,962
5	Self weight of structure	-	2999.29	2999.29	29,423.03
6	Fuel tank	-	250	250	2,452.5
7	Engine	-	900	900	8,829
Total sum of weight				10,141.98	99492.32

4.8. Boundary conditions used in the analysis

The boundary condition used in the analysis is different according to the operating conditions of the bus. The two major loads considered are bending load and torsional stiffness.
The bending load case is used to demonstrate the behaviour of the bus while it is travelling on the standard (smooth) road.

During the bending loading case the main loads that are considered are passenger weight, seat weight, luggage weight and engine weight and self weight of the bus which is taken into consideration by applying gravity as inertial load which is gravitation acceleration i.e. 9.81 m/s^2. The passenger weight together with seat weight is acted as a lumped mass. The point of application is on the nodes of the passenger seat. The luggage is assumed to be on the roof serves as a load bearing structure in addition to providing protection. Beside, the bus has compartment on the rear side and right side which is used to carry luggage.

During the torsional moment case the loads considered are passenger weight, seat weight, luggage weight, fuel tank weight and engine weight and self weight of the bus structure which is taken in to consideration by applying gravity as inertial load which is gravitational acceleration i.e. 9.81 m/s^2. The passenger weight together with seat weight is acted as a lumped mass on the respective nodes of the passenger seats.
Torsional moment helps to demonstrate the structure behaviour while the bus is travelling on none standard or bumpy road.
This loading case is same as bending load case except that in this case the front right side wheel vertical displacement (*z* direction) is given a *100 mm* value to create twisting moment on the bus structure. Figure 4.8 (a) shows the boundary condition to be applied in torsional moment case. Figure 4.8 (b) shows the bumpy road height.

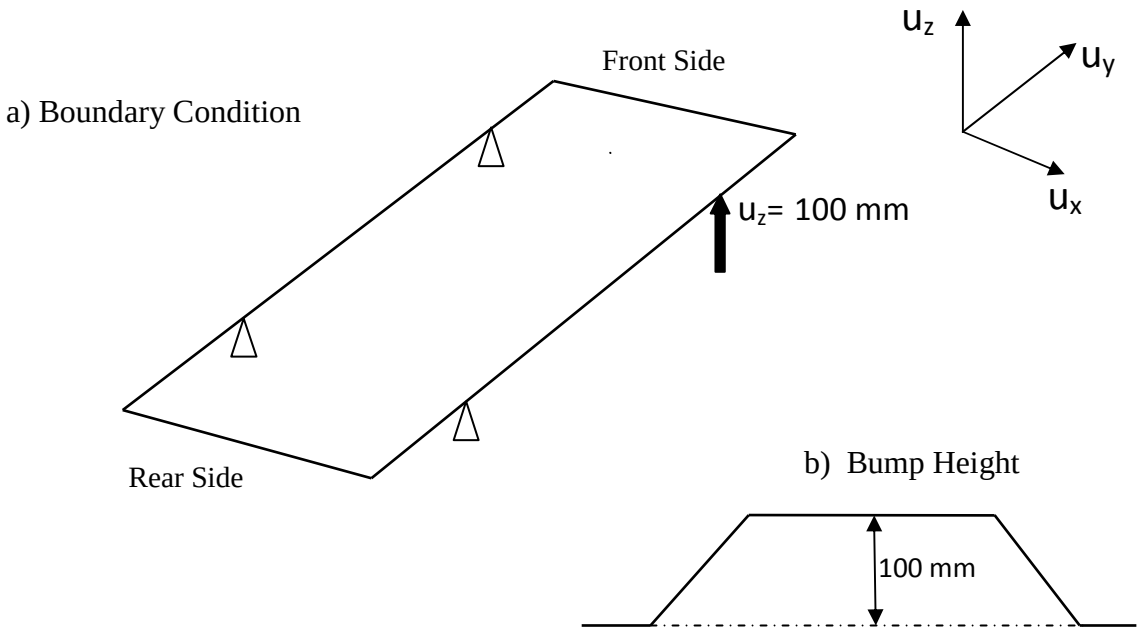

Figure 4.8 Boundary condition during torsional moment case

4.9. Results and discussion of static structure analysis

The static analysis solves the static equations of the problem, i.e., the equations resulting setting all time derivatives in Eq. 3.10 equal to zero. Doing so gives Eq. 4.1

$$\boldsymbol{KD = F} \qquad 4.1$$

Where ***K*** is the stiffness, ***D*** is the displacement and ***F*** is load vector

It demonstrates the bus traveling on standard road (smooth road). The deformed configuration of the system under the applied static loads is then computed. Static analysis is carried out on the model to get the weight of the bus structure, stress, deformation.

The static analysis is performed for two travelling road conditions. The first one, bending load case, is used to demonstrate the bus travelling on a smooth road and extract the deformation and stress values. The second case, twisting moment case, is used to find the values of stress and deformation while the wheels face bumpy road. In this case, the front right side wheel is subjected to bump.

4.9.1. Bending load case

- **Boundary condition for bending loading case**

The boundary condition for such loading case is both front and the rear wheels (left and right side wheel) are to be constrained in the three principal directions at the nodes and the displacements in *x, y,* and *z* directions are set as zero. Applying these boundary conditions on the finite element model, the calculate stresses and displacements on the critical members of the structure, obtained as an output from ANSYS work bench are summarized in table 4.5.

Analysis result

Table 4.5 Stress and displacements values in bending load case of original structure

Object Name	*Vertical Displacement*	*Normal Stress*	*Equivalent Stress*	*Total Displacement*
Minimum	0.1818 mm	0.4139 MPa	0.00501 MPa	0 mm
Maximum	-5.833 mm	90.36 MPa	122.57 MPa	5.73 mm
Minimum occurs on	Part 157	Part 20	Part 145	Part 37
Maximum occurs on	Part 314	Part 20	Part 23	Part 315

Table 4.5 shows the results of bending load. The negative sign in the displacement values show the direction of the displacement. Maximum value of displacement is 5.883 in the downward direction where as the minimum is 0.1818 in the upward direction. In addition, the maximum normal stress is 90.36 MPa and the minimum is 0.4139.

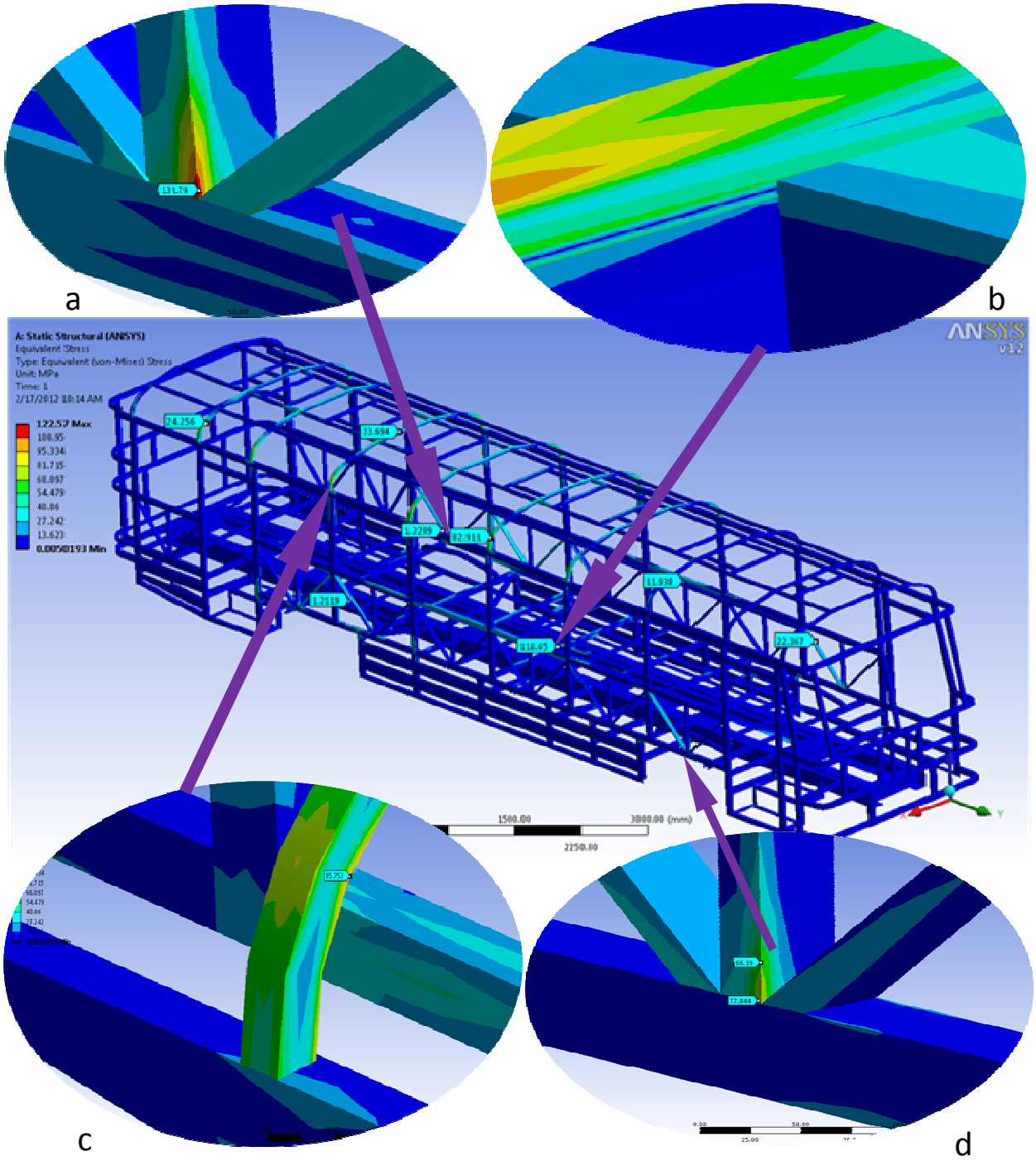

Figure 4.9 Equivalent stresses (Von miss stress) of original structure in bending load case

Fig. 4.9(a) shows the vertical member located around the rear wheel has maximum stress values. We can see that the maximum equivalent stress is 122 MPa which is lower than the yield stress (230 MPa) of the material which the structure is made. From the contour plot of

the figure, we see that most of the structure members are subjected to equivalent stress below 30 MPa. From figure 4.9(c), the roof members are subjected to stresses value of 83 MPa. Particularly, the periphery of the roof sections are subjected to relatively higher stress values.

The members located at the middle section are subjected to higher stress values; Figure 4.9(b) shows this in detail. The stress at this area reaches up to 95 MPa.

Overall look on the analysis result depicts that diagonal members of the structure are subjected to stress lower stress values. This shows that still we can work on the design modification of the bus structure. This proofs that largely the load is transferred through the vertical members.

Figure 4.9(d) shows details of the bus structure near the wheels. In this figure, the diagonals and vertical members are shown. These members of the structure which are close to the wheel are subjected to stress values which is relatively higher than other neighbouring members. This is due to the loads which are applied near the wheels and forced to be greater in value.

Figure 4.10 shows the contour plot of normal stress values of the structure. Here the diagonal members are subjected to lower normal stress values below 4 MPa, Figure 4.10(c) shows in detail. Figure 4.10(b) shows the periphery of the roof subjected to stress value of 80MPa. Figure 4.10(d) shows the front roof member in detail and depicts lower stresses occurs at that area.

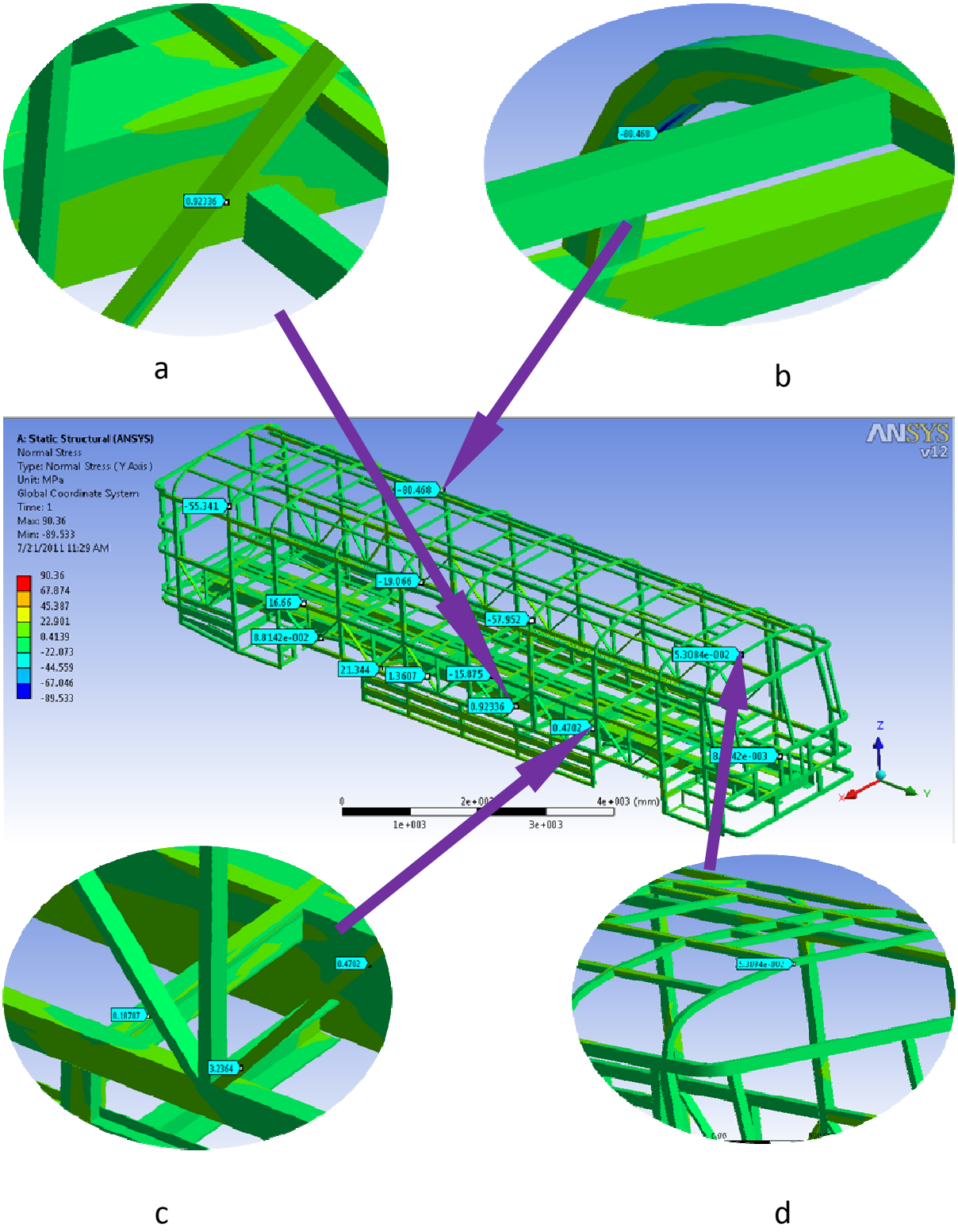

Figure 4.10 Normal stresses of original structure in bending load case

Figure 4.11 shows the contour plot of the total displacements of the structure. The front and rear sides of the structure experience lower displacement (below 0.95451mm) where as the middle section of the bus has deformation value between 1.909 mm and 3.8181 mm. Maximum displacements occurs at the middle section of roof structure with value of 5.7 mm. The directional displacement, Figure 4.12 shows this displacement is in downward direction.

Figure 4.11(a) shows that displacement of the floor is very low at the rear, this case holds for the front floor areas too.

The displacement values of the roof section are shown in detail in figure 4.11(b). Maximum displacement values occur at the middle section of the roof structure. It has a value of 5.7 mm. From figure 4.11(c), the rear area door is subjected to higher displacement than the corresponding left side of the bus. This is because of the unsymmetrical feature of the left and right side. The unsymmetrical feature is due to the rear side passenger door opening, so absence of diagonal and vertical members. As shown in the figure above the right side which is equipped with the passenger door opening, there is an excessive displacement due to the removal of the stiffener components from the door area.

Diagonal stiffeners of the original bus structure have lower displacement values. Figure 4.11(d) shows the diagonal members displacement.

The bottom rear section of the bus structure is subjected to lower displacement values. This is reasonable because most of the load carried by the bus lies at the middle section. This holds true for the front section of the bus.

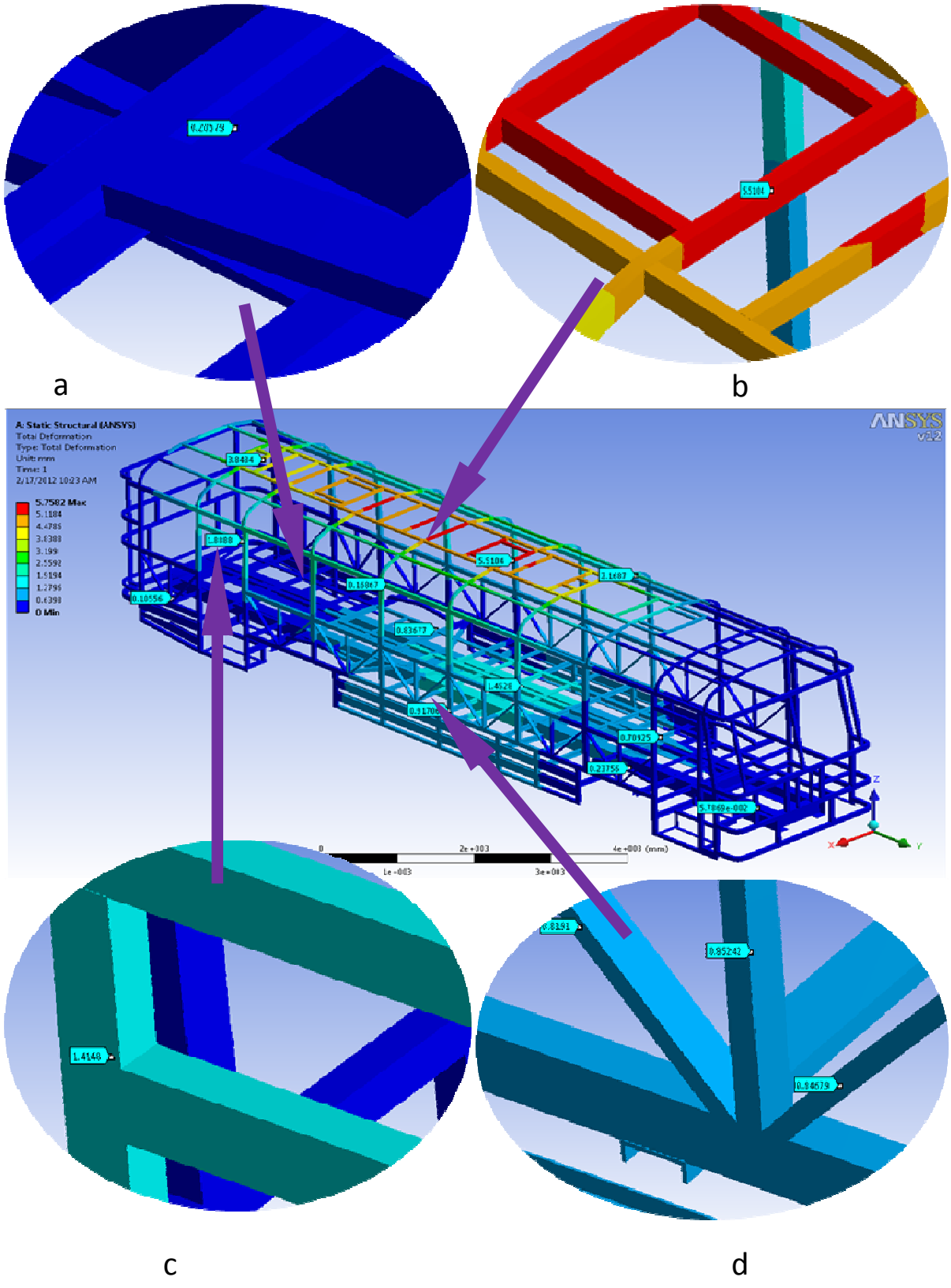

Figure 4.11 Total displacements of original structure in bending load case

The displacement in z-direction is shown below. From the figure, the highest displacement occurs on the roof of the structure with a value of 5.8mm in the downward direction. The rear and front members are subjected to an upward deformation where as the middle part of the structure is deflected in the down ward direction which can be seen from the Figure 4.12 shown below. This occurs because most of the loads carried by the bus are between the front and rear wheels. This displacement of the members near the wheels is relatively very low because it is the place where the structure is constrained to have zero displacement. The contour plot showed with red colour shows these values.

Figure 4.12(d) shows how the same colour coding has different results that are from -0.4mm to 2mm. The wheel node has a zero displacement because it is constrained there. So the neighbouring members of the wheel have much lower deformation.

Figure 4.12 (a) shows the displacement values of members near the wheel areas. The figure shows the horizontal and verticals. It has much lower displacement. This is due to the availability constrains near that areas.

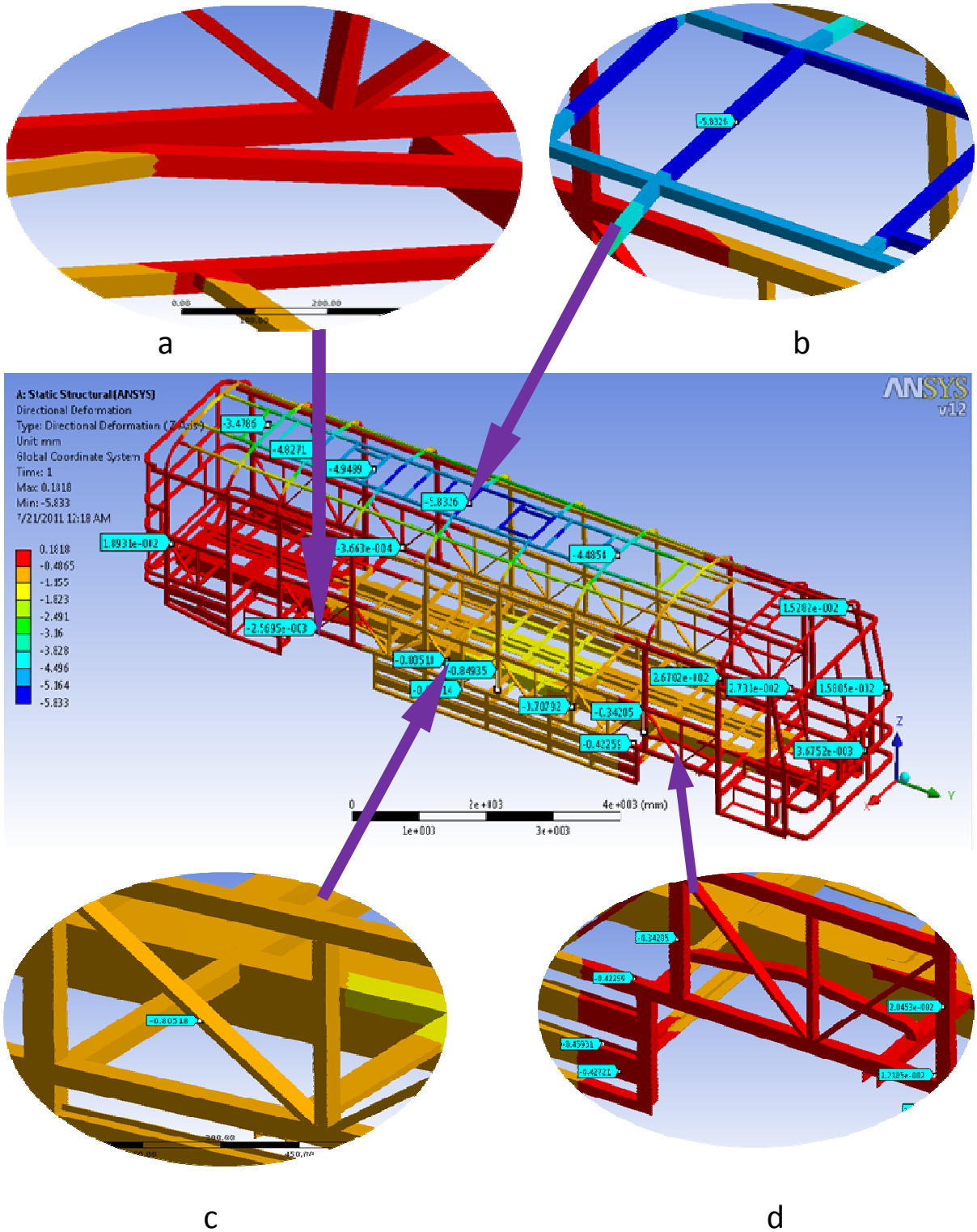

Figure 4.12 Vertical displacements (Z-Axis) of original structure in bending load case

Displacement of the members near the wheels is relatively very low because it is the place where the structure is constrained to have zero displacement. The contour plot with red colour shows these values.

4.9.2. Torsional Moment case

During the torsional moment case the loads considered are passenger weight, seat weight, luggage weight, fuel tank weight and engine weight and self weight of the bus structure which is taken in to consideration by applying gravity as inertial load which is gravitational acceleration i.e. 9.81 m/s^2. The passenger weight together with seat weight is acted as a lumped mass on the respective nodes of the passenger seats.

Twisting moment helps to demonstrate the structure behaviour while the bus is travelling on none standard or bumpy road. Two separate torsional moment cases are considered.

The first case is when only one wheel is subjected to a bump. The other case when diagonally opposite wheels are subjected to bump.

- **Boundary condition for torsional moment case 1**

This loading case is same as bending load case except that in this case the front right side wheel vertical displacement (u_z) is given a *100 mm* value to create twisting moment on the bus structure.

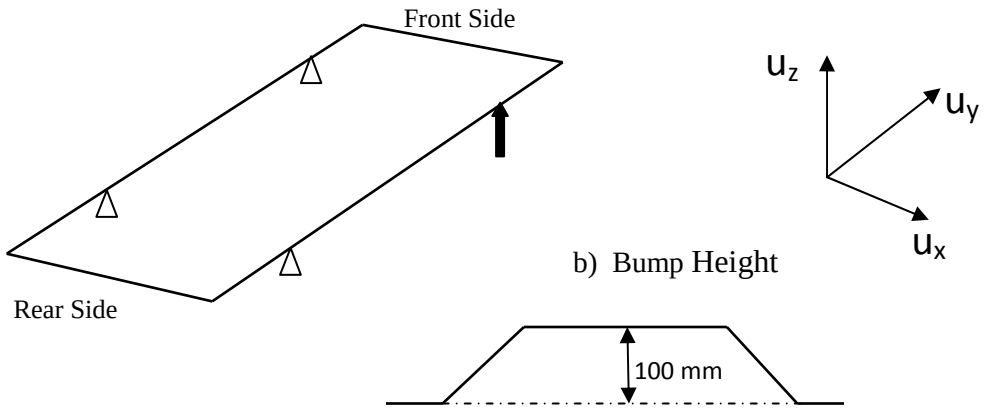

Figure 4.13. Boundary condition during torsional moment case 1

Figure 4.13 (a) shows the boundary condition to be applied in torsional moment case 1. Figure 4.13 (b) shows the bumpy road height.

Results of the analysis

The following table 4.6 summarise the stresses and deformation values on the structure members.

Table 4.6 Stress and displacement Values of original structure in twisting moment Case

Object Name	*Vertical Displacement*	*Normal Stress*	*Equivalent Stress*	*Total Displacement*
Minimum	-5.39 mm	9.76 MPa	0.01 MPa	0 mm
Maximum	13.77 mm	92.131 MPa	141.67 MPa	13.8 mm
Minimum occurs on	Part 324	Part 20	Part 232	Part 62
Maximum occurs on	Part 79	Part 345	Part 106	Part 50

Table 4.6 shows the displacement result in negative and positive values. The negative value it to mean the displacement values in down ward direction where as the positive one is to mean the displacement value on up ward direction.

Figure 4.14 shows the contour plot of total deformation of the structure after applying the loads and boundary conditions. A relatively higher displacement occurs at the point of application of the displacement (front left side of the structure), figure 4.14 (b) shows this in detail.

Figure 4.14(c) depicts displacement of members near rear door. Here again the rear door top left corner is deformed much higher than the corresponding left side of the bus members. This is due to the absence of horizontal, vertical and diagonal members of the structure for the door opening.

Figure 4.14(a) shows the displacement of roof member has value of 8.8 mm, which is higher than the bending load case displacement of the roof. The members near the wheel which face the bump are subjected relatively higher displacement values than the neighbouring members.

Figure 4.15 shows the directions of displacement for the members. The rear members of the structure are subjected to a downward displacement. Since the front right side is lifted, the rear structure tends to go downward direction, the rear load applied also have great contribution for this downward displacement. The rear load includes passengers, luggage and extra tire weight.

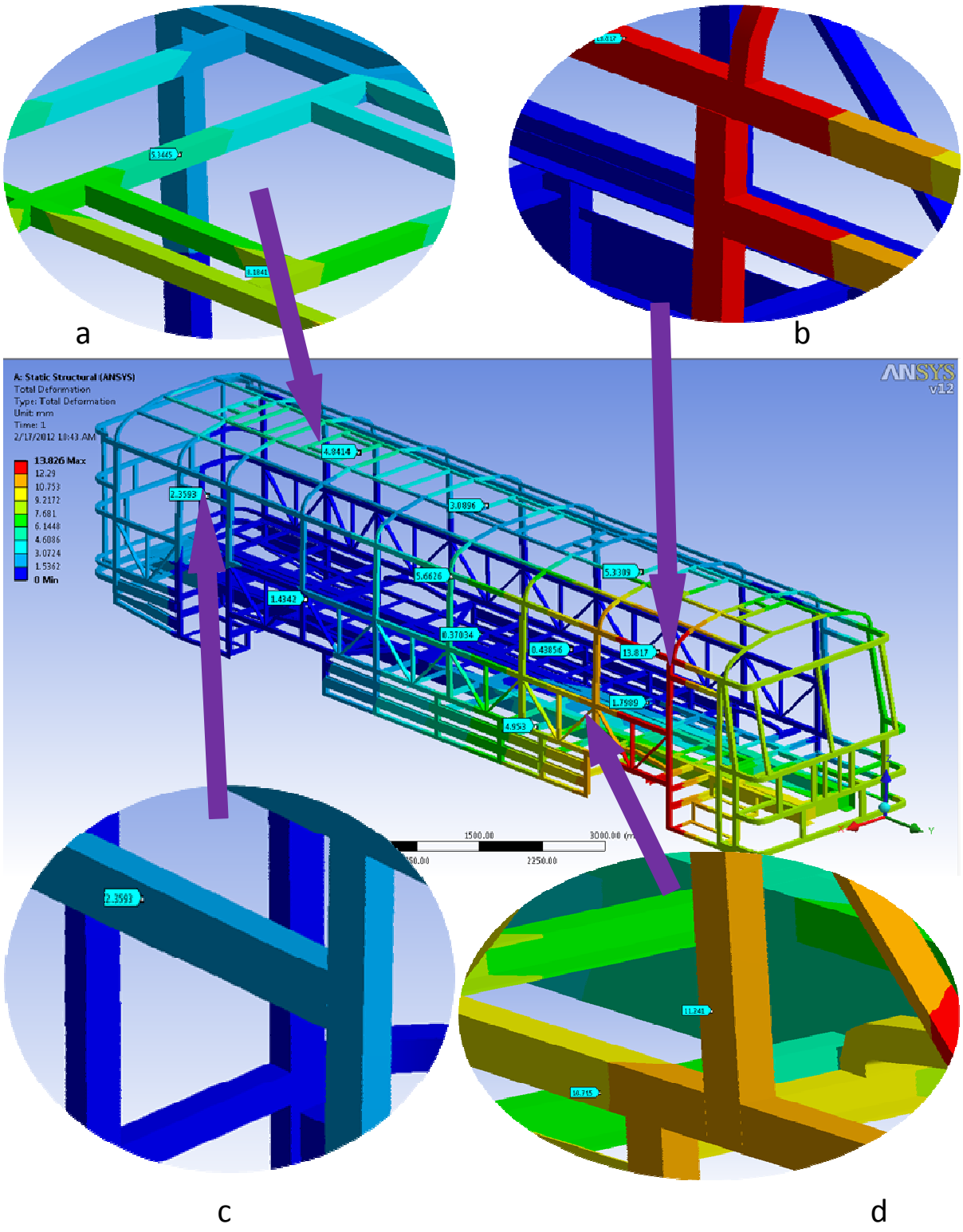

Figure 4.14 Total displacement of original structure in twisting moment case

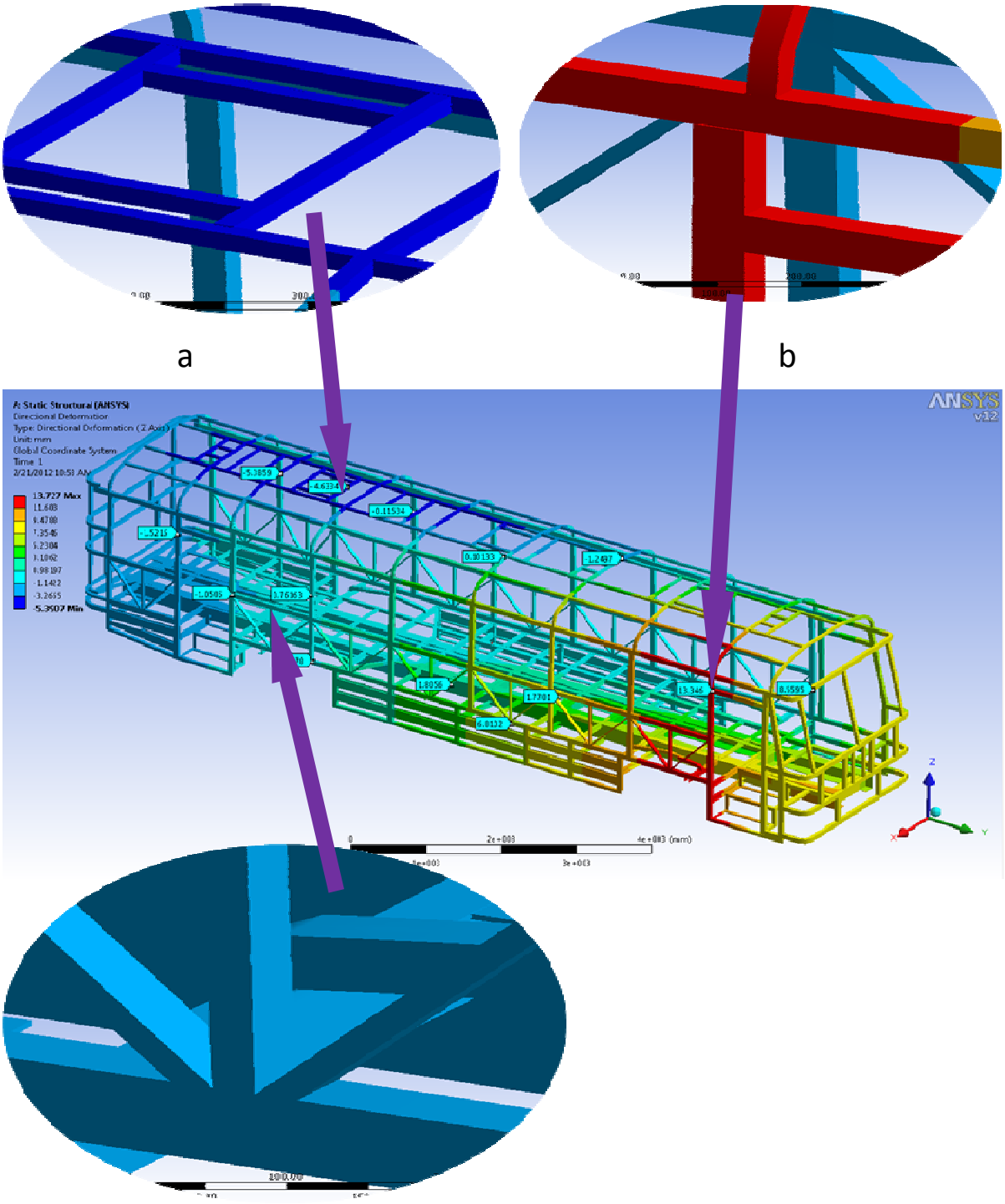

Figure 4.15 Directional displacements (z-direction) of original structure in twisting moment case

The figure above (figure 4.15) shows the vertical displacement (z-direction) of the structure. A relatively lower displacement occurs at the rear side of the bus structure. The front right side, front passenger door left top corner experience a higher displacement. This is due to the absence of horizontal and diagonal stiffener for the opening of the front passenger door.

Figure 4.16 shows contour plot of equivalent stresses on the structure. It can be seen from the figure that most of the structure members are subjected to equivalent stress values below 31 MPa. Figure 4.16(a) shows rear wheel area vertical member subjected to stress value of 130 MPa. Figure 4.16(b) shows stress values of members near the middle section of the bus structure, from this figure we can see a member subjected to equivalent stress value 102 MPa.

On the other hand, roof members are subjected to relatively higher stress values, figure 4.16 (b) shows a member subjected to stress value of 77 MPa. This occurs because the roof structure is the direct load bearing member, for luggage.

Figure 4.16 shows equivalent stress value of the front door. As it can be seen from the figure, the top left corner of the door is subjected to stress value of 46 MPa. This happens due to the applied bump at the front wheel node which makes the stress of the members grow big. Similarly, the driver door area members are also subjected to stresses of 53 MPa which relatively larger stresses than the neighbouring members.
Contour plot of normal stress figure is shown below (figure 4.17). Figure 4.17 (a) shows that the top periphery of the member is subjected to tensile stress of value 50 MPa and the lower periphery of the member is subjected to compressive stresses of 46 MPa.

The rear structure members are subjected to stress values of below 22 MPa.
The left side top corner of the front door experiences a relatively higher normal stress values because of the direct transmission of the bump to the structure.

The figure below (Figure 4.17) shows the bus side horizontal member top periphery is subjected to negative normal stress (-17 MPa) which indicates the member is in compression. This is true since the middle section of the bus is deformed in down ward direction which pulls the side horizontal members to become compressed.

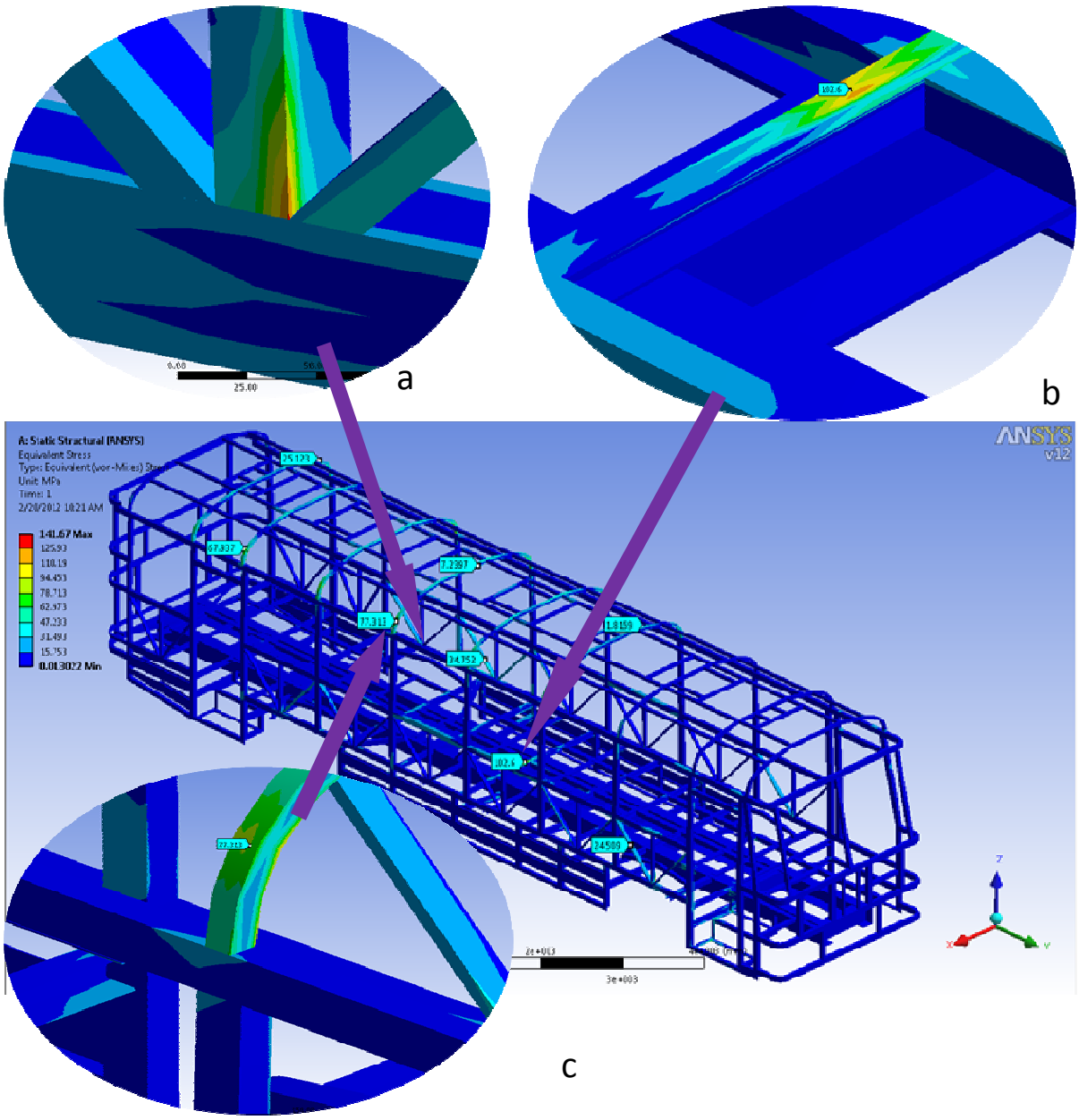

Figure 4.16 Von-Miss Stress of original structure in torsional moment case

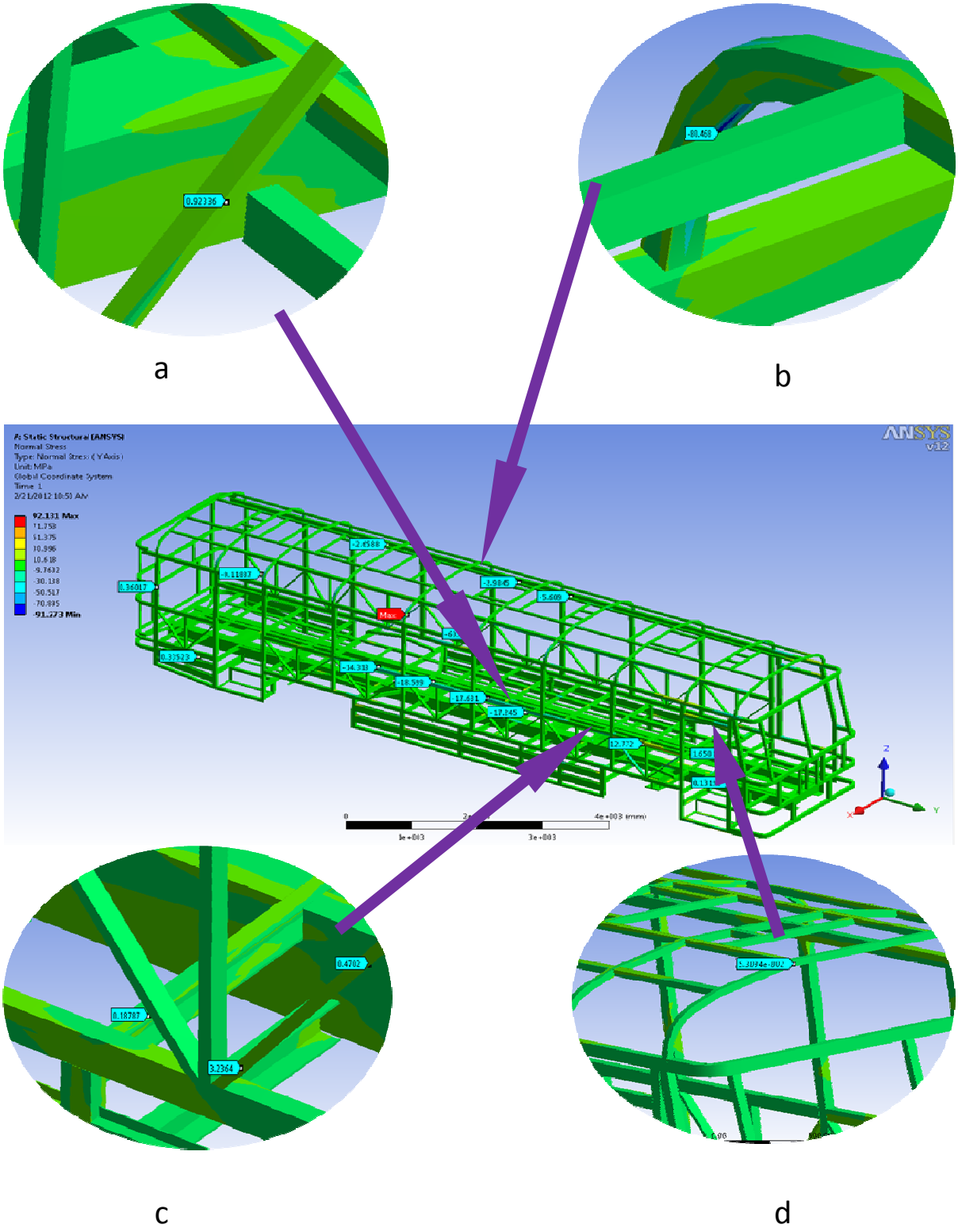

Figure 4.17 Normal Stress (y-direction) of original structure in torsional moment case

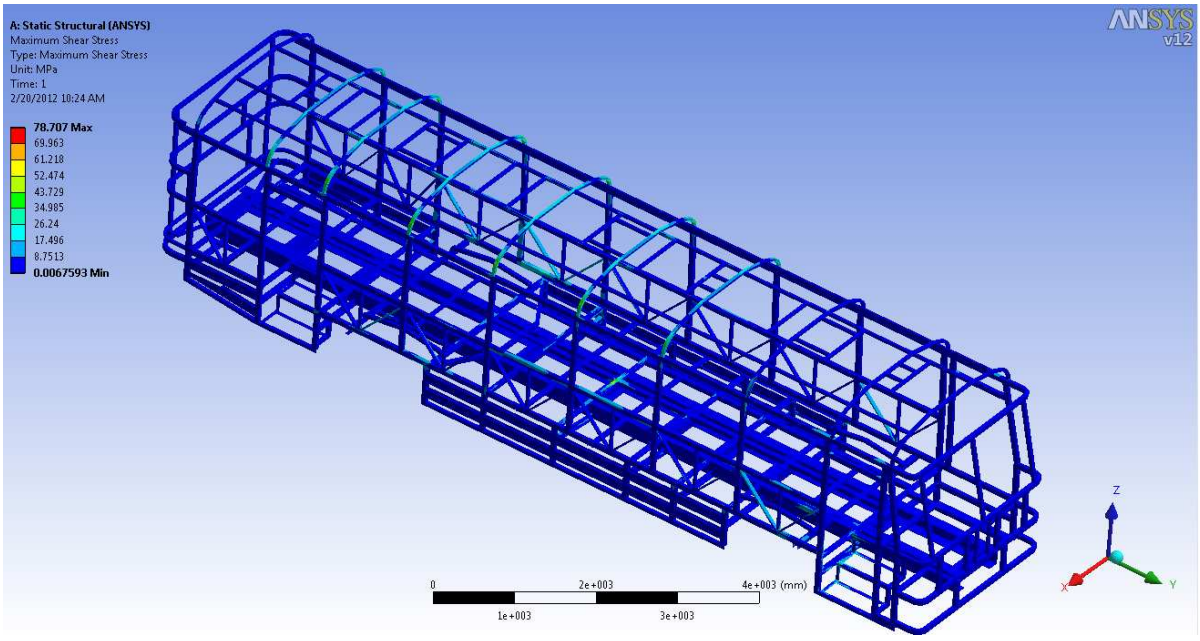

Figure 4.18 Shear stress of original structure in torsional moment case 1

Figure 4.18 shows the shear stress distribution of the bus structure. The maximum shear stress that occurs on the bus structure is 78.7 MPa. This is small compared to the allowable stress of the material. The middle section of the bus has higher values compared to the neighbouring members of the structure.

- **Boundary condition for torsional moment case 2**

  This case is used to simulate the structure response when the diagonally opposite wheels are on bump. The figure below indicates how boundary condition is applied on the structure.

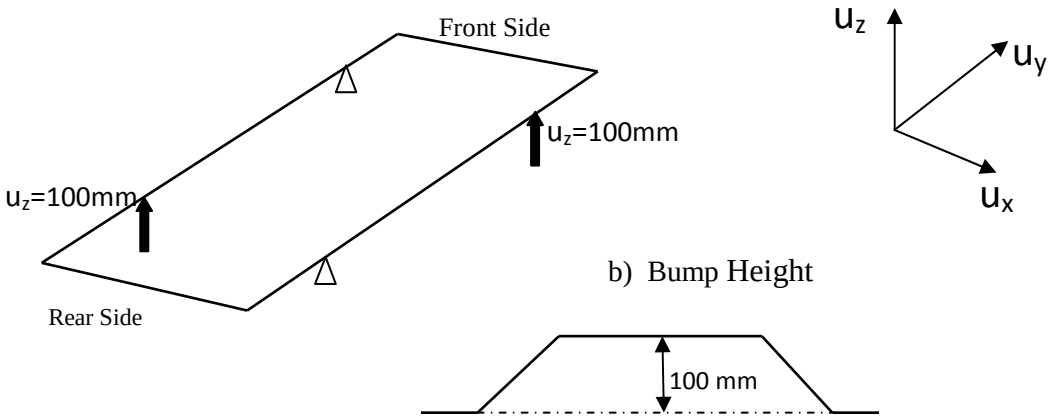

Figure 4.19 Boundary condition during torsional moment case 2

Result of the analysis

The following figure (figure 4.20) shows the total displacement of the structure for torsion moment case 2. As it can be seen from the figure, a maximum displacement occurs near the front right side wheel with value of 15 mm. In addition the rear left side of the structure is also subjected to large stress. This is due to the application of the bump near those areas.

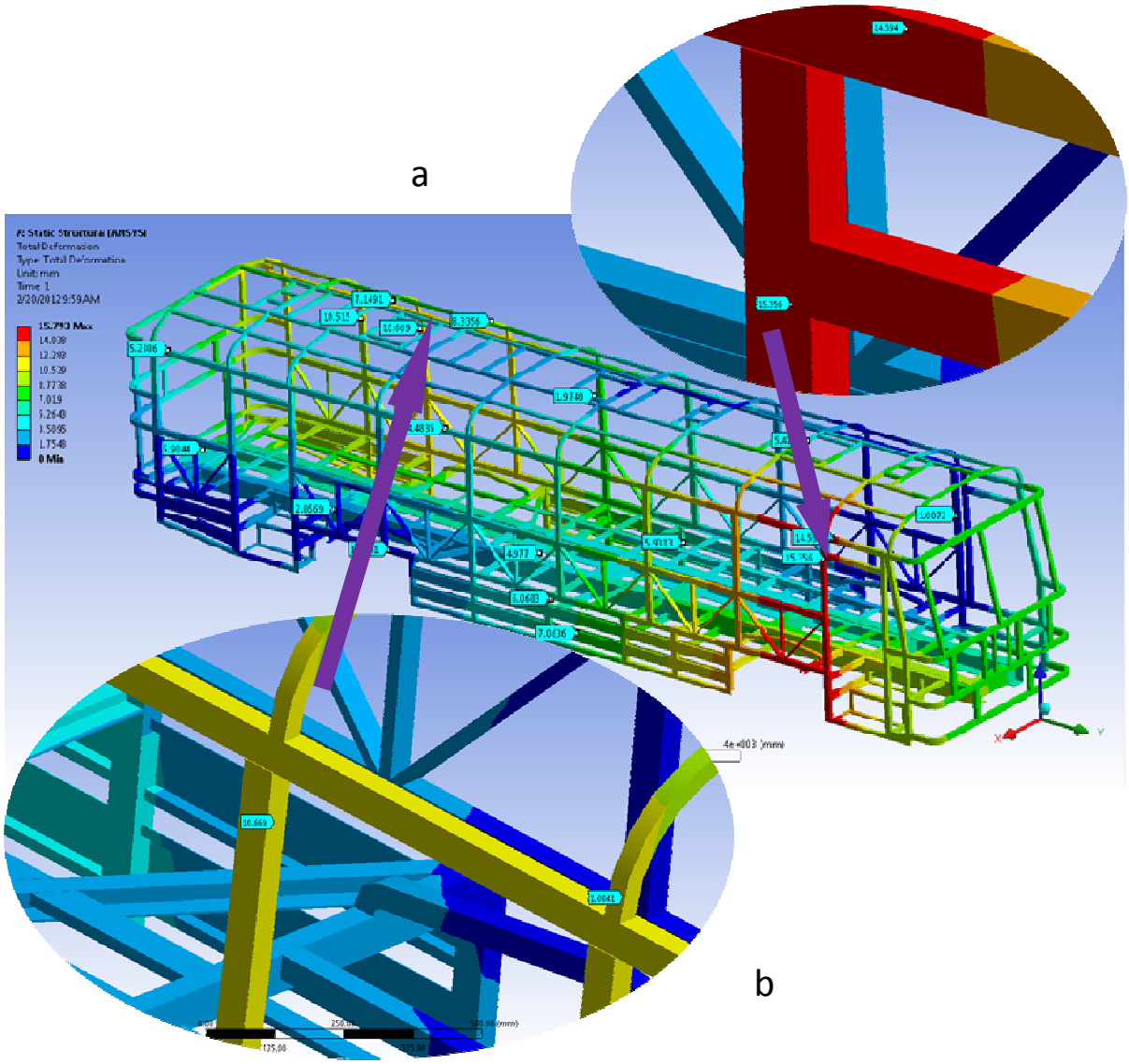

Figure 4.20 Total displacement of the original structure during torsional moment case 2

Figure 4.21 shows contour plot of equivalent stresses on the structure. It can be seen from the figure that most of the structure members are subjected to equivalent stress values below 21 MPa. Figure 4.42 (a) shows rear wheel area vertical member subjected to stress value of 130 MPa. Figure 4.21(b) shows stress values of members near the middle section of the bus structure, from this figure we can see a member subjected to equivalent stress value 102 MPa. Equivalent stress near the front door is shown by figure 4.21(d). As it can be seen from the figure, the top left corner of the door is subjected to stress value of 46 MPa. This happens due to the applied bump at the front wheel node which makes the stress of the members grow big. Similarly, the driver door area members are also subjected to stresses of 53 MPa which relatively larger stresses than the neighbouring members.

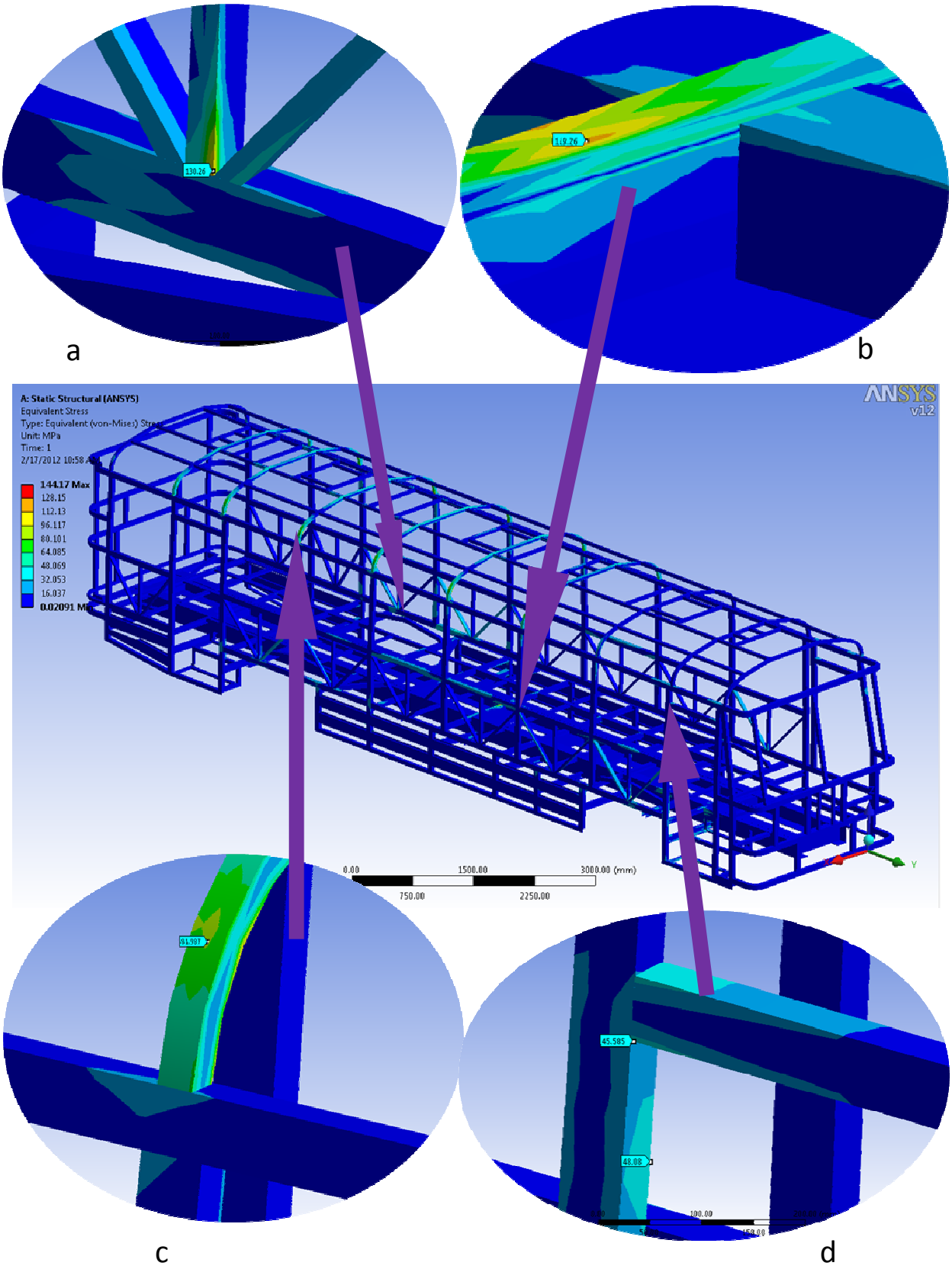

Figure 4.21 Equivalent stress of the original structure during torsional moment case 2

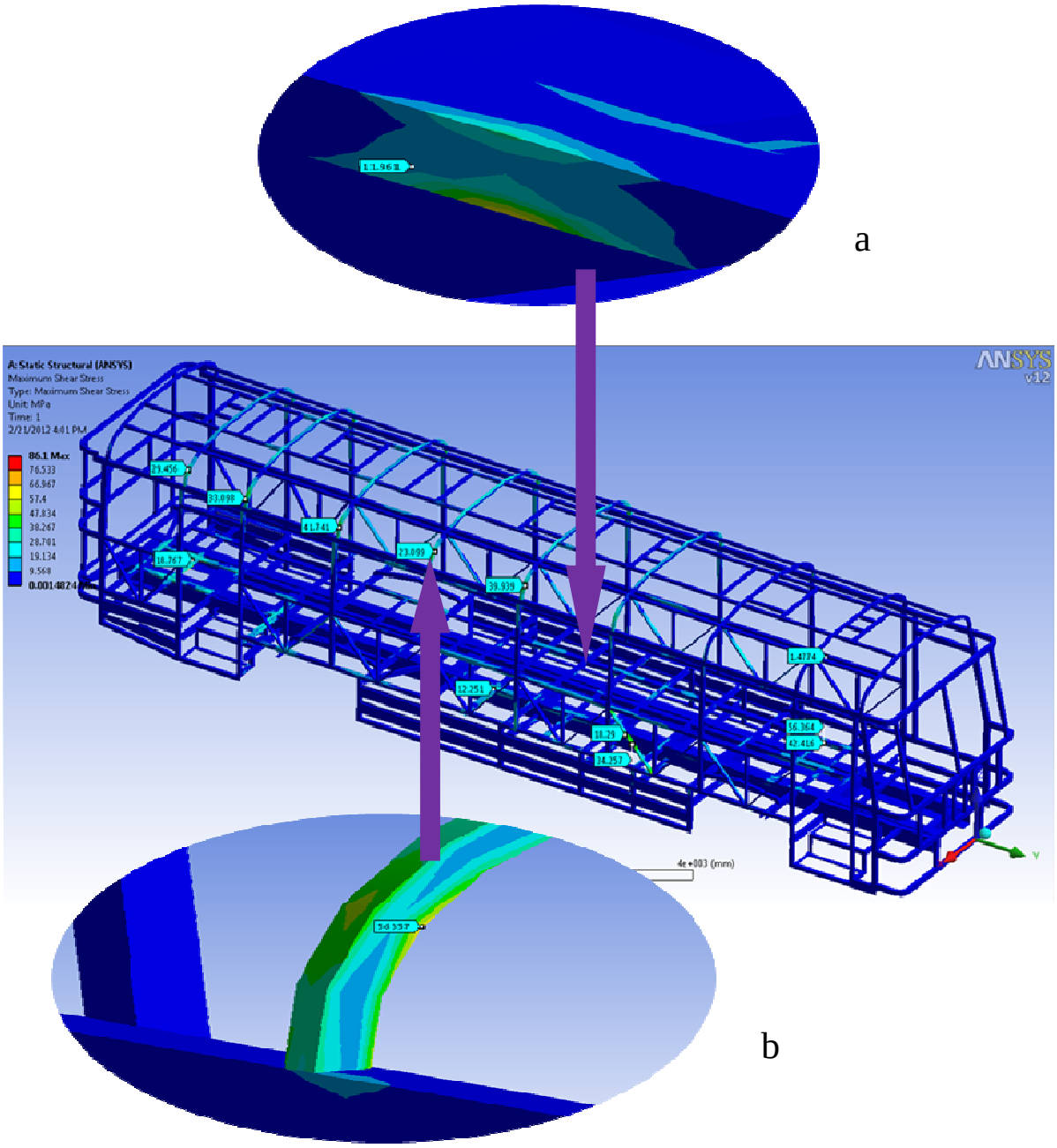

Figure 4.22 Shear stress of the original structure during torsional moment case 2

The above figure shows the shear stress of the bus structure for torsional moment case 2. The detail in figure (a) shows the middle section subjected higher values of shear stresses. The maximum shear stress that occurs is 86.1 MPa. Generally looking on the shear stress distribution of the original structure for torsional moment case 2, the members are subjected small stress of value below 26 MPa.

Therefore, the results of the two cases of torsional moment show the structure is subjected to stress values below the allowable of the material.

4.10. Vibration analysis of original structure

4.10.1. Vibration analysis of bus model

After modelling the bus structure using with CAD, by defining material properties and boundary conditions in ANSYS 12 workbench, the response at selected points of the structure is obtained by performing spectrum analysis when the vehicle moving at *20 km/hr* and *70 km/hr* on class H roads.

A spectrum analysis is one where the results of modal analysis are used with a known spectrum to calculate displacements and stresses in the model. It is mainly used in place of time-history analysis to determine the response of structures to random loading conditions such as earthquakes, road unevenness, wind loads, ocean wave loads, jet engine thrust, rocket motor vibrations and so on.

In this research the analysis is performed using power spectral density (PSD) analysis. A PSD spectrum is a statistical measure of the response of a structure to random dynamic loading conditions. It is a graph of power spectral density versus frequency, where the PSD may be a displacement PSD, velocity PSD, acceleration PSD or force PSD.

Similar to response spectrum analysis random vibration analysis may be single point or multi point. In a single point random vibration analysis, only one PSD spectrum is specified at different points in the model. In the present paper single point response analysis has been used.

The power spectral density (PSD) of random process provides the frequency composition of the data in terms of the spectral density of its mean square value. The track input PSD describes the frequency content of track.

The relation between the PSD and spatial frequency in general is represented as [17]

$$s_{pp}(\Omega) = c_{sp}\Omega^{-N} \qquad 3.17$$

Where $s_{pp}(\Omega) = PSD\ in\ m^2/cycles/m$

$$c_{sp}, N = constants\ depend\ upon\ type\ of\ road$$

$$\Omega = spatial\ frequency\ in\ cycles/m$$

The above relation in terms of actual frequency is given by

$$s_{pp}(f) = \frac{c_{sp}f^{-N}}{V^{1-N}} \qquad 3.18$$

$$s_{pp}(f) = PSd\ of\ displacment$$

$$f = frequency\ in \frac{cycles}{s}$$

$$V = vehicle\ speed\ in\ m/s$$

For ISO road standard of low quality road of Class H, the values of the constants and corresponding equations for plotting road roughness are given by,

$$For\ \Omega \leq {}^{1}/_{2\pi} \qquad s_{pp}(\Omega) = 0.032768(2\pi\Omega)^{-2}$$

$$and$$

$$For\ \Omega > {}^{1}/_{2\pi} \qquad s_{pp}(\Omega) = 0.032768(2\pi\Omega)^{-1.5} \qquad 3.19$$

Using Eq. 3.19, road roughness for Class H road is plotted using MATLAB.

Class H road is considered because it is highly rough road than the other class.

The values of graph (Figure 3.3) are used as input for the dynamic response analysis of the bus structure. These values are imported to ANSYS workbench to work on the random vibration of the bus.

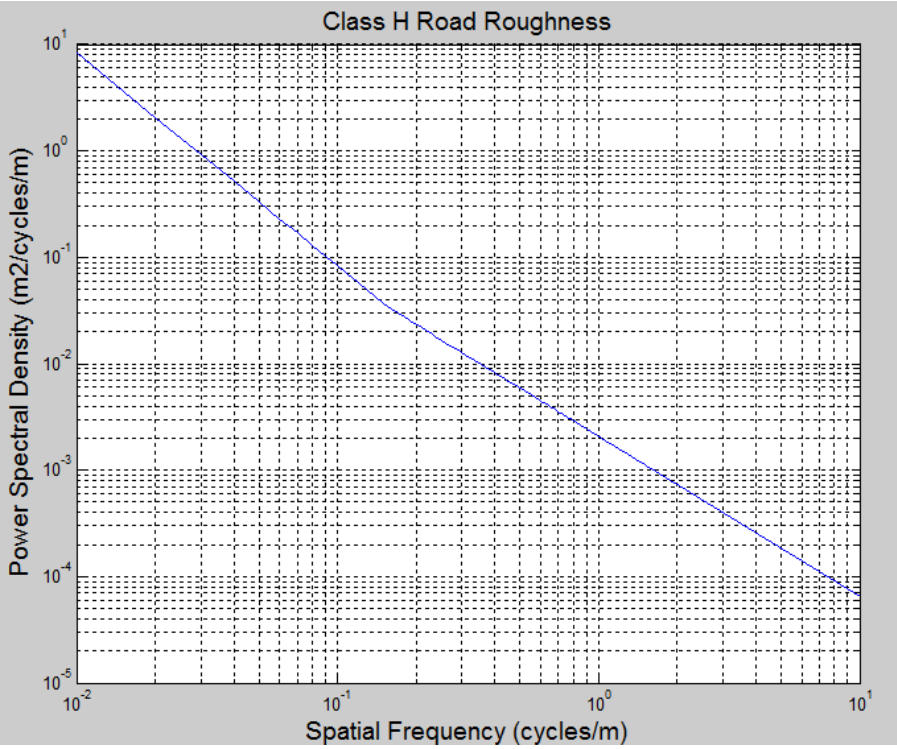

Figure 4.23 MATLAB plot of PSD of Road Roughness

The PSD plot in terms of frequency is plotted below for velocity of *70 km/hr* and *20km/hr* of the bus. This is then used as an input to the ANSYS 12 workbench for analysing response of the structure for such road condition.

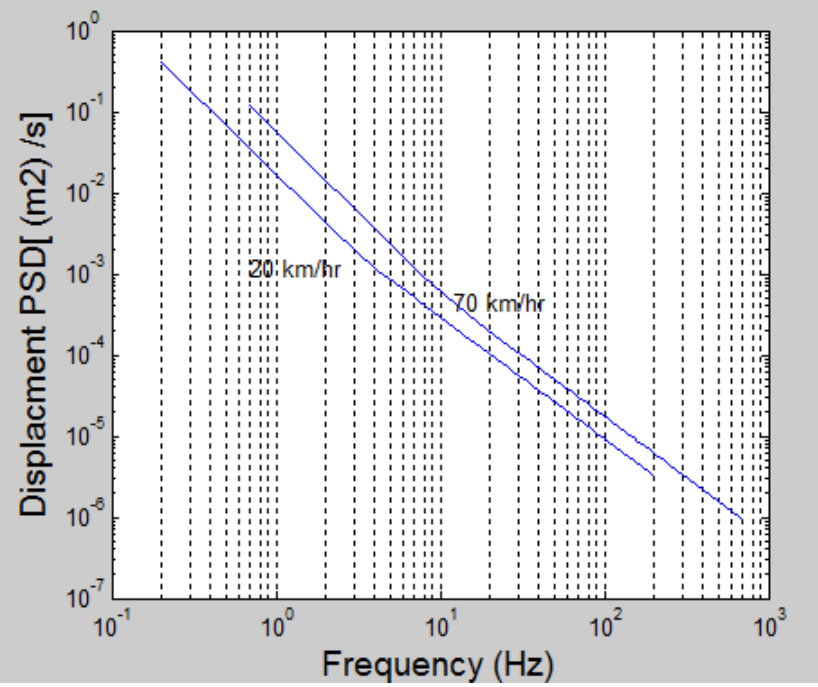

Figure 4.24 Displacement PSD of Class H road for 20 km/hr and 70 km/hr

4.10.2. Modal Analysis

The modal analysis is performed in order to extract the natural frequencies and mode shapes for vibration of the bus. The purpose of finding the natural frequency and mode shapes is to compare the original and improved bus structure in terms of these values and see the difference. In addition, it is used as input for dynamic analysis of the bus while it is travelling on standard road. The suspension has a spring stiffness of 35,000 N/m and damping of 1000 Ns/m.

The mode shapes and frequency values are tabulated as follows. The first four modes are considered in this analysis.

Table 4.7 Frequency value at each mode shape of original structure

Mode	Frequency [Hz]
1	6.2242
2	9.9311
3	12.308
4	14.4637

The following figures show the mode shapes of the bus structure. The equivalent stress values for each mode case shown separately below in figure

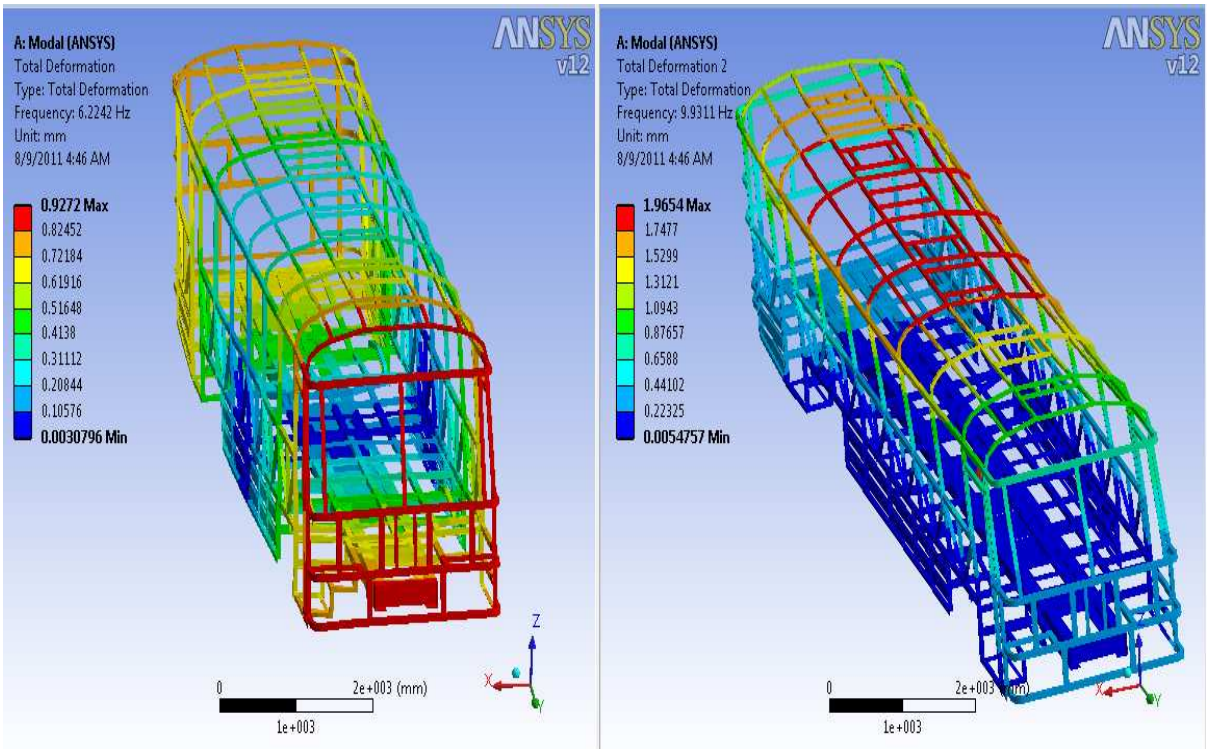

Figure 4.25 Deformation of bus for mode 1 and mode 2 of original structure

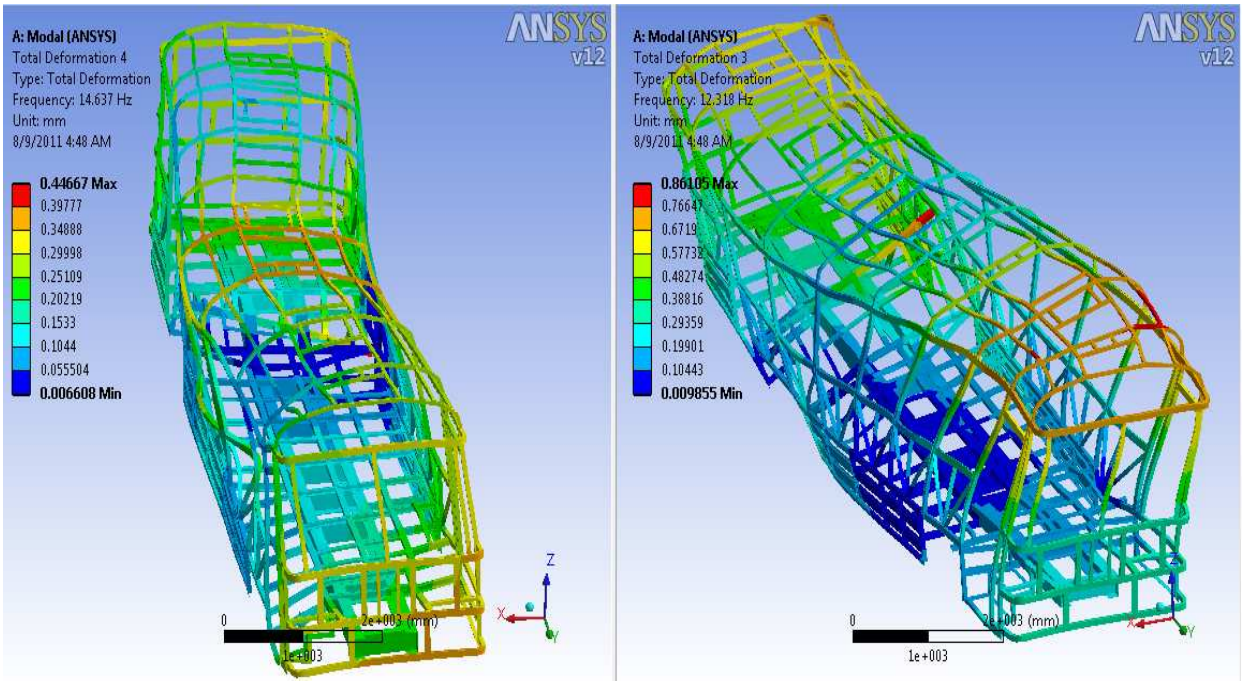

Figure 4.26 Displacement of bus for mode 4 and mode 3 of original structure

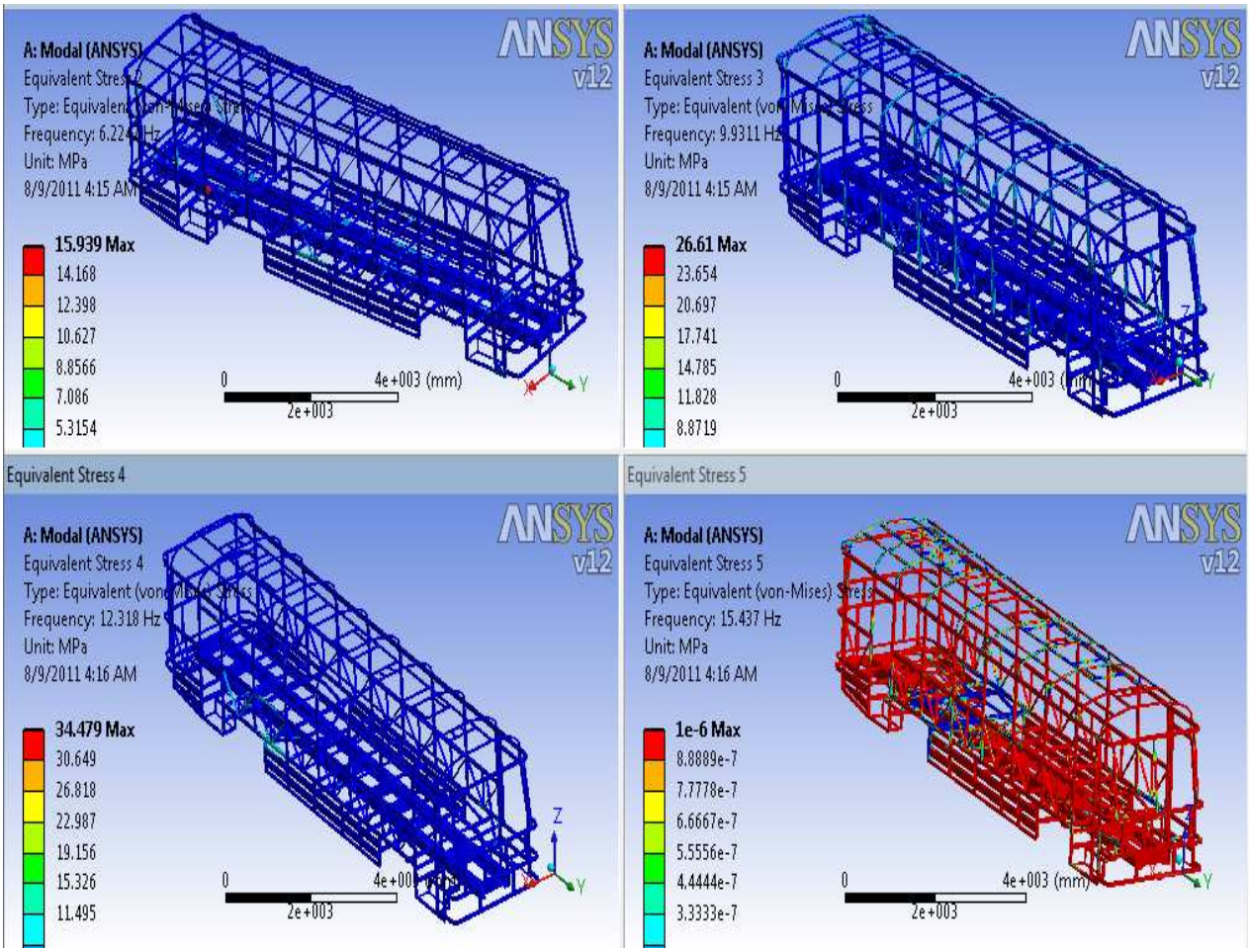

Figure 4.27 Equivalent Stress Values for modes 1, 2, 3, and 4

The following figures show the acceleration response of the bus structure at selected nodes. Node 147 and Node 20 is considered for both speeds of the bus. Node 147 is located at the rear door left top corner and Node 20 is at the front left top corner. That is for speeds of *20 km/hr* and *70 km/hr*. This node is found at the rear door top left corner.

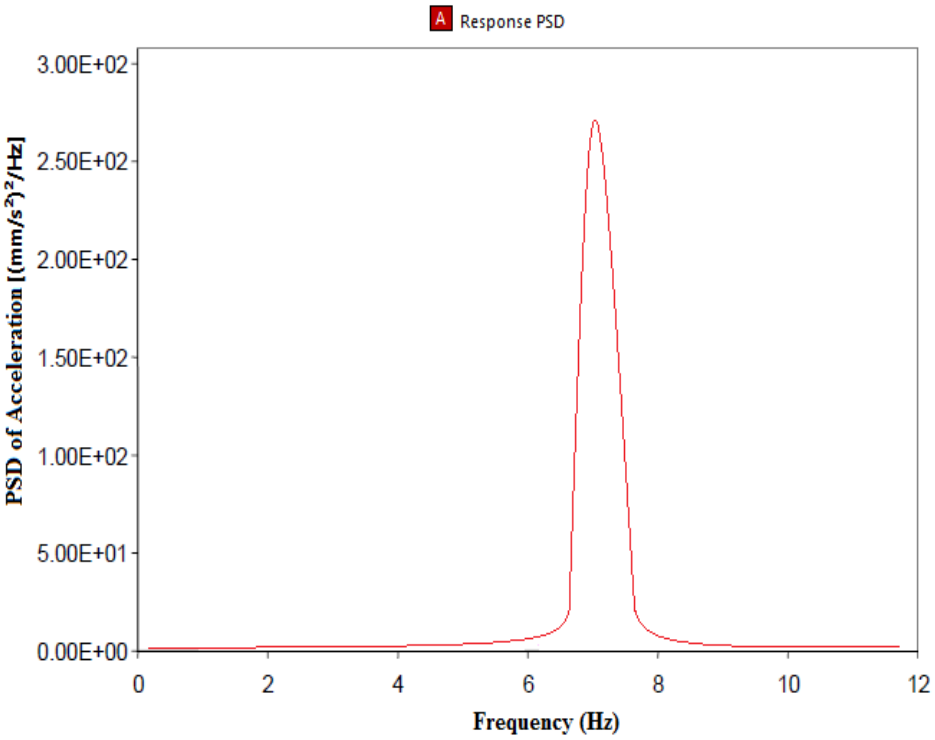

a) Response of Node 147 at rear door top right corner at speed of 70 km/hr

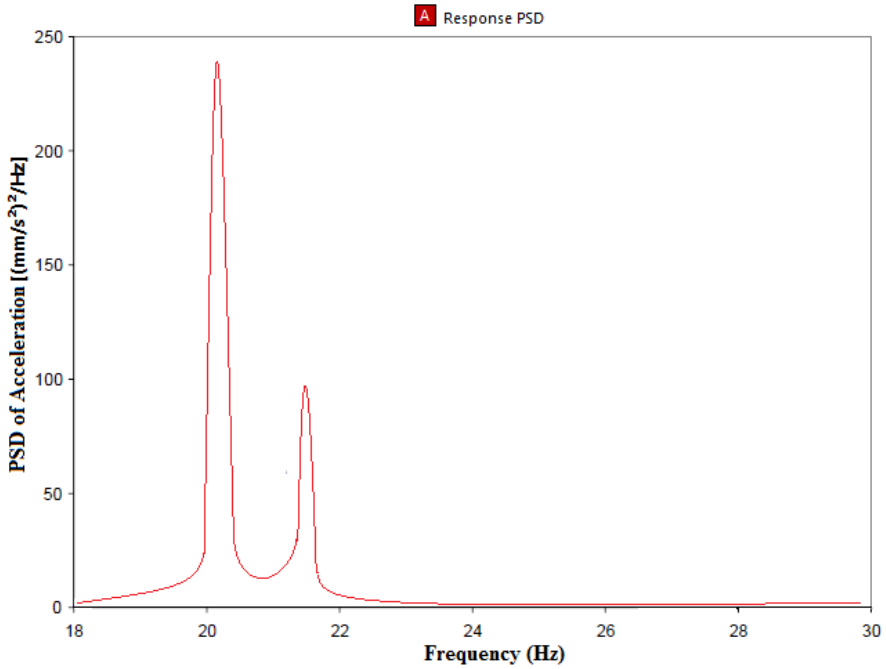

b) Response of Node 147 at rear door top right corner at speed of 20 km/hr

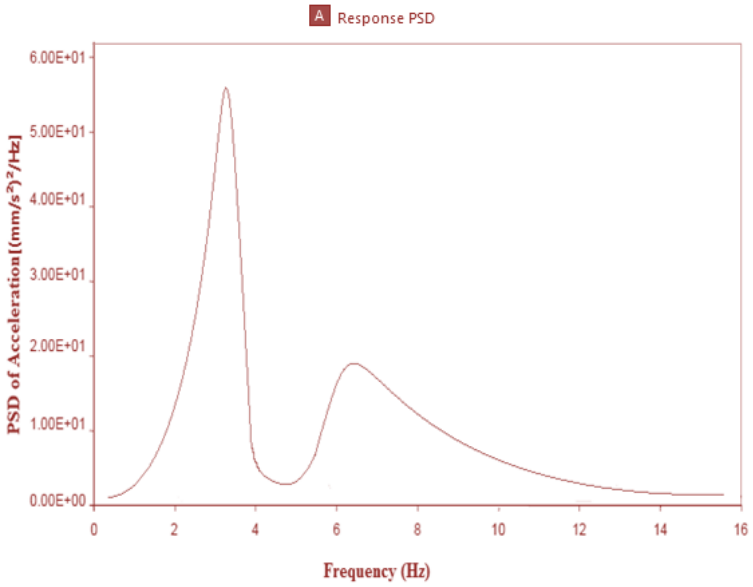

c) Response of Node 20 at front door top right corner at speed of 20 km/hr

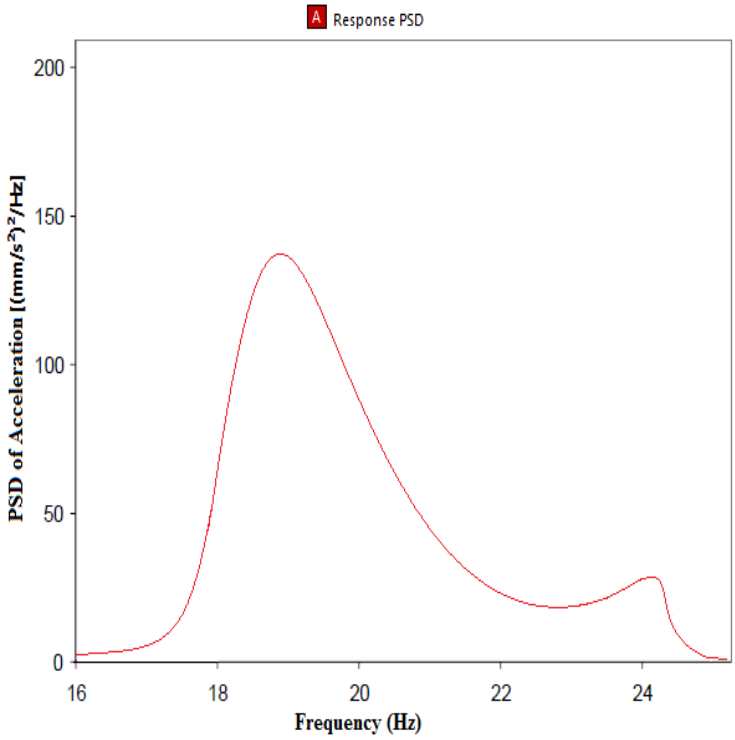

d) Response of Node 20 at front door top right corner at speed of 70 km/hr

Figure 4.28 PSD responses of selected nodes due to road roughness of original structure

From the above acceleration PSD results, while the bus traverses on Class H road at speed of *20 km/hr* experiences lower force on the stated nodes. But this becomes higher when the bus travels on the same road condition with speed of *70 km /hr*. As this force greatly affects the strength of the bus, it is recommended to drive with lower speed on such worst road case.

4.11. Improvement process

The critical objective of improvement of the structure is to reduce weight while keeping the structure strength in safe condition. As the results of the original structure in bending load and torsional stiffness depict, the stress and displacements found are very low. So there is a room to modify and improve the structure.

Therefore, the weight improvement of the structure is mainly based on the bending load and torsional stiffness results. The improved structure is again analysed for this two loading cases. The following figures (figure 4.23 and 4.24) show the components that have same RHS size. Those components of the structure that use RHS of size 70X50 and thickness of 3mm are assigned with number one where as those members which use RHS of 50X30 and thickness of 3mm are assigned with number two. The above stated sizes of RHS are used to build the bus structure in the factory.

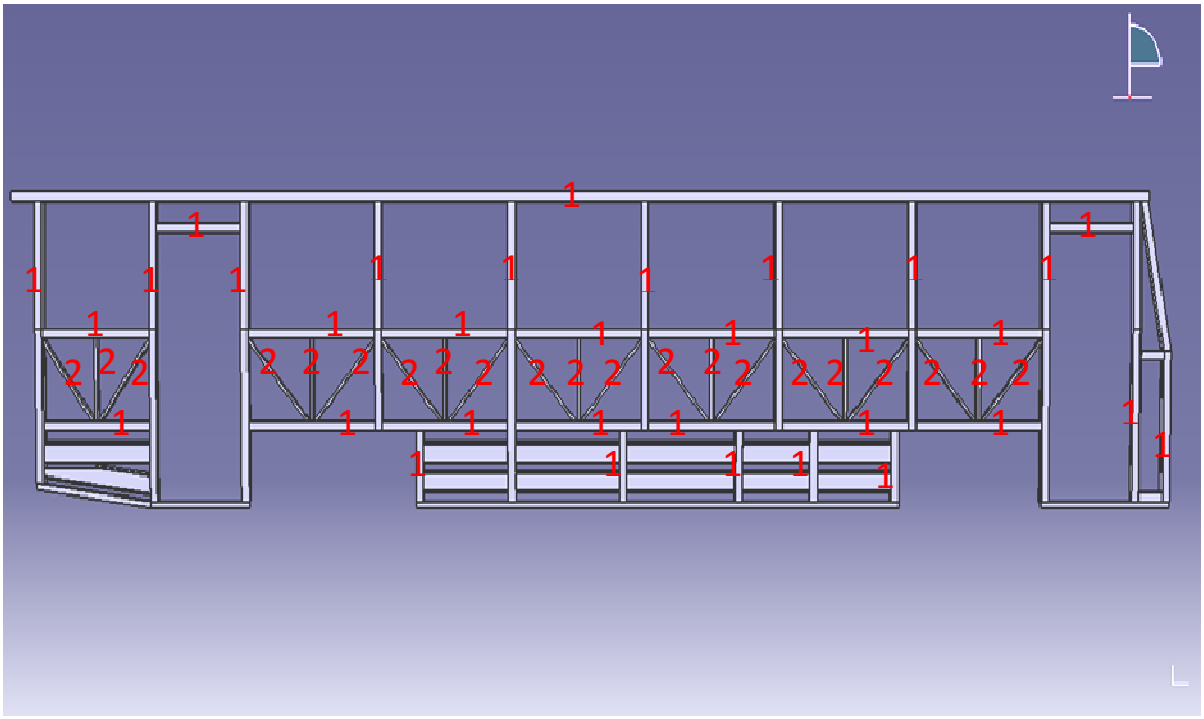

Figure 4.29 Passenger door side structure showing members which use same RHS

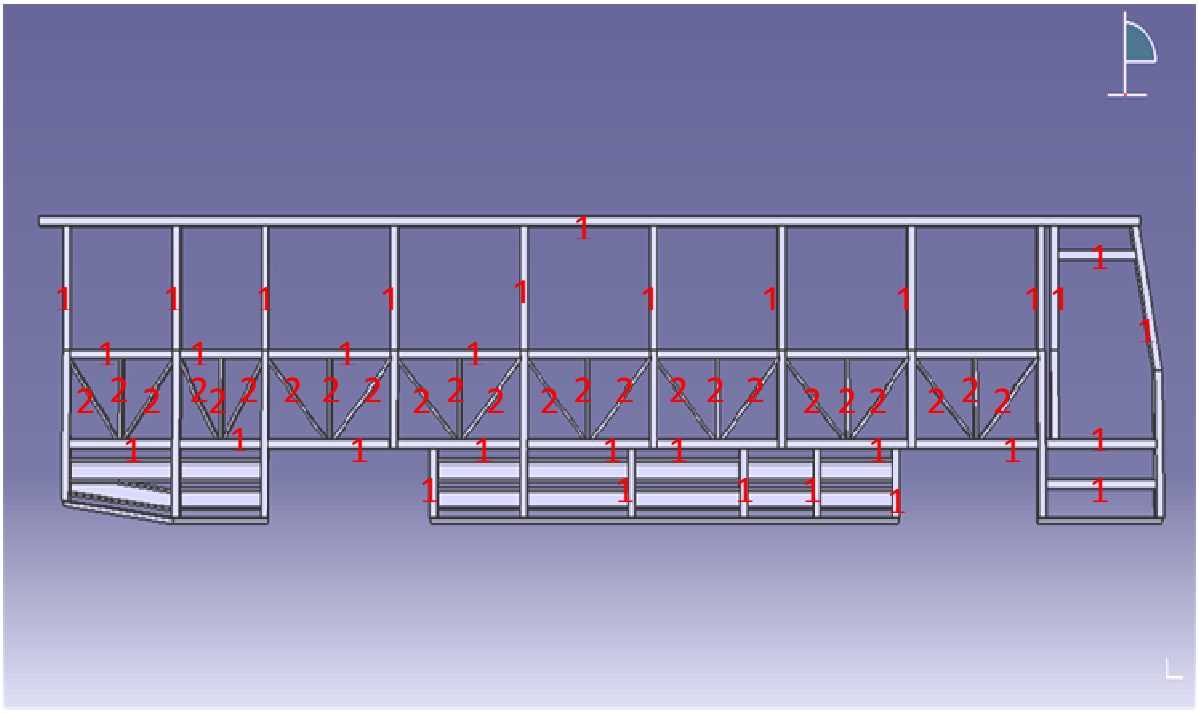

Figure 4.30 Driver side door structure showing members which use same RHS

4.11.1. Changing the size of RHS

The results of the original structure analysis depicts that the structure is subjected to low stress values. When we look at the results of bending load structure, the structure is subjected to lower stress compared to the torsional stiffness. The results of the torsional structure are higher in magnitude but generally the structure is subjected to very low stress values, very lower than the yield stress of the material. This provides a room for reducing the size of the structure members. Therefore, the sizes of the members can be reduced with lower sizes of members.

The improvement of the bus considers replacing of the members of the structure with lower sizes members. RHS size of 70X50X3 mm is replaced by 60X40X2.5 mm and RHS size of 50X30X3 mm is replaced by 40X40X2.5 mm. Therefore, the new model is made with new the replaced RHS.

The loading cases, the boundary conditions are also same as with the original structure. The new model will be analysed for bending load and torsional stiffness. The only change in the improved structure analysis is the use of the newly modelled bus with the newly replaced members of the structures.

4.12. Improved structure analysis

4.12.1. Finite element mesh of the improved model

The following figure shows the finite element mesh of the bus structure.

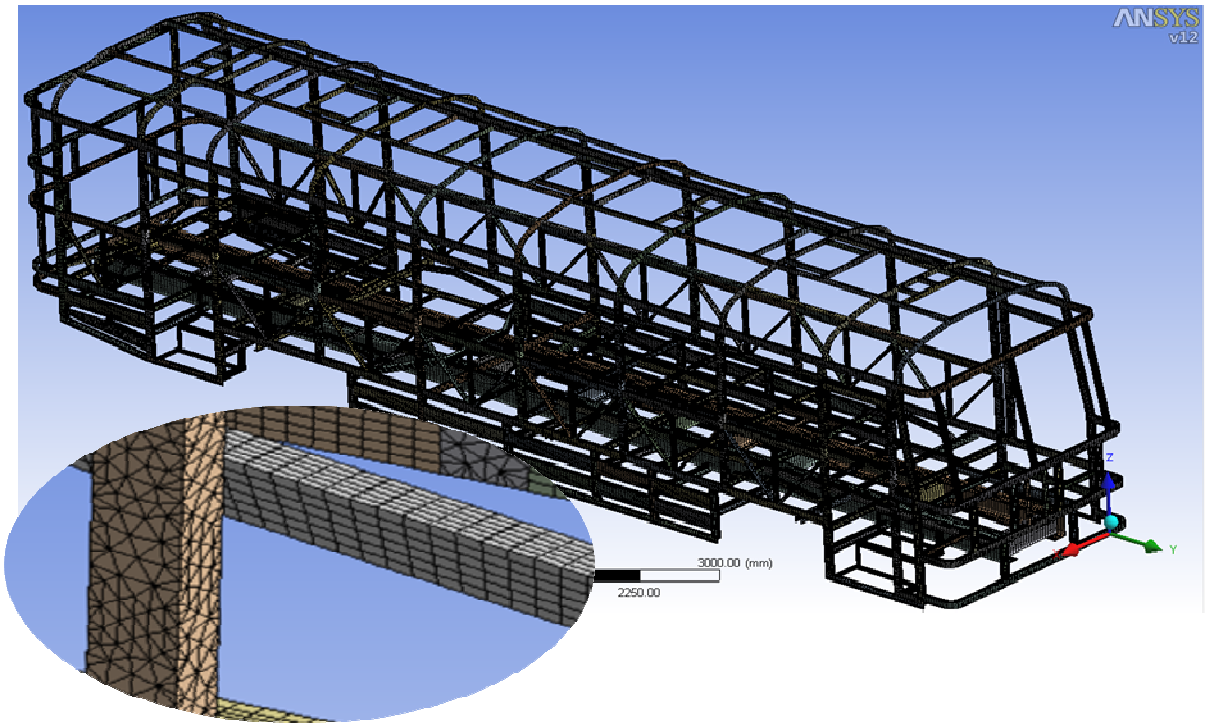

Figure 4.31 Finite element mesh of the improved bus structure

4.12.2. Boundary conditions of the improved structure analysis

The improved structure is analyzed in same way as the original structure is analyzed. The difference in the two analyses is the use of a different model for the improved structure of the bus. All the boundary conditions used in the original structure analysis are used for the improved structure too.

The load conditions considered for the original structure analyses is done here for the improved structure. These two major loads considered are bending load and torsional stiffness of the structure.

4.12.3. Bending loading case

Analysis Results

The following table 4.8 shows the values of stress and deformation of the improved structure in bending loading case.

Table 4.8 Values of stress and displacement for the improved bus

Object Name	*Equivalent Stress*	*Vertical Displacement*	*Normal Stress*	*Total Displacement*
Minimum	0.003 MPa	0.43093 mm	12.87 MPa	0 mm
Maximum	143 MPa	-6.5327 mm	121.6 MPa	6.5327 mm
Minimum Occurs On	Part 167	Part 341	Part 27	Part 33
Maximum Occurs On	Part 98	Part 7	Part 27	Part 307

The following figure (figure 4.32) shows the stresses and deformation of the bus for bending load case. The maximum equivalent stress is 143 MPa and the minimum is 0.003MPa. Most of the structure members are subjected to stress below 37.181MPa.

Figure 4.32 (b) indicates the middle bottom section of the bus structure member subjected stress value of 129.4 MPa.

The diagonal members are subjected to stress lower than 38 MPa. .

A relatively higher stress value occurs near the bottom members with value of 53 MPa compared to side members of the structure. This occurs at the rear side bottom section of the structure (figure 4.32(a)). The roof structure of the improved bus behaves in same way with original structure in that both are shown to have relatively higher equivalent stress. This is shown in figure 4.32(b). The stress value is 79.25 MPa.

In addition, members located at the middle section of the structure are subjected to high stresses as most of the load carried by the bus is located at the middle section. This is shown by figure 4.32(c).

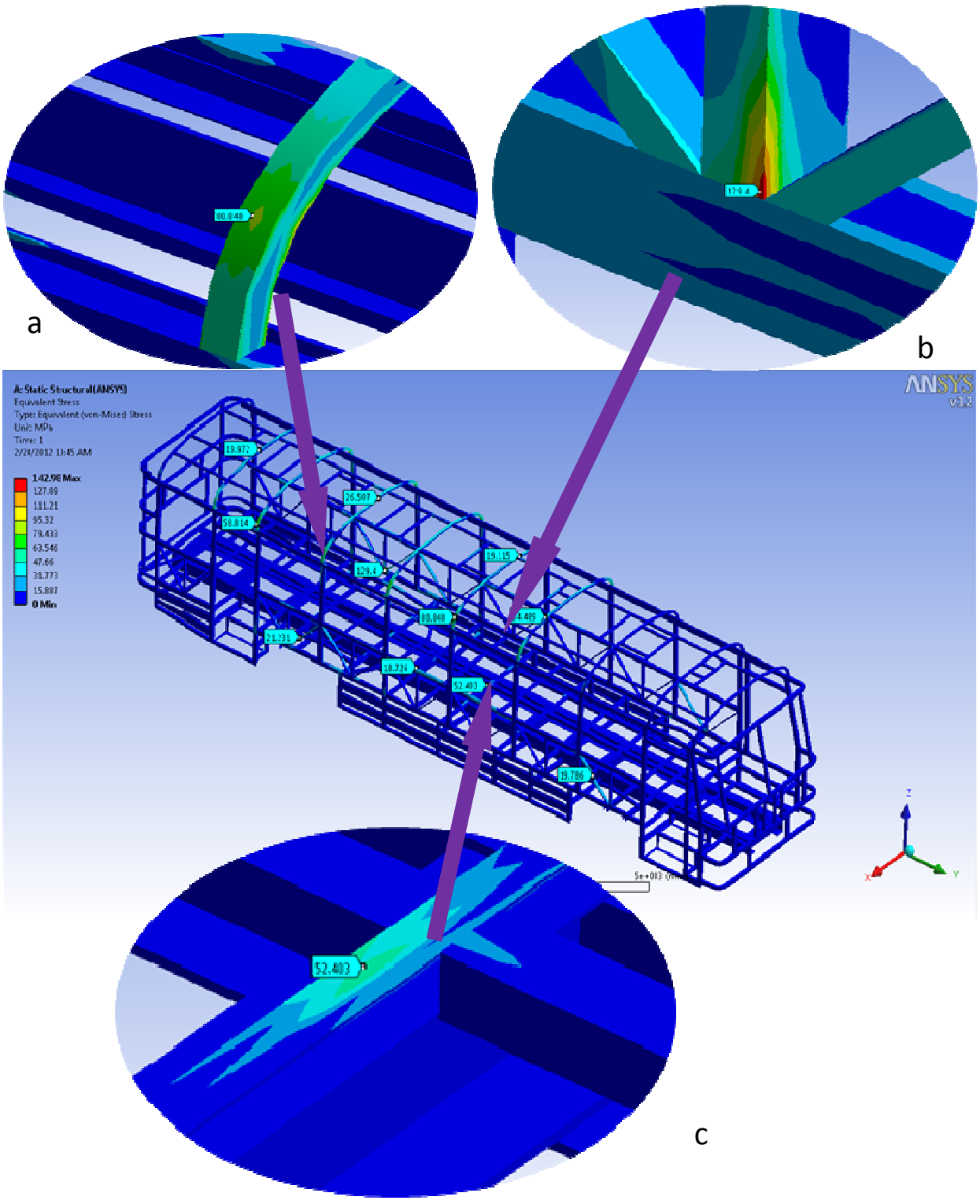

Figure 4.32 Von-Miss stress of improved structure in bending load case

The contour plot of normal stress figure (figure 4.33) shown below. Figure 4.33(a) shows the normal stress of members near the rear wheel. Here the top periphery of the horizontal member is subjected to compressive stress of value 45.96 MPa while the bottom is subjected to tensile stress of 106.5 MPa.

In addition, the side horizontal members, in the middle section of the bus are shown to have compressive stress on the top periphery and tensile stress at the bottom periphery. This is due sagging tendency of the bus structure in the middle section, i.e. between the front and rear wheels. It is shown by figure 4.33 (c).

The diagonal members are subjected to compressive stress of values 38 MPa. This is shown in figure 4.33 (b). Lower normal stress occurs at the front and rear section of the bus

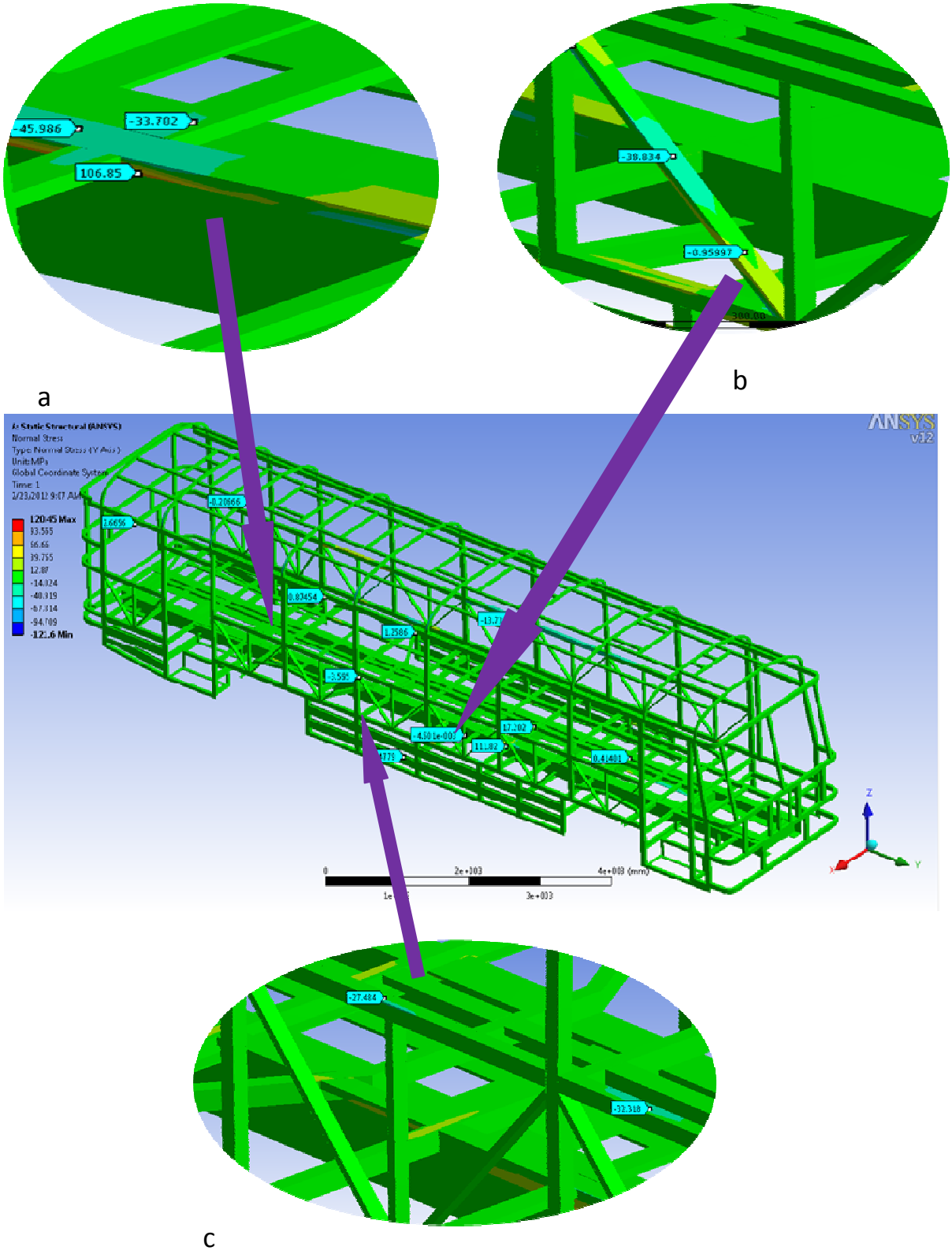

Figure 4.33 Normal stresses (y-direction) of improved structure in bending load case

The figure below (figure 4.34) shows the vertical directional displacement of the bus structure (z-axis). The maximum displacement is 6.5327 mm in down ward direction and the minimum is 0.43093 mm in upward direction.
It can be seen from directional displacement (figure 4.34(a)) of the structure, the structure deforms downward direction. The side members of the structure between the wheels exhibit a negative displacement values which can easily be seen from the directional displacement of the structure, figure 4.34. This is again due to the sagging tendency of the bus structure at the middle section. Figure 4.34(c) shows the diagonal members subjected to negative displacement values.

In addition, from figure 4.34(d) the chassis cross members which are found in between the front and rear wheels are subjected negative displacement values. The same is true for the diagonal members which are found in between the front and rear wheels. Such case happens because most of the load carried by the bus lies in between the rear and front wheels, that is middle section bus.

On the other hand, figure 4.34(b) shows the displacement of members near front door opening. There is lower displacement with positive value which indicates that it deforms in upward direction. The total displacement at this area is shown in figure 4.28(d) which has value of 4 mm. Similarly the displacement of the bus at the rear side has lower positive value which shows rear members deform in upward direction.

Besides, from the directional displacement figure 4.34, at this area has positive value which makes us to conclude the members are deformed in upward direction.
Structure member near to the place of constraints are subjected to lower displacement value.

Roof members of the structure experience higher displacement relative to other members. Figure 4.35 (a) shows the total displacement of the roof member. The displacement has a value of 6.5327 mm.
Also higher displacements occur at the middle section of the bus. This shown by figure 4.35(b).

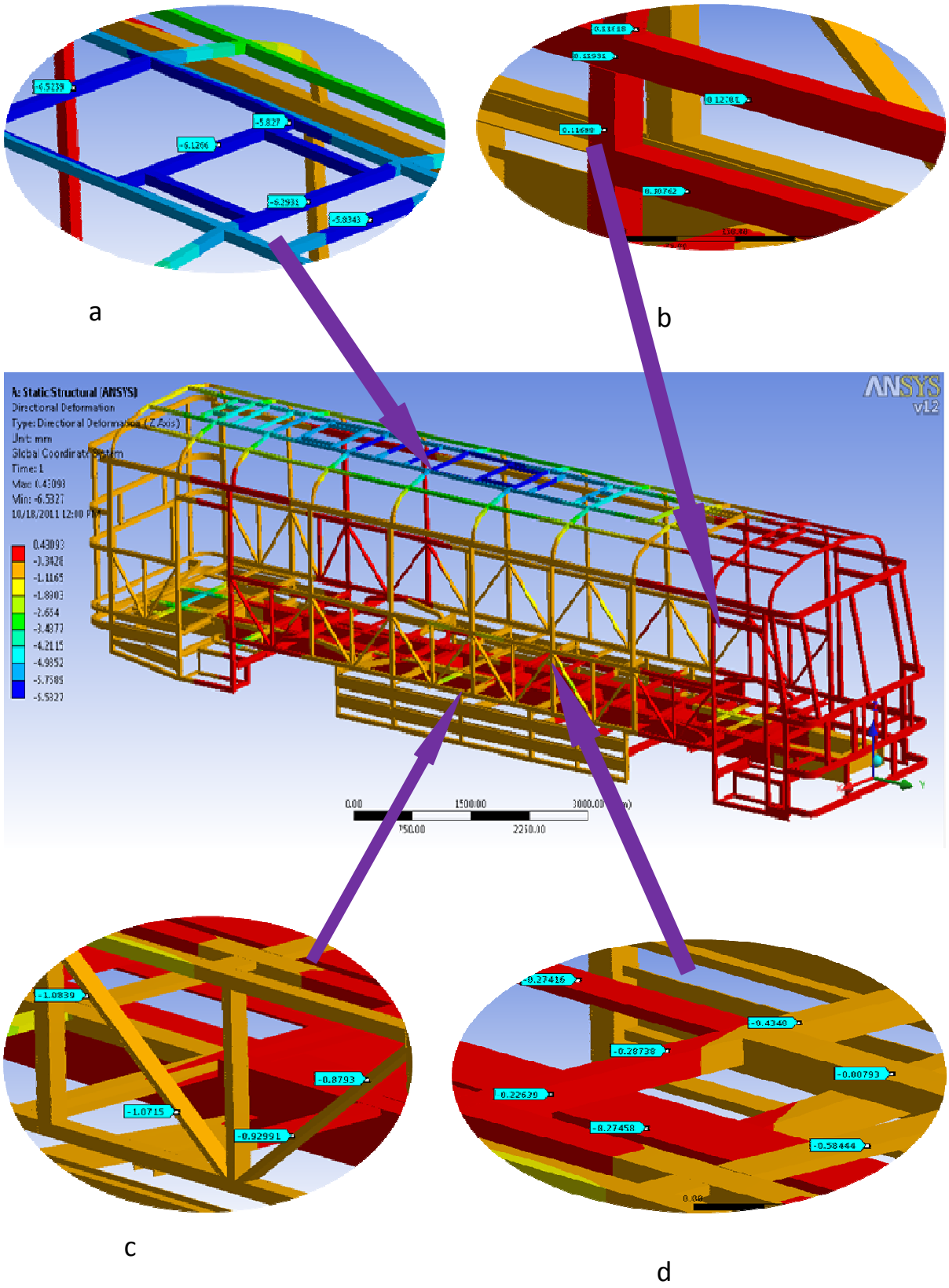

Figure 4.34 Directional displacements (z-direction) of improved structure in bending load case

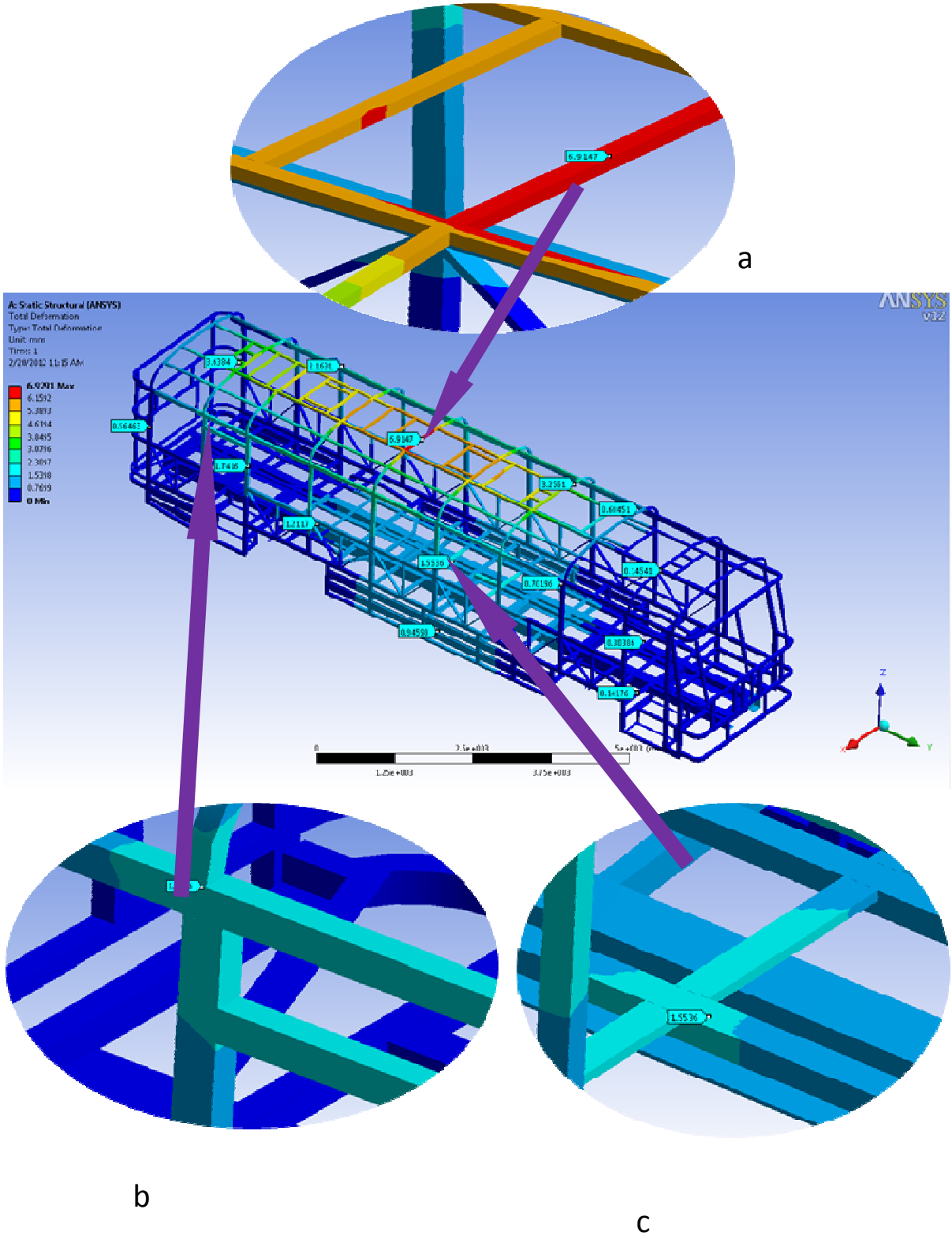

Figure 4.35 Total displacement of improved structure in bending load case

4.12.4. Torsional moment case

Analysis result

- **Torsional moment case 1**

The improved structure with newly replaced members is analysed for torsional stiffness. In the improved structure RHS 70X50X3 mm is replaced by RHS 60X40X2.5mm and RHS 50X30X3mm is replaced by RHS 40X40X2.5 mm. This case is similar with the original one except here the model used in the analysis is an improved one.

Table 4.9 Stress and displacement values in torsional loading case

Object Name	*Equivalent Stress*	*Vertical Displacement*	*Normal Stress*	*Total Deformation*
Minimum	0.00855 MPa	-7.1325 mm	14.61 MPa	0
Maximum	150 MPa	19.716 mm	137.89 MPa	19.713 mm
Minimum occurs on	Part 302	Part 316	Part 58	Part 123
Maximum occurs on	Part 190	Part 75	Part 63	Part 321

Table 4.9 shows the displacement values in positive and negative sign. The negative sign shows the direction of displacement is in downward whereas the positive sign shows upward displacement. The figure below (figure 4.36) shows contour plot of equivalent stress of the improved bus structure. Most of the bus members are subjected to equivalent stresses of below 43 MPa.

As it can be seen from the figure 4.36(a), the roof member is subjected to equivalent stress of 55 MPa. Figure 4.36(b) shows the stress near the front door which has a value of 41 MPa. Also higher stresses occur near the driver door. This is because of the bump applied at the front wheel node, figure 4.36 shows this. In addition, figure 4.36(c) it can be seen that higher stresses occur near rear wheels. Similarly relatively higher stresses occur at the bottom section of the structure around rear wheel areas which has value of 169 MPa. This is shown in figure 4.36(c).

The diagonal members are subjected to equivalent stress of 30 MPa, figure 4.36 shows this.

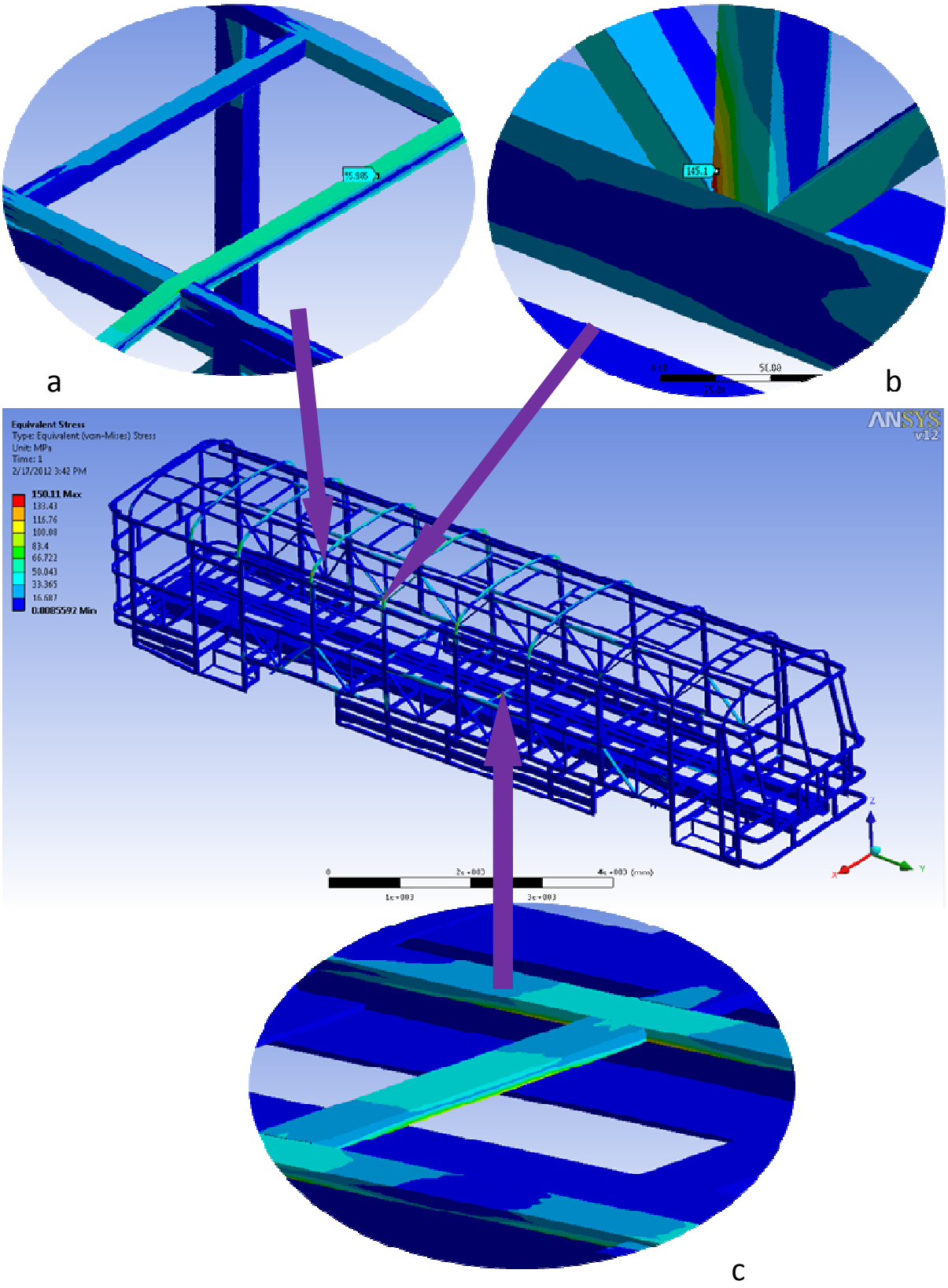

Figure 4.36 Equivalent stress of improved structure in torsional load case 1

The figure below (figure 4.37 (a)) shows the normal stress values of the structure. Similar to the original structure, the side horizontal members top periphery is subjected to negative stress values which indicate compressive stresses occur whereas the bottom periphery of the side members are subjected positive stress values.

Similar to the equivalent stress, relatively higher normal stress occurs near the rear wheel area members, which can be seen from figure 4.37(c). Figure 4.37(b) shows normal stress on the diagonal members with a value of 27 MPa.

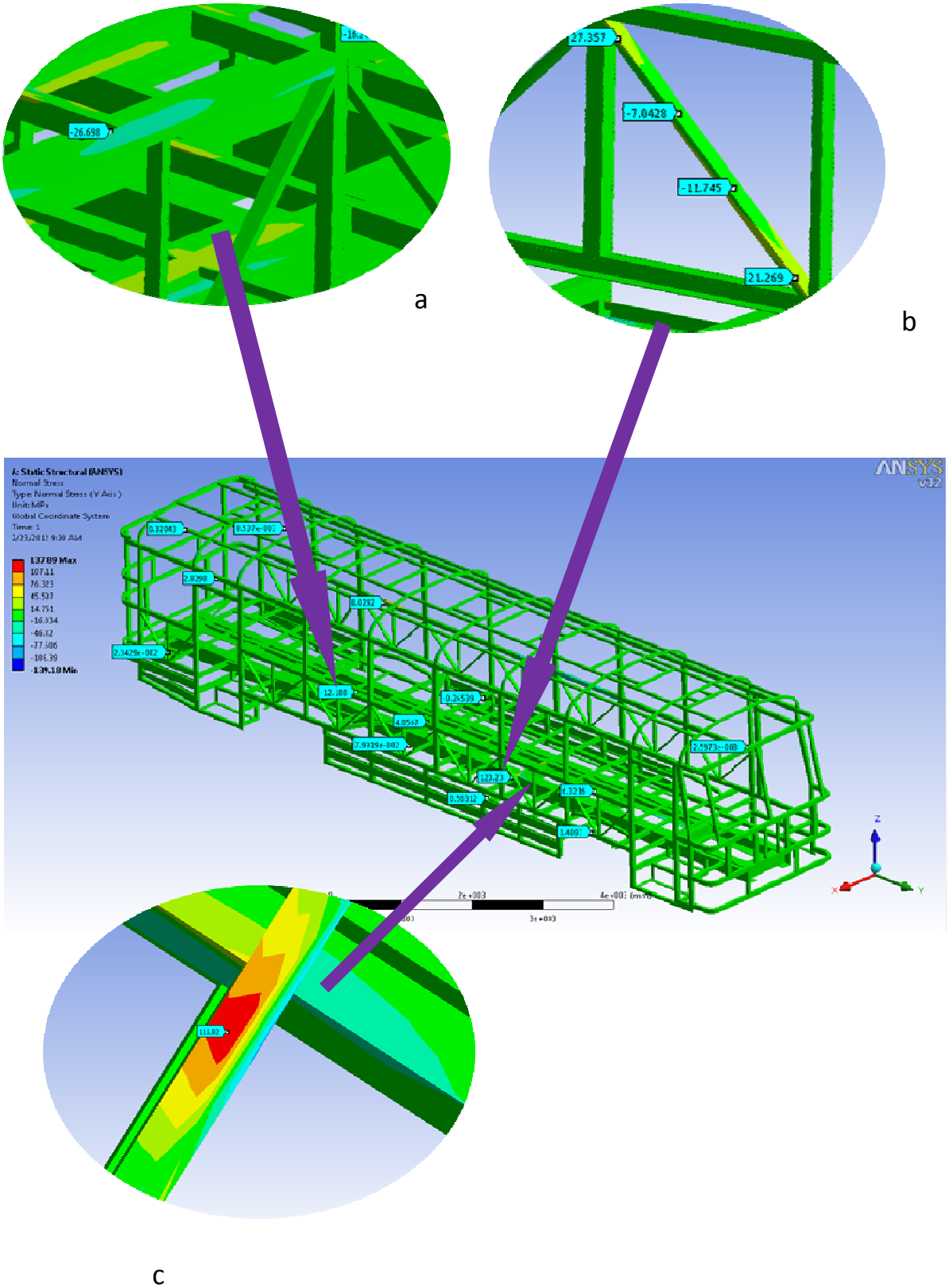

Figure 4.37 Normal Stress (vertical-direction) of improved structure in torsional load case 1

- **Shear Stress**

The following figure shows the shear stress distribution during the torsional moment case. This result shows that there is maximum shear stress at the middle section of the structure. Generally the structure is subjected to very lower values of shear stress compared to the allowable stress of the material. Therefore, here we do not fear failure that can occur due to the applied torsion moment.

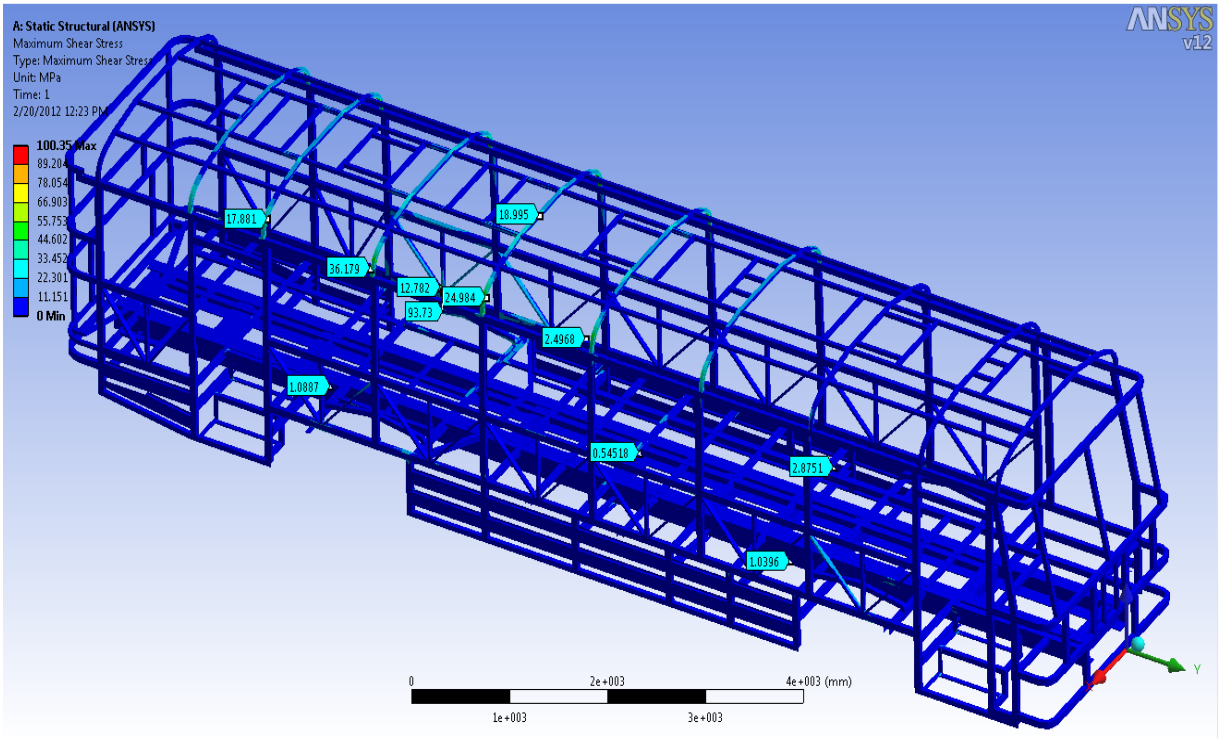

Figure 4.38 Shear stress of the improved structure for torsional moment case 1

The figure below (figure 4.39) shows the vertical directional displacement (z-axis) of the structure. The maximum displacement is 19.7 mm and the minimum is 7.1 mm in downward direction. A relatively lower displacement occurs at the rear side of the bus structure members. From figure 4.39(b), a higher deformation occurs near the point of application of the displacement (front right side of the structure). The front right side door members are subjected to relatively higher displacement values.

Rear side of the structure is subjected to downward displacement, figure 4.39. This is again due to the lifting of the front right side wheel and the added weight at the rear side, i.e. luggage passenger and extra tire weight. These loads tend to deform the rear side structure in downward direction.

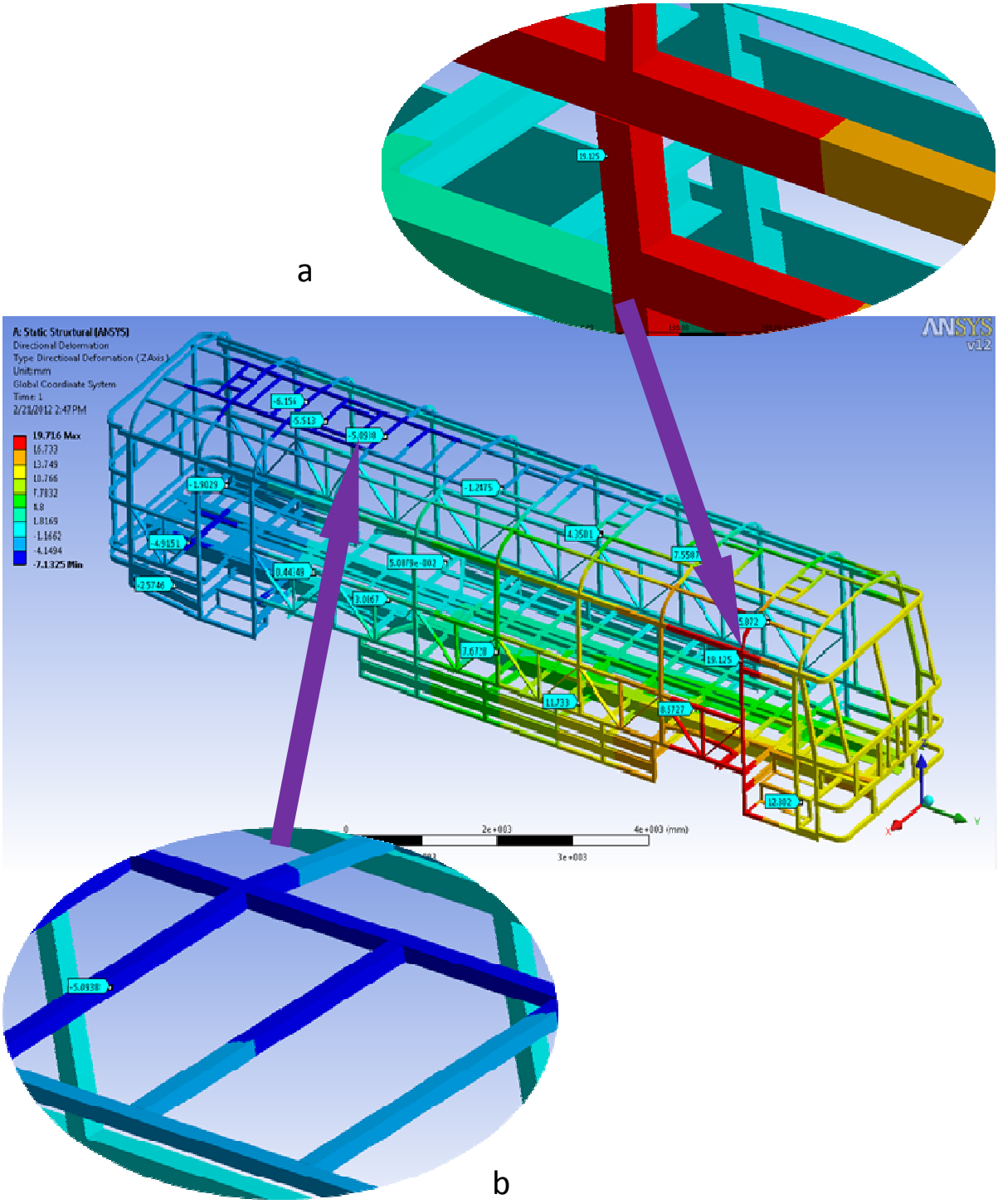

Figure 4.39 Directional displacements (vertical direction) of improved structure in torsional load case 1

From figure 4.40(a), the displacement of members near the rear door side is shown to have value of 1.804 mm. Relatively higher displacement occur by the side of wheel which is subjected to bump, i.e. front right side wheel. Figure 4.40(c) shows the displacement of the roof members to have value of 5.85 mm. The displacement of diagonal members around the application of the bump area is shown in figure 4.40(d).

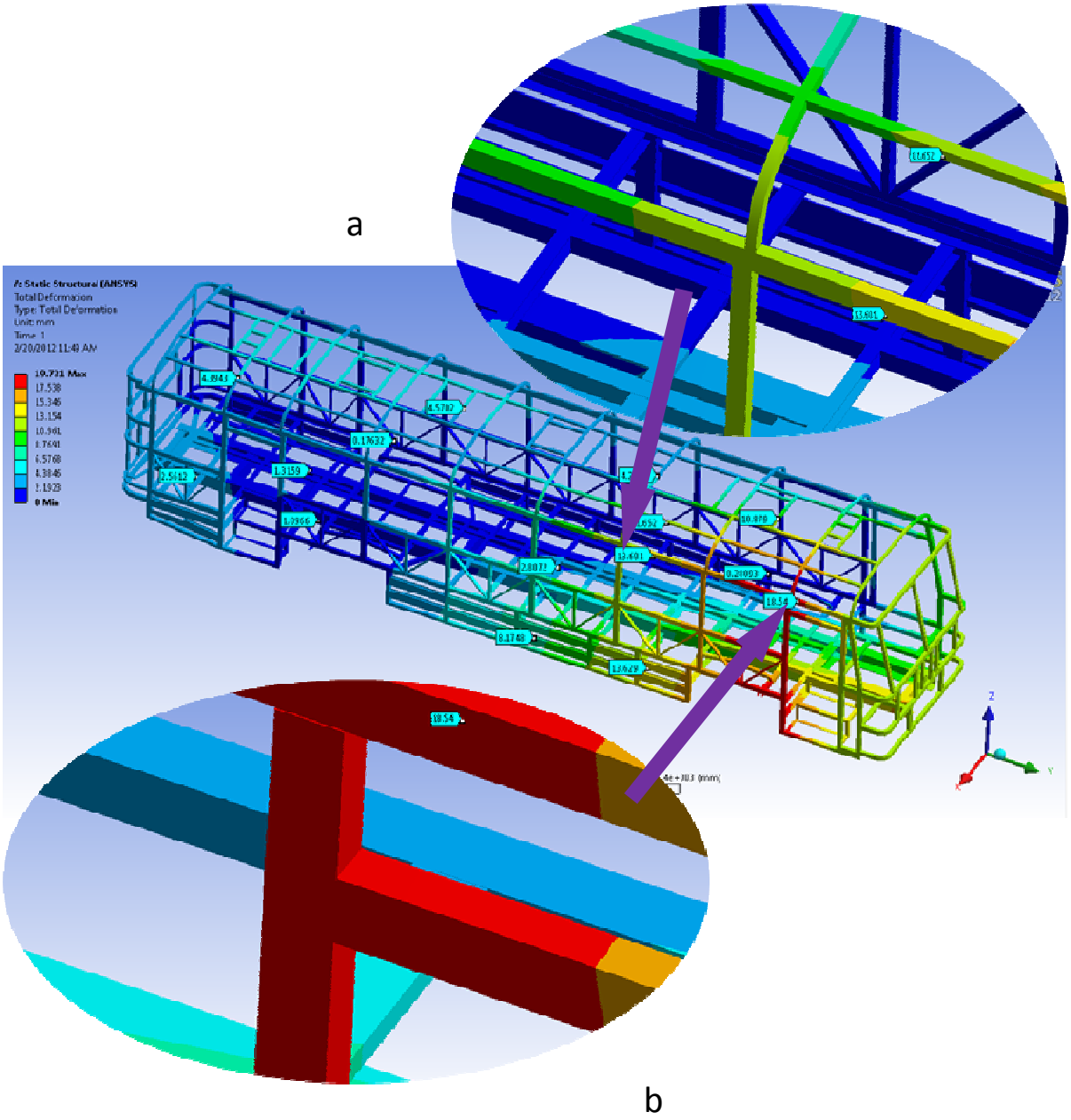

Figure 4.40 Total Displacement of improved structure in torsional load case 1

Figure 4.40 shows the maximum total displacement of the structure. This occurs near the front door top left corner. This is due to the bump applied at the front wheel.

- **Torsional moment case 2**

The following figure shows the equivalent stress of the bus structure when the diagonally opposite wheels face bumps. The result shows that the structure is subjected to maximum stress of 151 MPa. This occurs at the rear section of the bus structure where the left side wheel is located. Compared to the other neighbouring members, the roof structures are subjected to higher stress values. A relatively greater stresses occur at the middle section of

the structure. From the displacement values, here there is higher displacement in the downward direction.

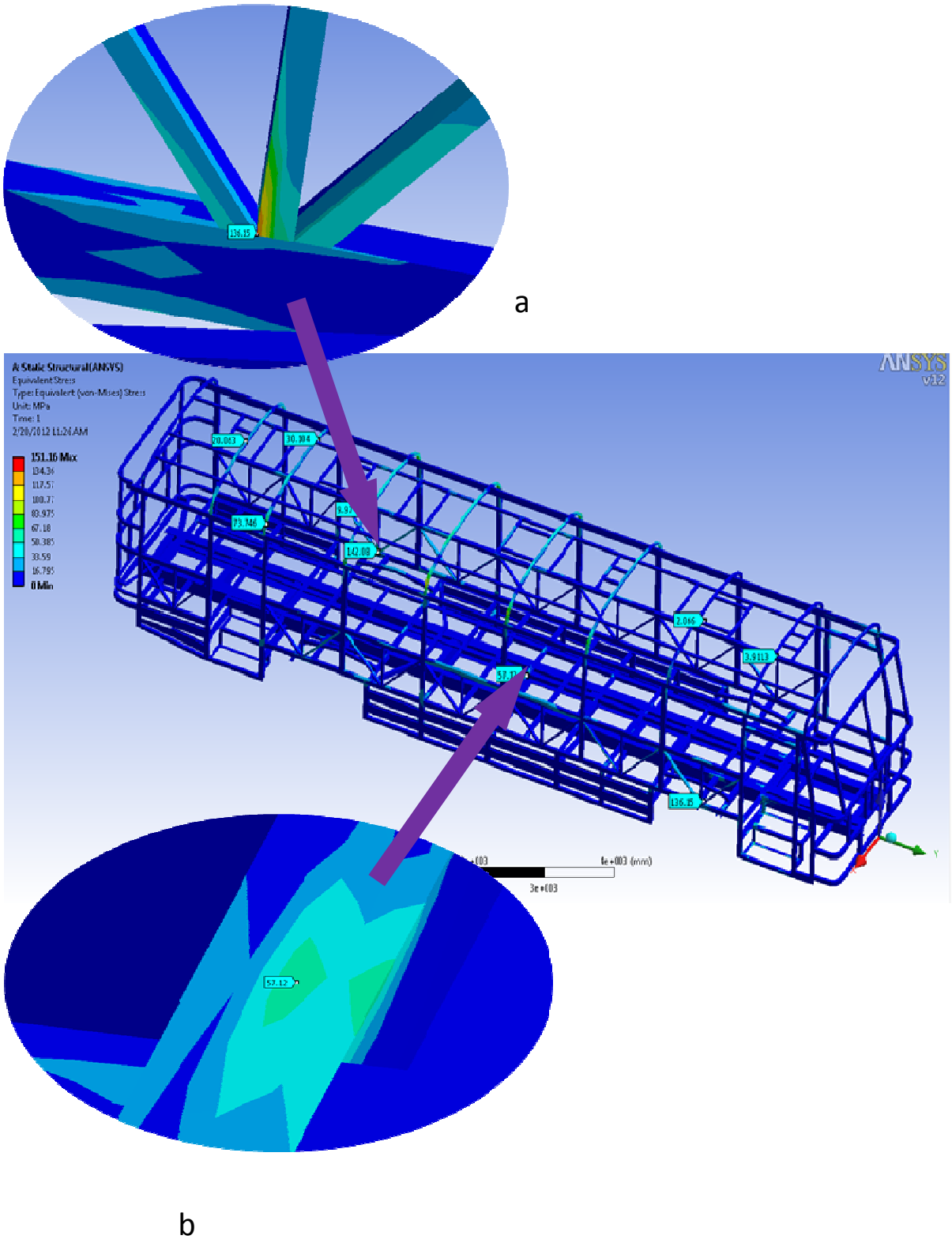

Figure 4.41 Equivalent stress in the improved structure for torsion moment case 2

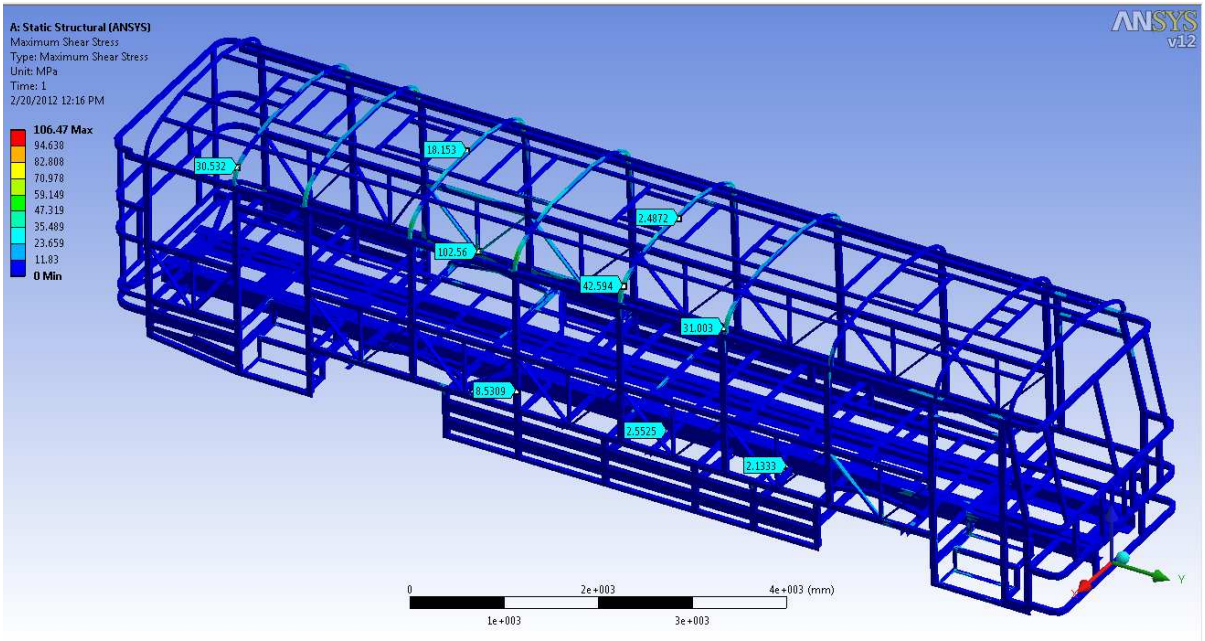

Figure 4.42 Shear stress of the improved structure for torsion moment of case 2

The above figure shows sheas stress distribution of the improved structure for torsion moment case 2. From the figure, there maximum value of the shear stress is 106 MPa which is greater than from the torsion moment of case 2. Minimum increment occurs in the shear stress value and the stress is still below the allowable stress.

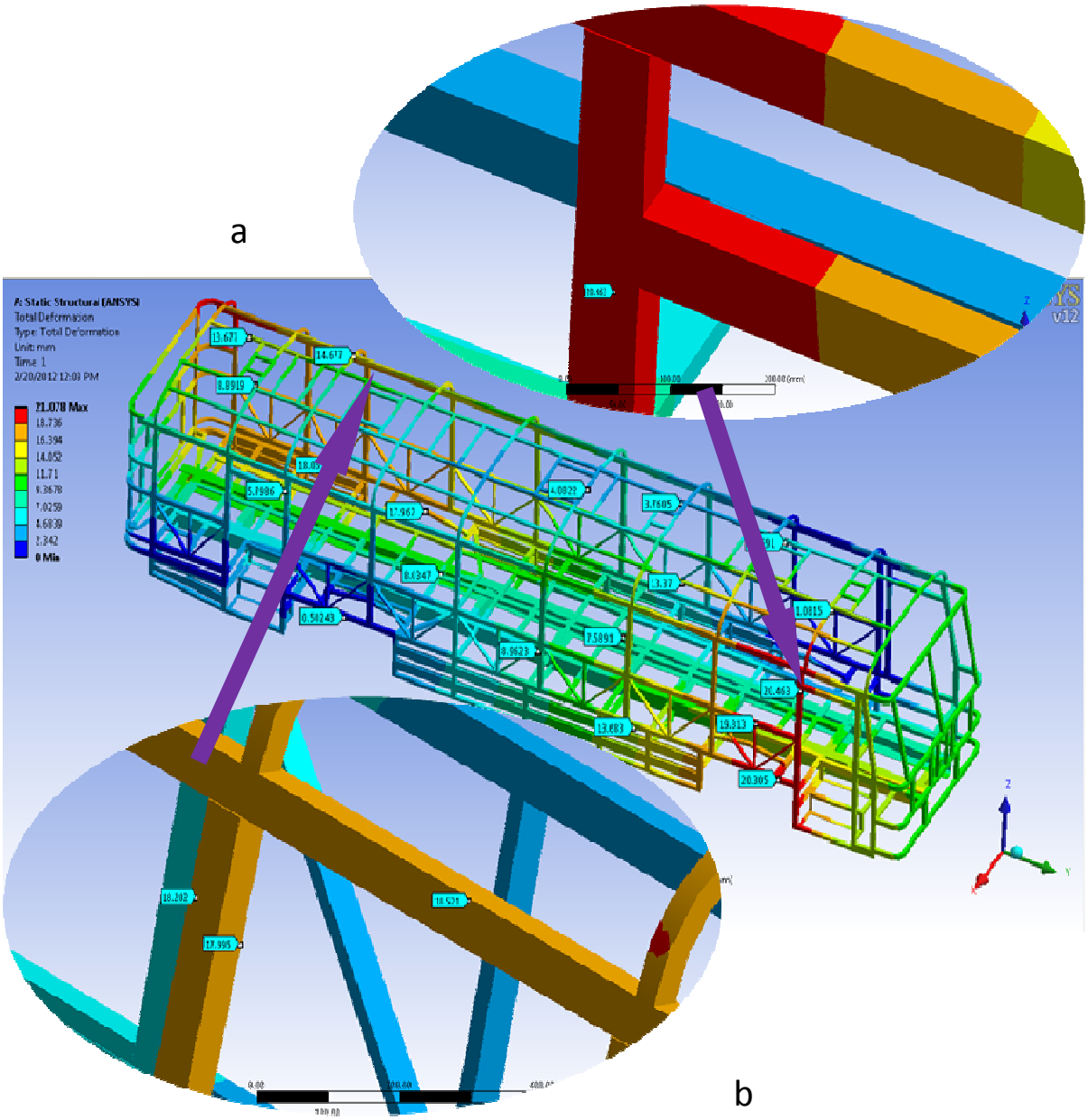

Figure 4.43 Total displacement of the improved structure for torsion moment case 2

Figure 4.43 shows the total displacement of the improved structure during torsion moment case 2. Similarly with the other torsion moment case, there are higher displacement values near the application of the bump. Here the figure shows that higher displacement occurs at the left side rear area where the bump applies directly. Greater displacement again occurs near the front right side wheel. This is due to the bumps applied on this wheel.

4.12.5. Vibration analysis of the improved structure

Modal analysis is carried out in order to extract the mode shapes and natural frequencies. The following table presents the modes and frequencies of the bus. In addition, we get the displacement and equivalent stress values of the structure at selected modes.

Table 4.10 Mode shape and frequencies of improved structure

Mode	Frequency [Hz]
1	10.38
2	12.907
3	14.158
4	18.89

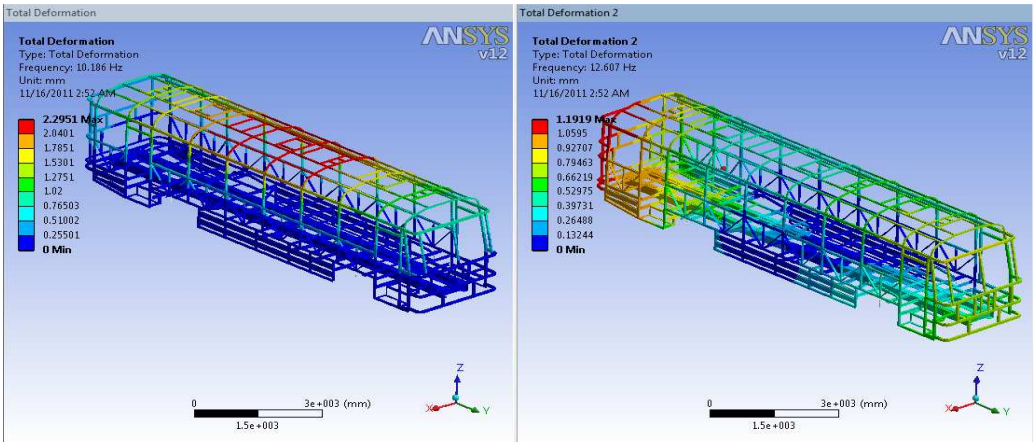

Figure 4.44 Displacement of improved bus structure for mode 1and mode 2

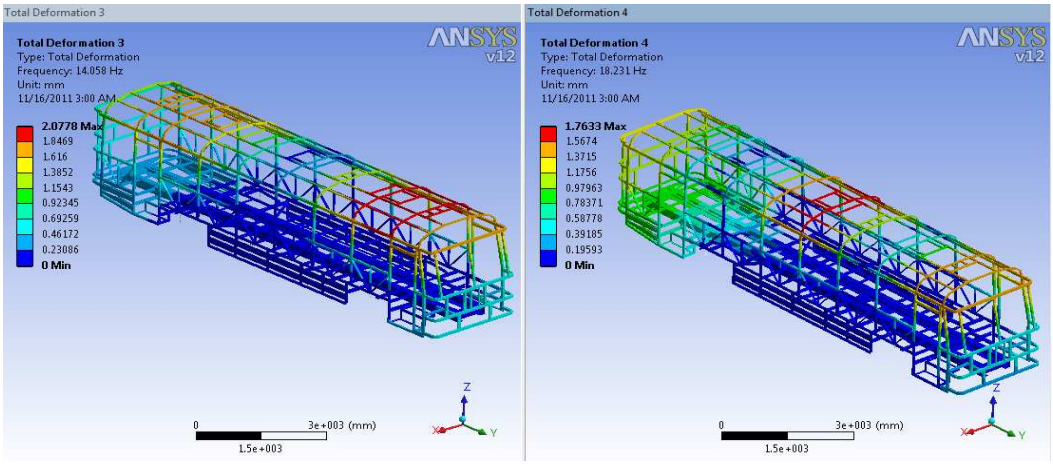

Figure 4.45 Displacement of improved bus structure for mode 3and mode 4

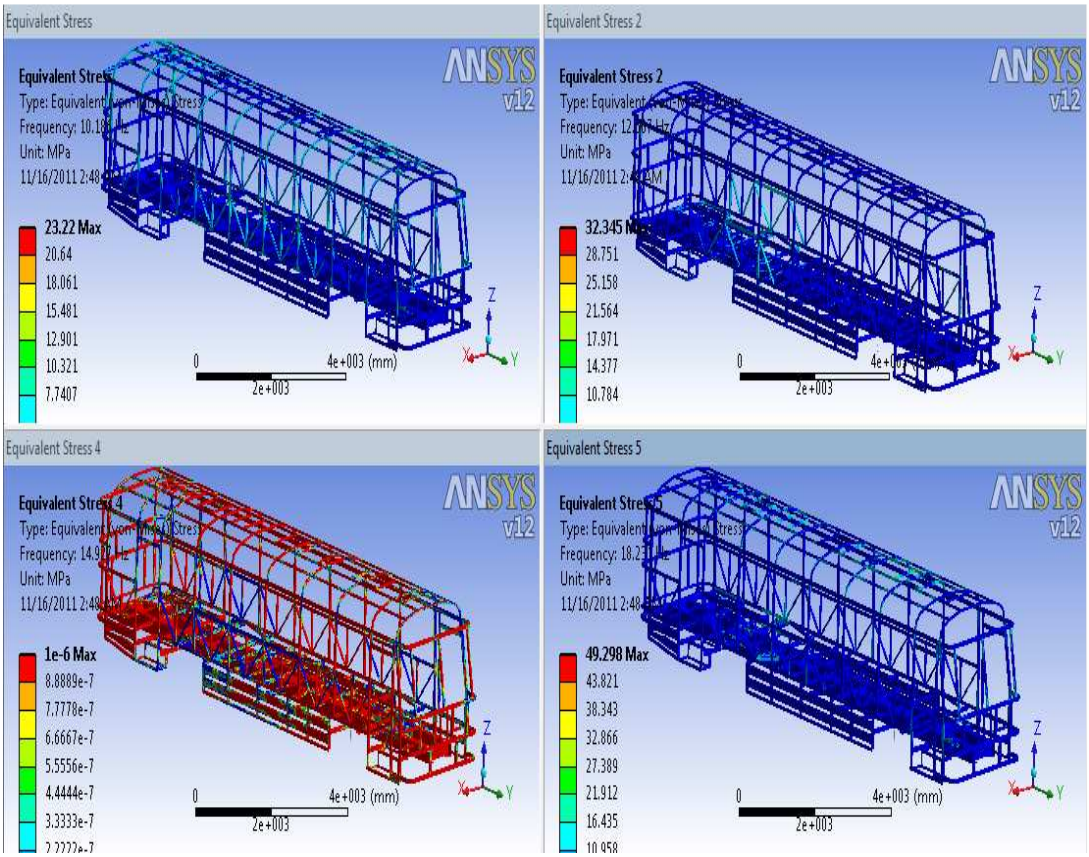

Figure 4.46 Equivalent stress values for the improved structure

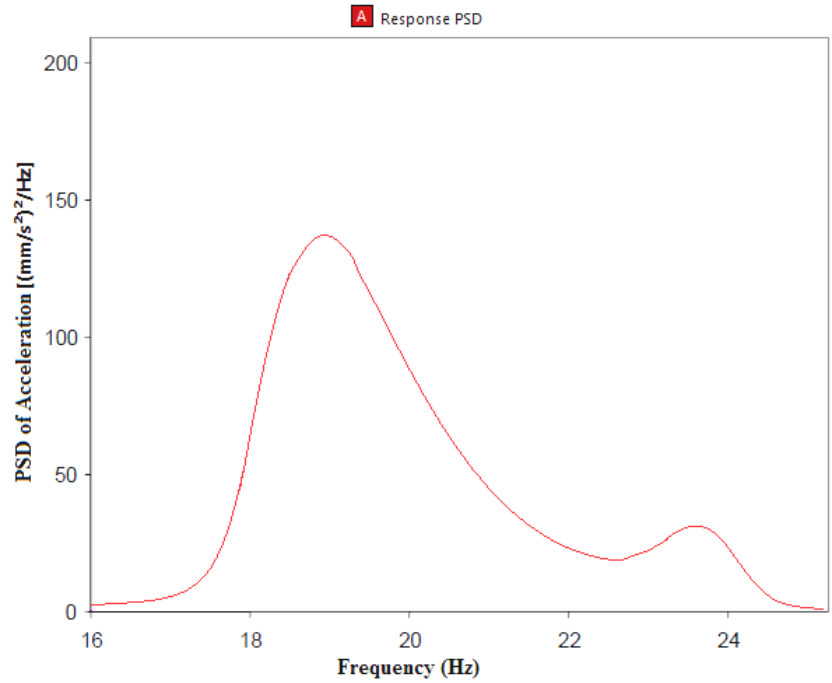

a) Response of Node at front door top right corner (20km/hr)

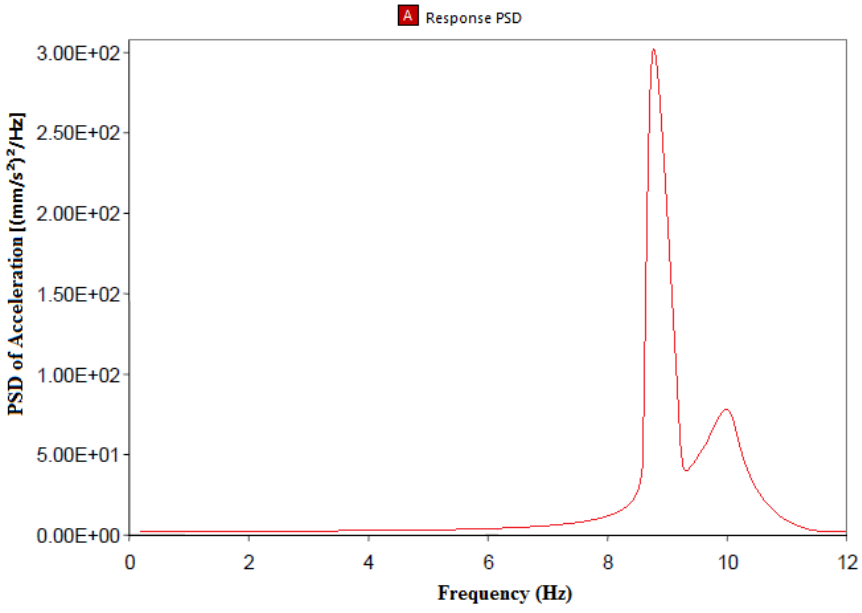

b) Response of Node at front door top right corner (70km/hr)

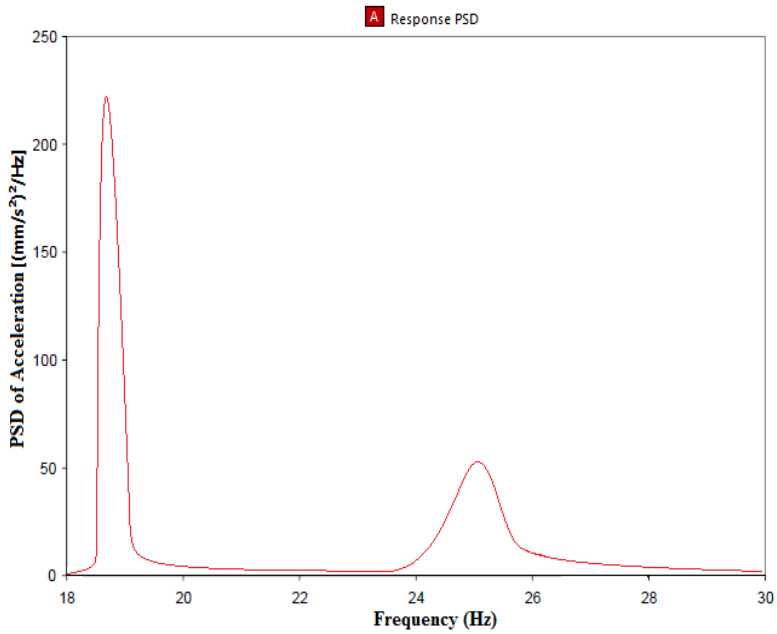

c) Response of Node at rear door top right corner (70km/hr)

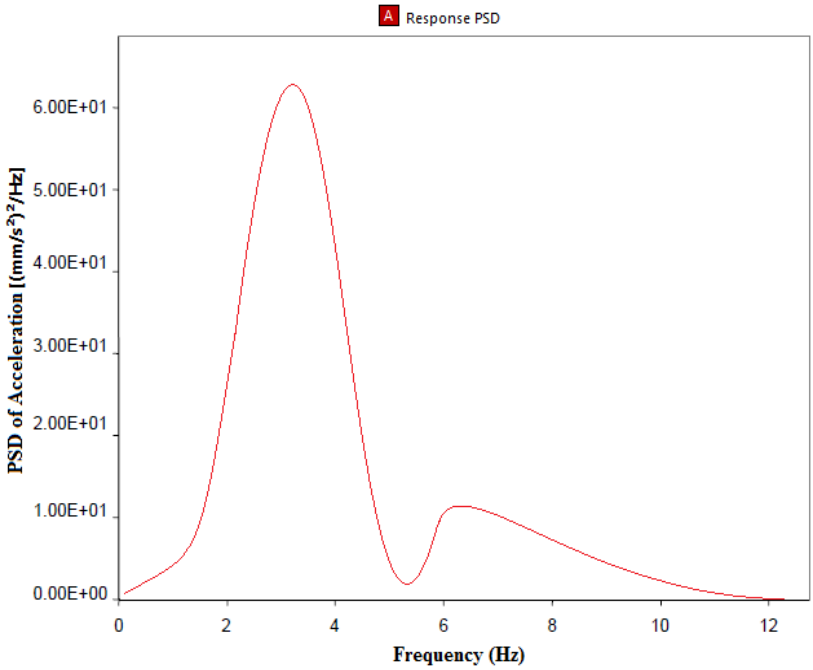

d) Response of Node at rear door top right corner (20km/hr)

Figure 4.47 PSD responses of selected nodes due to road roughness of original structure

Similar things can be stated here again for the improved structure of the bus. From the above acceleration PSD results, while the bus traverses on Class H road at speed of 20 km/hr experiences lower force on the stated nodes. But this becomes higher when the bus travels on the same road condition with speed of 70 km /hr.

4.13. Comparison between original and improved structure

- **Bending Load applied to the structure**

When bending load is applied on the structure, the comparison between the original structure and improved structure is shown.

Table 4.11 Comparison between original and improved structure during bending load case

	Original Structure	Improved structure
Mass	2999.29 kg	2809.49 kg
Max. Total Displacement	5.837 mm	6.5327 mm
Max. Normal Stress y-axis	90.36 MPa	121.647 MPa
Max. Equivalent Stress	122.57 MPa	143 MPa

- **Torsion moment applied to the structure**

When Torsion load is applied on the structure, the comparison between the original structure and improved structure is shown.

Table 4.12 Comparison between original and improved structure during torsion load case

	Original Structure		Improved Structure	
Mass	2999.29 kg		2809.49 kg	
	Torsion case1	Torsion case 2	Torsion case1	Torsion case 2
Max. Total Displacement	13.826 mm	15.793 mm	19.716 mm	21.078 mm
Max. Equivalent Stress	141.67 MPa	145.38 MPa	150 MPa	151.54 MPa

The structure mass is reduced by *189.8 kg* which is a great improvement for the bus body builders. It is improved by 6.33 %.

4.14. Verification of the method used

The following method is used as verification for the method used. The method is verified by using a simply supported overhanging beam of cross section used in the structure.

4.14.1. Bending Moment

The stress is given by

$$\sigma = \pm \frac{My}{I_z} \qquad 4.2$$

Where M= Bending moment

I_z=second moment of area and

σ is the stress at distance y from the N.A. of the beam cross-section

Now we should find the bending moment (M)

The applied loads are the load of the passenger and seat weight.

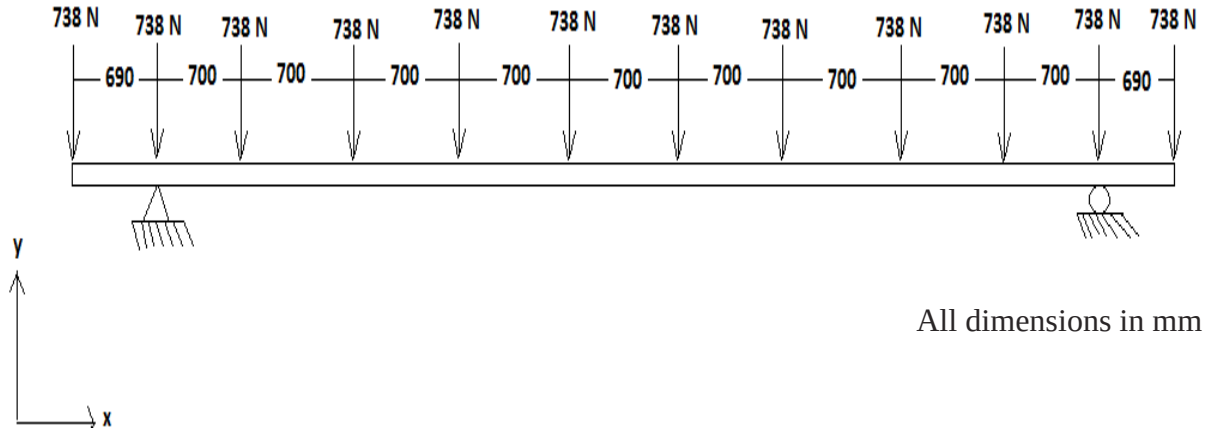

All dimensions in mm

Figure 4.48 Loads applied on the beam

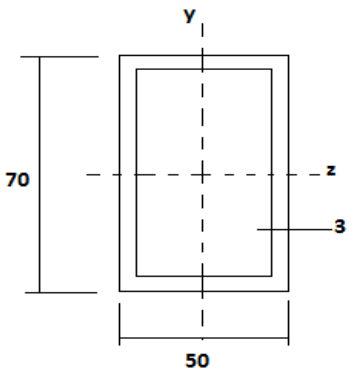

All dimensions in mm

Figure 4.49 Cross section of the beam used in the verification

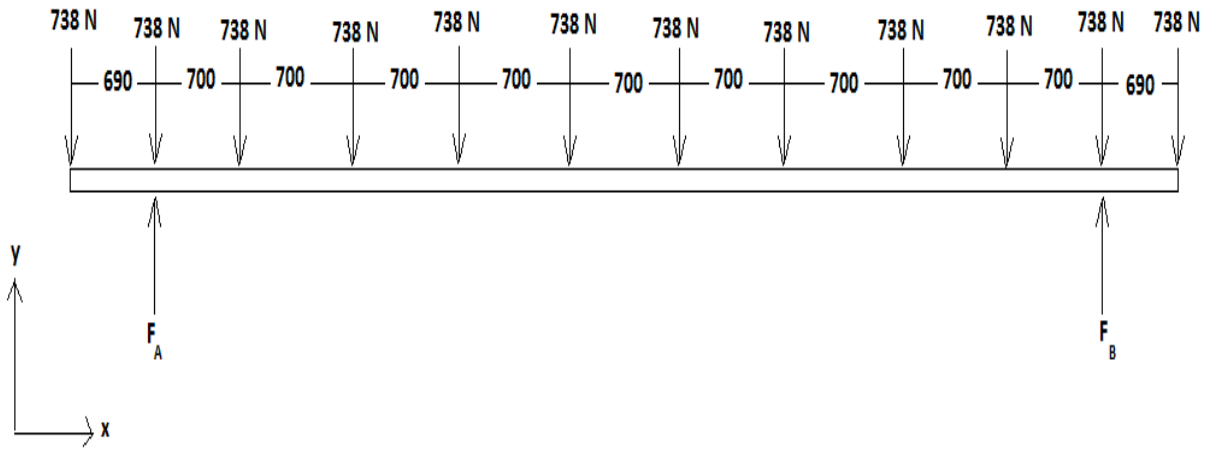

Figure 4.50 Reaction forces of the beam

Calculation of the reaction force,

$$F_A + F_B = 738 + 738 + 738 + 738 + 738 + 738 + 738 + 738 + 738 + 738 + 738 + 738$$

$$F_A + F_B = 8856 \text{ N}$$

$$-738\text{x}690 = 738\text{x}700 + 738\text{x}1400 + 738\text{x}2100 + 738\text{x}2800 + 738\text{x}3500 + 738\text{x}4200 + 738\text{x}4900 + 738\text{x}5600 - F_B\text{x}6300 + 738\text{x}6990$$

$$F_A = 4428\ N \qquad F_B = 4428\ N$$

The second moment of area is given by

$$I_z = \frac{1}{12} bh^3 \qquad 4.3$$

$b = 50\ mm\ and\ h = 70\ mm$

$$I_z = \frac{1}{12} x50x70^3 - \frac{1}{12} x44x64^3$$

$$I_z = 467971.99\ mm^4$$

The maximum bending moment is calculated to be $M_{max} = 4656780\ N\ mm$

The maximum tensile stresses occur at bottom periphery of the cross section, i.e. $y = 35mm$ where as the maximum compressive stress occurs at the top periphery of the cross section, i.e. for $y = 35\ mm$.

$$\sigma = \pm \frac{4656780x35}{467971.99}$$

$$\sigma = \pm 348.28\ MPa$$

The compressive stress occurs at the top side of the cross section and its value is calculated to be $-348.28\ \ MPa$. The tensile stress occurs at the bottom section of the beams cross section and its value is found to be $+348.28\ MPa$. Now to find the von miss stress (equivalent stress), we should first find the principal stresses.

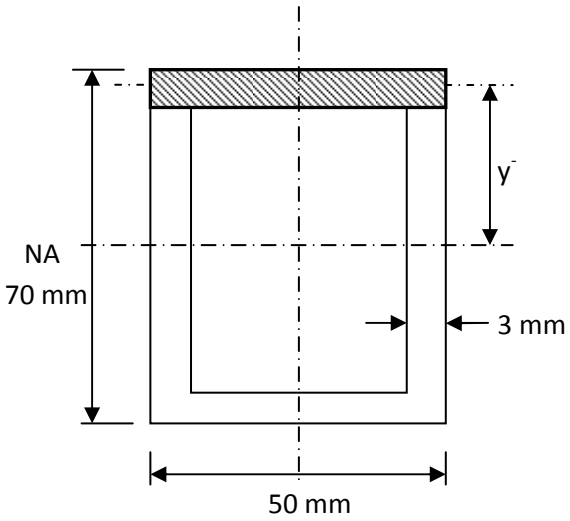

Figure 4.51 Cross section of beam for shear stress

For the shear stress at section, considering the shaded area above

$$Q = y^{-}A' \qquad 4.4$$

Where y^{-} is the distance from the nutral axis to the centroid of the area considered and A' is the area of the considered section.

$$y^{-} = \frac{64}{2} + 1.5 = 33.5\ mm$$

and

$$A' = 50 \times 3 = 150\ mm^2$$

$$Q = 33.5 \times 150 = 5025\ mm^2$$

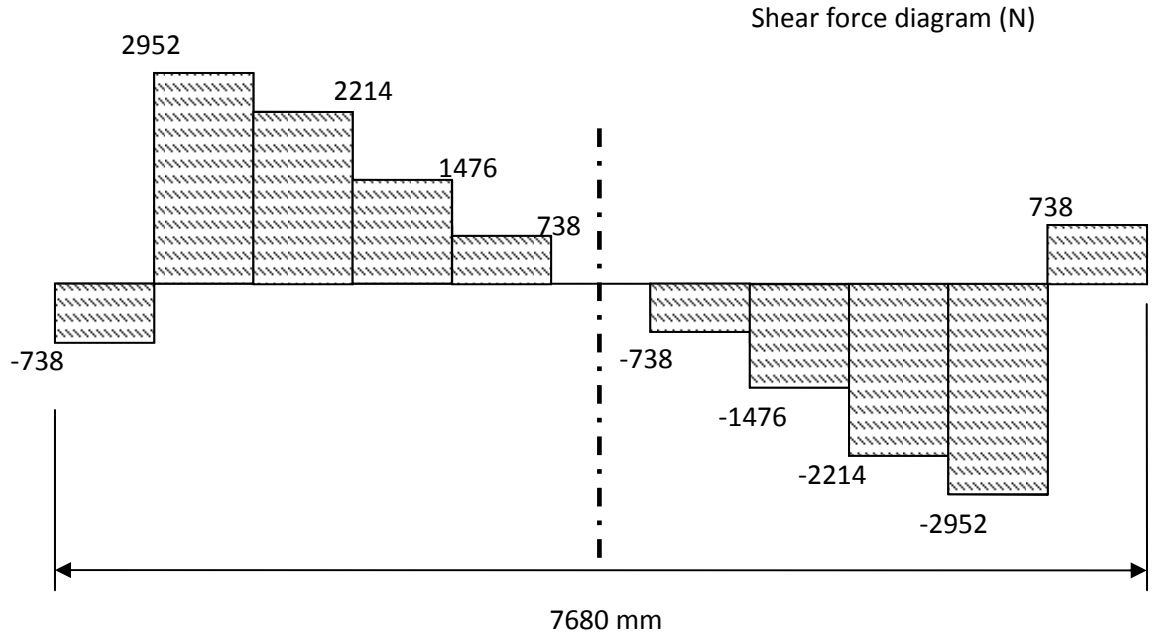

Figure 4.52 Shear force diagram

Now shear force at the middle of the beam becomes zero.

$$\tau_{xy} = -\frac{VQ}{Ib} \qquad 4.5$$

Since shear force has a zero value, the shear stress becomes zero, i.e. $\tau_{xy} = 0$

to find the principal stresses, the following equation is used.

$$\sigma_1, \sigma_2 = \frac{\sigma_x + \sigma_y}{2} \pm \sqrt{\left(\frac{\sigma_x - \sigma_y}{2}\right)^2 + {\tau_{xy}}^2} \qquad 4.6$$

$\sigma_x = -348.28 \ \ MPa \quad and \ \ \sigma_y = 0$

$$\sigma_1 = 0 \qquad \sigma_2 = 0 \qquad \sigma_3 = -348.28 \, MPa$$

$$\sigma_{von-miss} = \left[\frac{(\sigma_1 - \sigma_2)^2 + (\sigma_2 - \sigma_3)^2 + (\sigma_3 - \sigma_1)^2}{2}\right]^{1/2} \qquad 4.7$$

$$\sigma_{von-miss} = 348.28 \, MPa$$

4.14.2. Deflection of the beam

Macaulay's method is used to find the bending moment at any general section X-X of the beam. The Macaulay's method helps to find a single expression for bending moment throughout the complete span of the beam. It is used to cover all loading conditions.

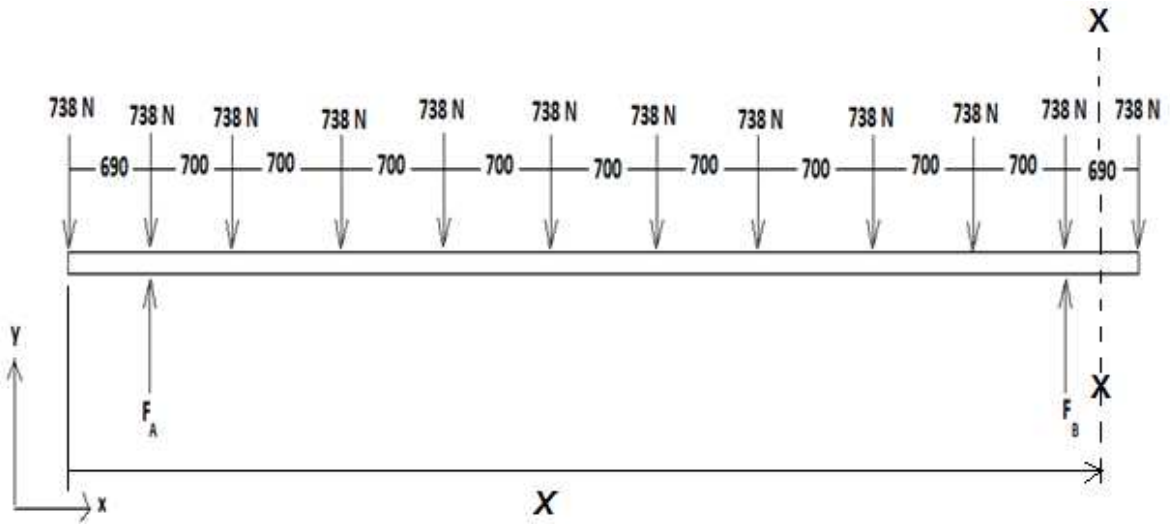

Figure 4.53 Section X-X of Beam

$$F_A = 4428\ N \qquad F_B = 4428\ N$$

$$M_{xx} = -738x - 738(x-690) + 4059(x-690) - 738(x-1390) - 738(x-2090) - 738(x-2790) - 738(x-3490) - 738(x-4190) - 738(x-4890) - 738(x-5590) - 738(x-6290) - 738(x-6990) + 4059(x-6990)$$

But the bending moment is given by the following equation

$$M = EI\frac{d^2y}{d^2x} \qquad 4.8$$

By integrating this equation, slope is found.

$$\theta = \frac{dy}{dx} \qquad 4.9$$

The second integration of this equation gives deflection (δ) of the beam.

$$\delta = y$$

Therefore, integrating twice the above bending moment equation will provide the following deflection equation along the length of the beam.

$$y = \delta = \frac{1}{EI}\left[-738\frac{x^3}{6} - 738\frac{(x-690)^3}{6} + 4059\frac{(x-690)^3}{6} - 738\frac{(x-1390)^3}{6} - 738\frac{(x-2090)^3}{6} - 738\frac{(x-2790)^3}{6} - 738\frac{(x-3490)^3}{6} - 738\frac{(x-4190)^3}{6} - 738\frac{(x-4890)^3}{6} - 738\frac{(x-5590)^3}{6} - 738\frac{(x-6290)^3}{6} - 738\frac{(x-6990)^3}{6} + 4059\frac{(x-6990)^3}{6} + Ax + B\right] \qquad 4.10$$

Where A and B are integrating constants to be solved from the boundary conditions.

When $x = 690 \quad y = 0$ also $x = 6990 \quad y = 0$

Therefore, the values of A and B is

$$A = -9.0688 \times 10^9 \qquad B = 6297.922 \times 10^9$$

$$EI = 200 \times 467971.99 \times 10^3 = 9.36 \times 10^{10} \quad N\,mm^2$$

Substituting these values in Eq. 4.9, the following values are found.

Table 4.13 Deformation values of the beam calculated analytically

Length of Beam (mm)	Deflection (mm)
0	67.2895
690	0
1390	-68.6697
2090	-129.6382
2790	-174.7913
3490	-198.7199
3840	-201.7671
4190	-198.7199
4890	-174.7895
5590	-129.6353
6290	-68.6657
6990	0
7680	67.2957

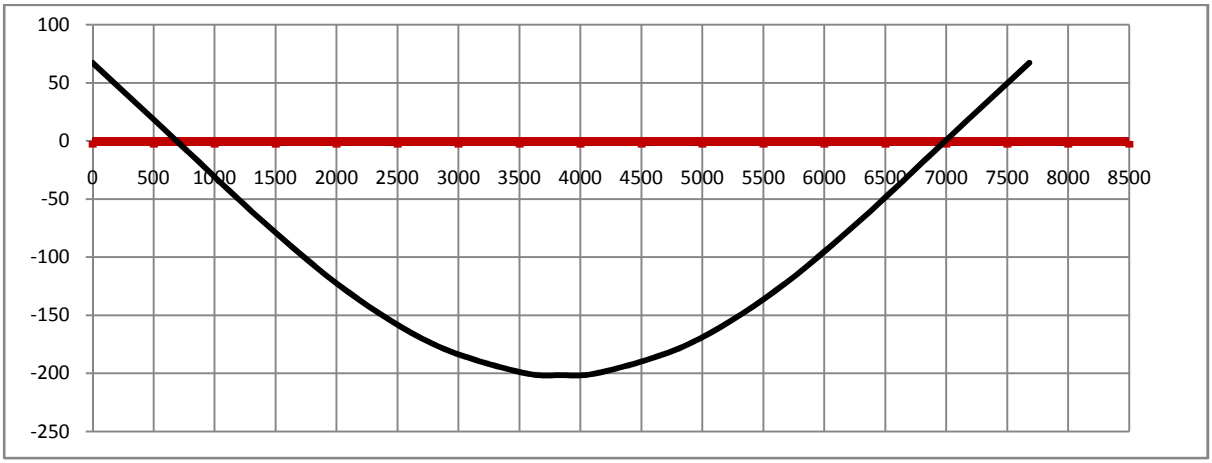

Figure 4.54 Deflection curve of the beam plotted in Microsoft Excel

4.14.3. Verification of manual analysis of the beam with ANSYS 12 Workbench

The following figure shows finite element mesh of the beam. BEAM 44 elements are used in meshing of the beam.

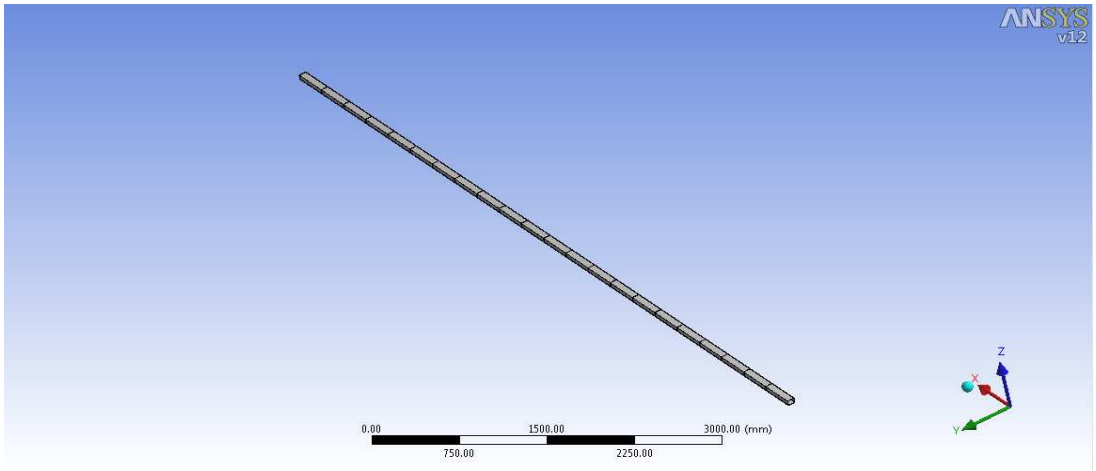

Figure 4.55 Finite element mesh of the beam

The loads on the beam are applied on the structure on the places where they are applied on the structure.

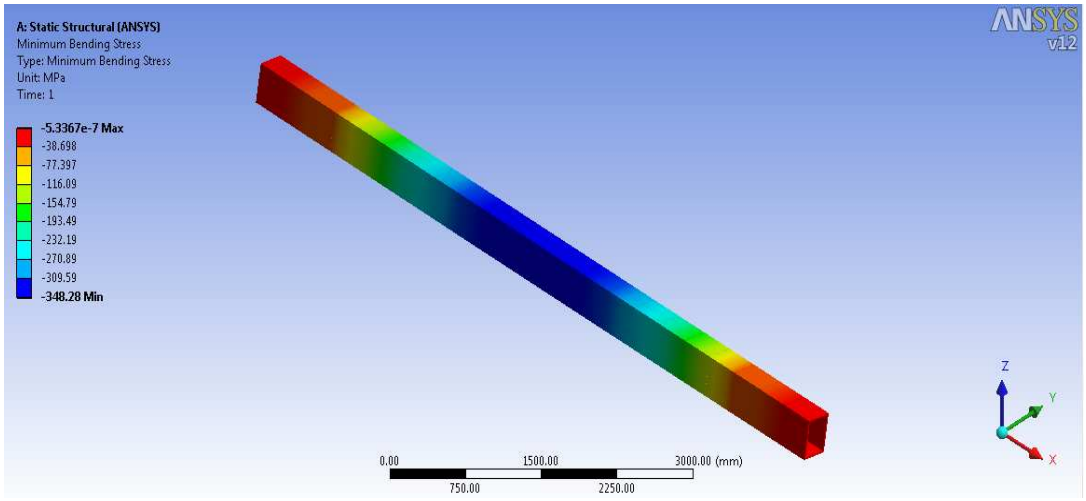

Figure 4.56 Minimum bending stress

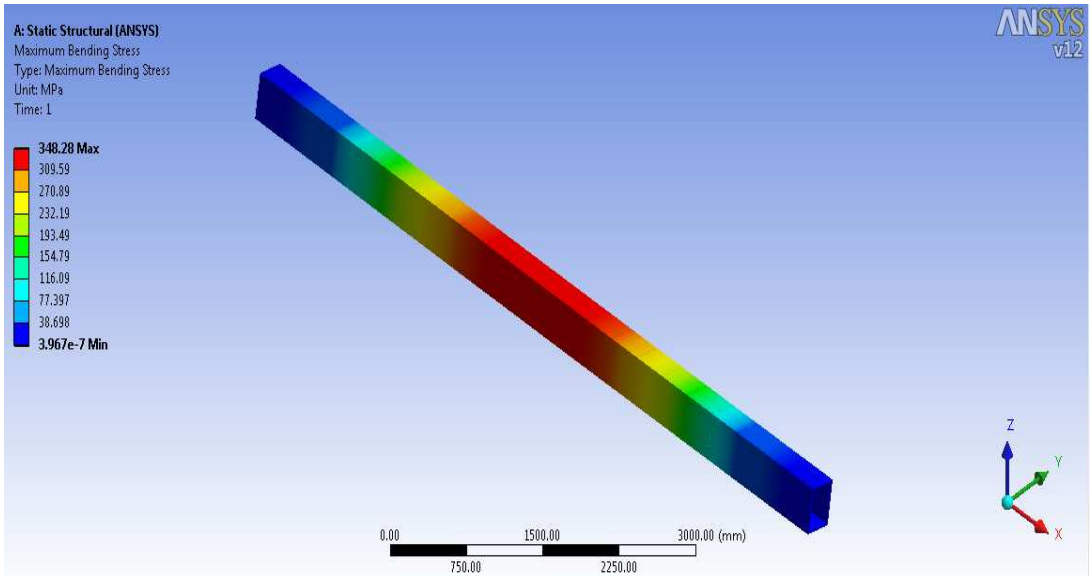

Figure 4.57 Maximum bending stress

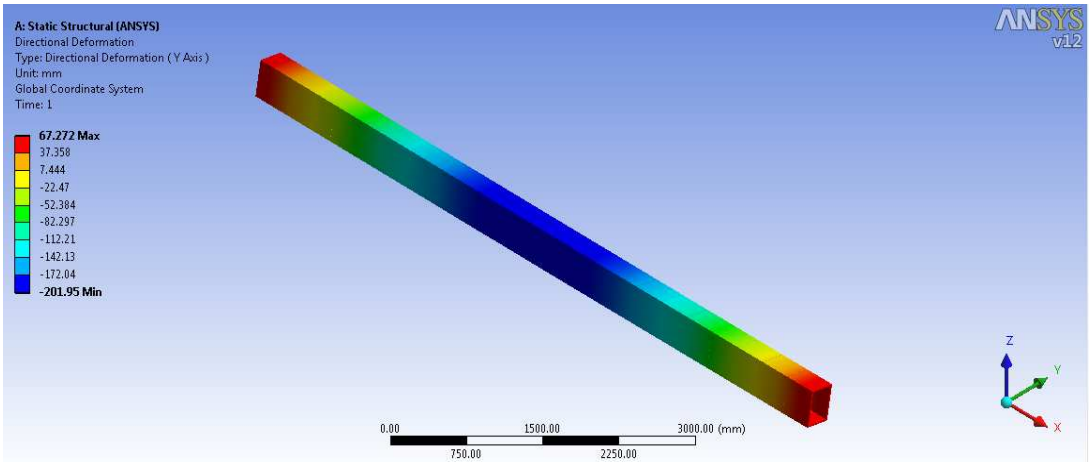

Figure 4.58 Deformation of the beam

The maximum displacment is 201.95mm. As we obsreve from the analtical and software analysis of the beam, there is a close similarty in bending and deflection results. This shows the procedure used in the analsyis of the bus strucutre is correct. Specifically, looking in to the deformation of the beam, there is close similarity. The beam deflected in up ward direction at its ends whereas it deflected in down ward direction in the middle section. This is what we have seen in the bus strcutre case.

Chapter Five

Cost Analysis

Cost analysis is carried in order to show the difference in cost between the original and improved structure. The analysis is based on the current cost of the materials in the market.

The following table shows the types of the RHS used in the original and modified bus structure.

Members marked with number 1 use RHS of 70X50X3mm in the original structure whereas those members which are marked with number 2 use RHS of size 50X30X3mm.

Table 4.14 Sizes of RHS used in the bus Structure

No.	Previous RHS used	Newly used RHS
1	70X50X3 mm	60X40X2.5 mm
2	50X30X3 mm	40X40X2.5 mm

In order to estimate cost, we need to find the total length of RHS steel used in the bus structure. First we examine the passenger side structure.

Total length of RHS 70X50X3mm used in passenger door side structure

Table 4.15 Total length of RHS 70X50X3mm used in passenger door side structure

	Member	Length(mm)	Amount in Number	Total length (mm)
1	Vertical stand	2300	5	11500
2	Vertical Stand (Short)	1720	4	6880
3	Verticals (Bottom)	530	5	2650
4	Top Horizontal	11000	1	11000
5	Vertical (Rear)	2100	1	2100
6	Front vertical stand	2272	1	2272
7	Horizontal window frame	1250	12	15000
8	Horizontal window frame (rear)	1020	2	2040
9	Top door side	810	2	1620
10	Small horizontals (Front)	300	2	600
			Sum Total of Length	55662 mm

Total length of RHS 50X30X3mm used in passenger door side structure

Table 4.16 Total length of RHS 50X30X3mm used in passenger door side structure

	Member	Length(mm)	Amount in Number	Total length (mm)
1	Diagonal stiffener	906	12	10872
2	Small vertical stiffeners	670	7	4690
3	Rear diagonal stiffeners	782	2	1564
			Sum Total of Length	17126

Total length of RHS 70X50X3mm used in Driver door side structure

Table 4.17 Total length of RHS 70X50X3mm used in Driver door side structure

	Member	Length(mm)	Amount in Number	Total length (mm)
1	Vertical stand	2300	5	11500
2	Vertical Stand (Short)	1720	4	6880
3	Vertical stand driver side door	1650	1	1650
4	Verticals (Bottom)	530	5	2650
5	Top horizontal	11000	1	11000
6	Vertical (Rear)	2100	1	2100
7	Front Vertical Stand	2272	1	2272
8	Horizontal window Frame	1250	12	15000
9	Horizontal window frame (Rear)	1020	2	2040
10	Top Rear door side	810	2	1620
11	Driver door horizontal bottom	1090	2	2180
12	Top of driver door horizontal	765	1	765
			Sum Total of Length	59657 mm

Total length of RHS 50X30X3mm used in passenger door side structure.

Table 4.18 Total length of RHS 50X30X3mm used in passenger door side structure

	Member	Length(mm)	Amount in Number	Total length (mm)
1	Diagonal stiffener	906	12	10872
2	Small verticals	670	8	5360
3	Rear diagonals	782	2	1564
4	Rear diagonals (door)	740	2	1480
			Sum Total of Length	19276

From the above calculation, the total length of RHS 70x50x3mm employed in the left and right sides of the structure is 115,319mm and RHS of 50X30X3mm is 36,402 mm.

From market the following prices of the RHS is obtained.

Table 4.19 Prices of RHS

No.	Profile type	Price/6m (birr)
1	RHS 70X50X3 mm	790.00
2	RHS 50X30X3 mm	480.00
3	RHS 60X40X2.5mm	560.00
4	RHS 40X40X2.5 mm	350.00

Table 4.20 Length of RHS and cost saved

No.	Profile type	Length (m)	Cost (Birr)
1	RHS 70X50X3 mm	115.319	15183.67
2	RHS 60X40X2.5mm	115.319	10763.10
3	RHS 50X30X3 mm	36.402	2912.16
4	RHS 40X40X2.5 mm	36.402	2123.45

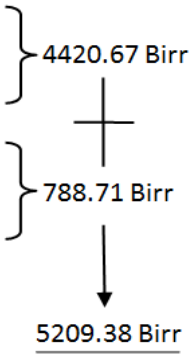

The total cost that will be saved by replacing of the RHS with the newly ones is 5209.38 Birr. The factory saves 5209.38 Birr per Bus produced. The annual production of the factory reaches 90 to 110 Buses. Consequently, the average cost saved from manufacturing of the structure with the newly replaced RHS reaches 520, 938.00 Birr in a year.

Chapter Six

Conclusions and Recommendations

6.1. Conclusions

This research focuses on improving of the bus structure weight. The strength of bus structure is the most important thing to be considered in the design process. The bus model used in this research for simulation was developed with the same dimensions of a real bus manufactured in Ethiopia. The strength of the bus structure is analysed for two major load cases. The first case bending load case and the other is torsional stiffness. The results of the original structure analysis show the stresses found are small, which directly implies the bus structure is overdesigned. It was seen that the highest displacement occur at the roof section of the bus structure because the members used to build the roof are smaller in cross section than other members.

This gives us a room to further improve the bus structure by redesigning. In the improvement process, the members of original structure are replaced with reduced thickness and cross section profile. The total weight reduced during the improvement process is *189.8 kg*. Again this improved structure is analysed for bending load and torsional stiffness. It is found that the stress is raised in some members, however looking at the overall structure, the stresses found are still small. The procedure used in the analysis is validated using simply supported overhanging beam. Specially, the deformation of the bus is very similar with the beam deformation. So, with improvement made on the structure, the total cost saved by replacing with the new members is *5209.38 Birr* per bus produced. Generally the factory will save a total of 520, 938.00 birr annually.

The acceleration PSD response analysis reveals that when driving at high speed on gravel road of standard Class H, larger force will be induced on the structure, which leads to easy failure of the RHS. However, driving with lower speed significantly reduces the forces where by leaving the structure in safe condition.

6.2. Limitations of the study

The results of this study clearly showed that with the considered cases of operating scenarios, the structure is improved. But limitations of the study are:

- ✓ Shape of the structure is not analysed which has aerodynamic effect on the structure.
- ✓ Welding quality in assembling of the structure members is not analysed.

6.3. Recommendation for Future Study

- The sheet metal which is covered on the structure should be included in the finite element analysis in order to find a more refined result.
- The behavior of the structure during rollover, specially the roof section of the bus need to be analyzed.
- Further redesign of the bus structure considering individual members.

References

1) B.L. Boada, A. Gauchia, M.J.L. Boada, V. Diaz, A genetic-based optimization of a bus structure as a design methodology. *Paper presented at the 12th IFToMM World Congress, Besancon*, France, 2007.
2) C. Theodosiou, G. Georgiou and S. Natsiavas, 2008, Periodic Steady State Response of a Large Scale City Bus Model With Nonlinear Characteristics. ENOC, Saint Petersburg, Russia.
3) Lan F., Chen J. and Lin J., 2004, Comparative analysis for bus side structures and lightweight optimization. *Journal of Automobile Engineering*, 218, 1067−1075.
4) Zhang Daqian, Zhang Tianxia, Zhang Guosheng and Zhao Weitao, Structural Reliability Analysis of Bus Body in Consideration to the Correlation of Working Conditions, 2009 *International Conference on Measuring Technology and Mechatronics Automation*, China,2009.
5) Balazs Gombor, 2005 Dynamic analysis of a bus body frame: 'Determination of the loads and stresses'. *International Journal of Vehicle Mechanics and Mobility*, 43(11), 807–822
6) Manokruang S., Butdee S., 2009, Methodology of Bus-Body Structural Redesign for Lightweight Productivity Improvement, *AIJSTPME*, 2(2): 79-87.
7) Liang, Cho-Chung and Le, Giang-Nam, 2009, Bus rollover crashworthiness under European standard: an optimal analysis of superstructure strength using successive response surface method, *International Journal of Crashworthiness*, 14: 6, 623 – 639.
8) M. Gobbi G. Mastinu.,1998, Expected Fatigue Damage of Road Vehicles due to Road Excitation, *International Journal of Vehicle Mechanics and Mobility, Vehicle System Dynamics*, 29: 1, 778 -788.
9) S. Butdee , F. Vignat, 2008, TRIZ method for light weight bus body structure design, *Journal of Achievements in Materials and Manufacturing Engineering*,31:2, 456-462
10) H Kim, M W Suh and D H Bae, 2000, Development of an optimum design technique for the bus window pillar member, *Journal of Automobile Engineering*, 215, 11−19.
11) K.A.Ahmed M.B.A.Abdelhady A.M.A.A.Abouelnour, The Improvement of Ride Comfort of a City Bus Which is fabricated on a Lorry Chassis. *Engineering Research Journal*, Vol.53, 1997.

12) Zhang Xingwang and Tao Zhen, A Study Shape Optimization of Bus Body Structure Based on Stiffness Sensitivity Analysis, *IEEE Journal*, 2009,1225-1229, China.
13) A. GAUCHIA, V. DIAZ, M. J. L. BOADA and B. L. BOADA, 2010, Torsional Stiffness and Weight Optimization of a Real Bus Structure, *International Journal of Automotive Technology*, 11:1, 41-47.
14) R. Sidhu, J. Burgueno, R.C. Averill, E.D. Goodman, 2003, Shape Optimization for Improved Vehicle Safety and Reliability, *ABAQUS Users' Conference*
15) P. Neves, A. A. Fernandes , A. Ferreira , A. T. Marques , N. Correia, B. Almada-Lobo, *Use of Composite Materials in Public Service Vehicles*, Instituto de Engenharia Mecânica e Gestão Industrial, Porto, Portugal.
16) Martin Hornung and Michael Hajj, 2009, Structural Bonding for Lightweight Construction, *Materials Science Forum*, Switzerland, Vol 618-619, pp 49-56.
17) Y-H Wang and M-C Shih, 2010, Design of a genetic-algorithm-based self-tuning sliding fuzzy controller for an active suspension system, *Proc. IMechE Journal of Systems and Control Engineering*, Vol. 225,367-383 P.
18) Finite element analysis and concepts,*" Guide for the Use and Applicability of Workbench Simulation Tools from ANSYS, Inc."2009.*

Bibliography

1) Young W. Kwon, Hyochoong Bang, *Finite Element Using Mat Lab*, New York, CRC press, 1997.
2) David V. Hutton, *Fundamentals of Finite Element Analysis*, New York, McGraw-Hill, 2004.
3) Douglas Thorby, *Structural Dynamics and Vibration in Practice, An Engineering Handbook*, USA, Elsevier Ltd., 2008.
4) Knut O. Kverneland, *World Metric Standard for Engineering, Industrial Press inc.*, New York, 1978.